Structural analysis of N-phenyl-N'-sulfinylhydrazines and their hydrogen bonded dimers

Pratibha Malla

A Thesis

in

The Department

of

Chemistry and Biochemistry

Presented in Partial Fulfillment of the Requirements
for the Degree of Master of Science at
Concordia University
Montreal, Quebec, Canada

September 2005

Your file Votre référence
ISBN: 978-0-494-20666-9
Our file Notre référence
ISBN: 978-0-494-20666-9

Abstract

Structural analysis of N-phenyl-N'-sulfinylhydrazines and their hydrogen bonded dimers

Pratibha Malla

N-phenyl-N'-sulfinylhydrazine (PhNHNSO) is known to form hydrogen bonded dimers in the solid. Recent experimental studies have shown that the dimerization of PhNHNSO is very sensitive towards the position of a substituent on the aromatic ring. It was found that upon introduction of a substituent in ortho position, dimerization did not occur. However, substitution in meta and para position did not hinder dimer formation.

This study was carried out to understand why certain PhNHNSOs dimerize, while others do not. The effects of substituent and solvent on dimerization were investigated by means of different computational methods. In general, density-functional theory calculations were combined with topological analyses of the electron density.

The relative energies revealed a preference of the *syn* configuration over other configurations of the unsubstituted monomer. The introduction of substituents in ortho position led to less stable monomers as well as dimers, whereas meta and para substitution had only a small effect on monomer and dimer stabilities. The geometries, frequencies and electron densities of N-H and S=O bonds are more affected by ortho than by meta and para substitution, and the ortho dimers showed weaker intermolecular interactions because of twisted geometries. The observed intermolecular N-H---O and C-H---O interactions in the dimers are characterized as hydrogen and anti-hydrogen bonds, respectively. Increasing solvent polarity weakens the dimers. The topological properties, structural parameters and energies showed an unfavourable dimerization for ortho substituted PhNHNSO monomers, which is consistent with the experimental results.

Acknowledgements

First, I would like to offer my sincere thanks to my supervisor Dr. Heidi M. Muchall for her advice, support and patience throughout my graduate studies. I am very grateful for her encouragement and for giving me an opportunity to present our research at the annual meeting of the Canadian Society for Chemistry in London, Ontario. I would also like to extend my thanks to my committee members Dr. Gilles H. Peslherbe and Dr. Christine E. DeWolf for their guidance and support.

I am also thankful to Dr. Robert Mawhinney, Dr. Francis Djapa, Sunjun Li and Ying Zhao for their advice. My special thanks go to Elena Ivanova, Lei Zhang and Petrina Kamya for their useful suggestions and for their help during group meetings, seminar and committee meetings.

Finally, I would like to thank my husband, parents-in-laws (Bhava K. Khayargoli and Laxmi Khayargoli), my parents (Shyam Lal Malla and Menuka Malla), sisters and brother and other family members for their continuous support and encouragement.

Dedicated to my husband Praduman Khayargoli and

my daughters Pranamika Khayargoli and Primika Khayargoli

Table of contents

List of figures ..... **x**

List of schemes ..... **xiii**

List of tables ..... **xiv**

List of abbreviations and symbols ..... **xviii**

Chapter 1 Introduction **1**

1.1 Weak interactions 1

1.1.1 The hydrogen bond 1

1.1.2 The (improper blue shifting or) anti-hydrogen bond 4

1.1.3 Classification of hydrogen bonds 5

1.1.4 Characterization of hydrogen and anti-hydrogen bonds 5

1.2 Computational methods 7

1.3 Substituent effects 9

1.3.1 The Hammett substituent constant 9

1.3.2 The isodesmic reaction approach 11

1.4 Methodologies 12

1.4.1 Supermolecular approach 12

1.4.2 Topological analysis of the electron density 13

1.4.3 Solvent effect 15

Chapter 2 Historical background to N-phenyl-N'-sulfinylhydrazine and objectives and organization of Chapters 3, 4 and 5 ..... **16**

2.1 The hydrogen bonding network in the dimer of the syn-N-phenyl-N'-sulfinylhydrazine 19

2.2 The influence of substituents on hydrogen bond forming bonds in N-phenyl-N'-sulfinylhydrazine 20

2.3 Chloro and methyl substituted N-phenyl-N'-sulfinylhydrazines: experimental and computational analyses 21

Chapter 3 The hydrogen bonding network in the dimer of the syn N-phenyl-N'-sulfinylhydrazine 22

3.1 Introduction 22

3.2 Experimental section 24

3.3 Computational details 24

3.4 Results and discussion 25

3.4.1 Vibrational spectra 25

3.4.2 PhNHNSO Monomer 28

3.4.2.1 Energies and geometries 28

3.4.2.2 Frequencies 31

3.4.3 PhNHNSO Dimer 33

3.4.3.1 Energies and geometries 33

3.4.3.2 Frequencies 37

3.4.4 Identification and characterization of the weak interactions 38

3.5 Conclusions 44

Chapter 4 The influence of substituents on hydrogen bond forming bonds in N-phenyl-N'-sulfinylhydrazine 45

4.1 Introduction 45

4.2 Computational details 46

4.3 Results and discussion 47
4.3.1 Energies 48
4.3.2 Barrier height 52
4.3.3 Geometry and frequency 53
4.3.3.1 N-H bond 54
4.3.3.2 C-H bond 56
4.3.3.3 S=O bond 57
4.3.4 Electron densities 58
4.3.5 Hammett correlations 61
4.3.5.1 Bond distances, frequencies and electron densities 61
4.3.5.2 Atomic charges on hydrogen and oxygen atoms 64
4.3.6 Stability of substituted compounds 68
4.4 Conclusions 70
Chapter 5 Chloro and methyl substituted N-phenyl-N'-sulfinylhydrazines: experimental and computational analyses 71
5.1 Introduction 71
5.2 Experimental section 73
5.3 Computational details 73
5.4 Results and discussion 74
5.4.1 Vibrational spectra 74
5.4.2 Energies 76
5.4.3 Geometries 81
5.4.4 Frequencies 85

5.4.5 Identification and characterization of the weak interactions 87

5.5 Conclusion 98

Chapter 6 Conclusions and future work 99

References 103

Appendix A: Supplemental information related to Chapter 3 110

Appendix B: Supplemental information related to Chapter 4 112

Appendix C: Supplemental information related to Chapter 5 140

Appendix D: Internal coordinates and total energies 144

Appendix E: Contour plots and molecular graph 192

List of figures

Fig. 1.1: Examples of intra- and intermolecular H-bonds with donor (D) / acceptor (A) designation. 2

Fig. 1.2: Variation in the number of intermolecular H-bonds in different systems..... 3

Fig. 1.3: Schematic H-bond pattern with (a) bifurcated donor and (b) bifurcated acceptor atoms. 3

Fig. 1.4: Anti-H bond in the T-shaped benzene dimer..... 4

Fig. 1.5: Molecular graphs of ethene. (a) Contour plot of $\rho(r)$ with interatomic surfaces and bond paths, (b) AIM 2000 representation. Only one BCP is identified in each. 14

Fig. 2.1: Predicted H-bond network in PhNHNSO from X-ray and neutron diffraction studies.[44,45] 16

Fig. 2.2: (a) *Syn*, (b) *sickle*, (c) *anti1* and (d) *anti2* configurations of PhNHNSO. 17

Fig. 2.3: Substituted PhNHNSO compounds to be studied and their notation. 18

Fig. 3.1: H-bonding network in the PhNHNSO dimer as suggested from diffraction studies.[44,45] 23

Fig.3.2: Configurations of the PhNHNSO monomer: (a) *syn*, (b) *sickle*, (c) *anti1*, (d) *anti2*..... 28

Fig. 3.3: Contour maps of the electron density of (a) the *syn* configuration, (b) the *sickle* configuration and (c) the dimer with only one monomer plus one oxygen atom from the second monomer in the plane of the plot. Saddle points for weak interactions are indicated by arrows. (d) Molecular graph of the dimer at the B3LYP/6-311+G(2d,p). The outermost contour in (a)-(c) is 0.001

au and the remaining contours increase in value in steps equal 2×10^n, 4×10^n, 8×10^n with n starting at -3 and increasing in steps of unity. 39

Fig. 4.1: Configurations/conformers of substituted PhNHNSO and numbering of compounds. (X= OH, OCH_3, CH_3, F, Cl, Br, CN and NO_2)..... 47

Fig. 4.2: Plots of bond distance (d, pm) and frequency (ν, cm^{-1}) for (a) N-H bond at the cc-pVTZ level, (b) ortho C-H bond at the cc-pVTZ level (c) S=O bond at the 6-31+G(d) level. All basis sets are for the B3LYP method. 55

Fig. 4.3: Plots of bond distance (d, pm) and electron density (ρ, e/$Å^3$) for (a) N-H bond at the cc-pVTZ level, (b) ortho C-H bond at the cc-pVTZ level (c) S=O bond at the 6-31+G(d) level. All basis sets are for the B3LYP method. See text for the correlations..... 60

Fig. 4.4: Dependencies for the S=O bond: (a) bond distance (d, pm) (b) frequency (ν, cm^{-1}) and (c) electron density (ρ, e/$Å^3$) versus. σ from B3LYP/6-31+G(d). (Δ p, · m3, * m5 substitution)..... 62

Fig. 4.5: Dependencies for the N-H bond of para substituted compounds: (a) bond distance (d, pm) (b) frequency (ν, cm^{-1}) and (c) electron density (ρ, e/$Å^3$). and σ_p^+ from B3LYP/6-311+G(2d,p). 63

Fig. 4.6: Correlations for the ortho C-H between electron density (ρ, e/$Å^3$) and σ for (a) m3 (b) m5 from B3LYP/cc-pVTZ. (· m3, * m5 substitution)..... 63

Fig. 4.7: Correlation between atomic charges (au) and σ for (a) the oxygen atom of the S=O bond (b) the hydrogen atom of the N-H bond and (c) the hydrogen atom of the C-H bond from B3LYP/6-31+G(d).(Δ p, · m3, * m5 substitution) 67

Fig. 4.8: Correlation between isodesmic reaction energies (ΔE) (kcal/mol) and σ for (a) meta and (b) para substituted compounds from B3LYP/6-31+G(d). (Δ p, • m3, ⋆ m5 substitution). 69

Fig. 5.1: Notation of the substituted PhNHNSO dimers and numbering of the ring carbon atoms. 73

Fig. 5.2: Contour maps of the electron density of (a) the mCl3 dimer with only one monomer plus one oxygen atom from the second monomer in the plane of the plot and (c) the oCl2 dimer with S atoms of two monomers in the plane of the plot. Saddle points for weak interactions are indicated by arrows. The outermost contour is 0.001 au and the remaining contours increase in value in steps equal 2×10^n, 4×10^n, 8×10^n with n starting at -3 and increasing in steps of unity. (c) and (d) show the molecular graphs for the mCl3 and oCl2 dimers, respectively. 88

List of schemes

Scheme 1.1: Isodesmic reaction for p-substituted benzoic acids 11

Scheme 4.1: Isodesmic reaction for the substituted PhNHNSO and aniline. 68

List of tables

Table 1.1: Common distances (Å) and angle (degrees) of strong, moderate and weak hydrogen bonds. 6

Table 3.1: Frequency (cm^{-1}) of the N-H stretching vibration of neat PhNHNSO and in CCl_4, $CHCl_3$ and CH_2Cl_2 solution. Concentration in mol/L. 27

Table 3.2: ZPVE corrected total energies (au) of four configurations of the PhNHNSO monomer. Relative energies (kcal/mol) are given in parentheses. 29

Table 3.3: Selected geometrical parameters (distances in pm, angles in degrees) of four configurations of PhNHNSO from B3LYP/6-31+G(d). 30

Table 3.4: Scaled frequency[a] (cm^{-1}) of the N-H stretching vibration in four configurations of the PhNHNSO monomer. 32

Table 3.5: Free energies of solvation, ΔG_{solv}, and their electrostatic contributions, ΔG_{el} (kcal/mol) of the *syn* PhNHNSO monomer and dimer in three solvents. 34

Table 3.6: Selected calculated and experimental geometrical parameters (distances in pm, bond angles in degrees) of the PhNHNSO dimer. 36

Table 3.7: Electron density $\rho(r)$ ($e/Å^3$) and Laplacian $\nabla^2\rho(r)$ ($e/Å^5$) for BCPs of (N)H---O and (C)H---O interactions, and mutual penetrations[a] (pm) of H and O atoms of the PhNHNSO dimer from B3LYP/6-31+G(d). 40

Table 3.8: Integrated properties[a] (au) of hydrogen atoms of interacting N-H and C-H bonds in the dimer and their differences from the *syn* monomer, with B3LYP/6-31+G(d). 42

Table 3.9: Bond critical point (BCP) data ρ(r) in e/Å^3 and $\nabla^2\rho(r)$ in e/Å^5 for the ortho C2-H bonds and distances (pm) from the BCP to the C and H nuclei in the PhNHNSO *syn* monomer and dimer. 43

Table 4.1: Relative ZPVE corrected total energies[†a] (kcal/mol) of the substituted[†b] compounds PhNHNSO at the B3LYP level with three different basis sets. ... 50

Table 4.2: Equilibrium population (%) at room temperature of the substituted conformers from B3LYP/6-31+G(d). 52

Table 4.3: Barrier heights (kcal/mol) from C2-C-N-H torsion for o2-o6 and m3-m5 conversion and in para and unsubstituted compounds PHNHNSO from B3LYP/6-31+G(d). 53

Table 4.4: Dihedral angles C2-C-N-H (degree) of o2 and o6 conformers from B3LYP/6-31+G(d). 54

Table 4.5: Experimental and calculated[a] N-H stretching frequencies (cm^{-1}) for Cl and Me substituted compounds. 56

Table 4.6: AIM integrated atomic charges (au) from B3LYP/6-31+G(d). 65

Table 4.7: Calculated isodesmic reaction energies (ΔE) from B3LYP/6-31+G(d). 68

Table 5.1: Frequency (cm^{-1}) of the N-H stretching vibrations of chloro and methyl substituted PhNHNSOs in $CHCl_3$ solution at concentration of 0.1 and 0.5 mol/L. 75

Table 5.2: ZPVE corrected relative energies ΔE[a], interaction energies ΔE_{inter} and free energies of dimerization ΔG (kcal/mol) of chloro and methyl substituted PhNHNSO dimers. 77

Table 5.3: Free energies of solvation, ΔG_{solv}, and their electrostatic contributions, ΔG_{el} (kcal/mol) of the methyl substituted PhNHNSO monomers and dimers in three solvents.....79

Table 5.4: Free energies of solvation, ΔG_{solv}, and their electrostatic contributions, ΔG_{el} (kcal/mol) of the methyl substituted PhNHNSO monomers and dimers in three solvents.....80

Table 5.5: Distances (pm) of the N-H, ortho C-H and S=O bonds involved in intermolecular interactions in PhNHNSO dimers and their difference from the respective monomers.....82

Table 5.6: H-bond distances (pm) and bond angles on hydrogen (degrees) of all PhNHNSO dimers.....84

Table 5.7: CCNN dihedral angle (degree) of the substituted PhNHNSO dimers.....85

Table 5.8: Scaled frequency (cm^{-1}) of the N-H and the C-H stretching vibration of the PhNHNSO dimers and their shift from the respective monomers.....86

Table 5.9: Electron density $\rho(r)$ ($e/Å^3$) and Laplacian ($\nabla^2\rho$) ($e/Å^5$) for BCPs of (N)H---O and (C)H---O interactions of chloro and methyl substituted dimers.....89

Table 5.10: Mutual penetration of nonbonded (r^0) and bonded (r) radii (pm) of H and O atoms of all dimers.....92

Table 5.11: Integrated atomic properties[a] (au) of hydrogen atoms of interacting N-H and C-H bonds of chloro substituted dimers and their difference from the respective monomers.....94

Table 5.12: Integrated atomic properties[a] (au) of hydrogen atoms of interacting N-H and C-H bonds of methyl substituted dimers and their difference from the respective monomers..... 96

List of abbreviations and symbols

AIM	Atoms in molecules
Anti-H bond	Anti-hydrogen bond
B3LYP	Becke's three-parameter hybrid exchange/Lee-Yang-Parr correlation functional
BCP	Bond critical point
COSMO	Conductor-like screening model
CP	Critical point
DFT	Density-functional theory
E	Energy
EDG	Electron-donating group
EWG	Electron-withdrawing group
FTIR	Fourier Transform Infrared
G	Free energy
HF	Hartree-Fock or hydrogrn fluoride
H-bond	Hydrogen bond
K_x	Equilibrium constant for substituted compound
K_H	Equilibrium constant for unsubstituted (or hydrogen substituted) compound
M	Dipolar polarization
PES	Potential energy surface
q	Charge
$\rho(r)$	Electron density

$\nabla^2\rho(r)$	Laplacian of the electron density
ρ	Hammett reaction constant
σ	Hammett substituent constant or signature of a CP
σ_+	Hammett substituent constant
ω	Rank of a CP
SCRF	Self-consistent reaction field
ν	Stretching vibration

Chapter 1

Introduction

1.1 Weak interactions

Weak interactions are the foundations of chemistry and nature. From simple water to complex biological molecules like proteins and nucleic acids, and from the self-assembly of cylindrical, helical and spherical structures to supramolecular channels and cavities, all show various types of these interactions.[1-5] Basically, ion-ion, ion-dipole, dipole-dipole, hydrogen bond (abbreviated as H-bond) and van der Waals interactions fall into the category of weak interactions. Although all have the same fundamental principle, an interaction between opposite charges, they differ in magnitude, effective range and mode of operation. Amongst them, the most prominent interaction is the H-bond.

1.1.1 The hydrogen bond

Recognition and description of the H-bond began in 1920, when Latimer and Rodebush introduced the concept of the H-bond as a weak bond that exists when the hydrogen nucleus is held by two octets.[6] The term "hydrogen bond" was first introduced by Pauling in 1931.[7] He suggested that such bonds are formed to some extent by oxygen and, in some cases, by nitrogen atoms. In 1936, Huggins further illustrated the concept of the H-bond as a hydrogen-bridge in ice and in organic compounds.[1] He described a wide variety of both inter- and intra-molecular H-bonds with N-H and O-H as donors and O and N as acceptor atoms. Pimental and McClellan in 1960 used letters A and B for the hydrogen bond donor and acceptor atoms.[1,2] The nature of the H-bond was established by Morokuma in 1971.[1] The author decomposed the H-bond into terms that represent

electrostatic, polarization, exchange repulsion, charge transfer and dispersion contributions.

In general, conventional H-bond interactions A-H---B involve the sharing of a hydrogen atom between two electron-withdrawing atoms (A, B), where both atoms are usually C, N, O and F. The H-bond is thus a bridge that connects atoms A and B that have electronegativities larger than that of hydrogen. The A-H group is generally referred to as the "proton donor" (D) group and the B atom is called the "proton acceptor" (A). When hydrogen is attached to an electronegative atom the bonding electrons are drawn strongly towards that atom creating a bond dipole. The hydrogen atom acquires a small positive charge and becomes capable of attracting negatively charged atoms of either the same or a different molecule. In the latter case, this attraction leads to the association of two molecules by formation of an intermolecular H-bond.[8] A H-bond is represented by a dotted line as illustrated in Fig. 1.1.

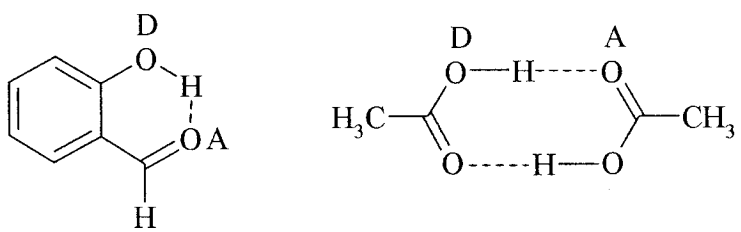

Fig. 1.1: Examples of intra- and intermolecular H-bonds with donor (D) / acceptor (A) designation.

The number of H-bonds between molecules can vary. A variety of molecules such as phenols, amines, and sulfonamides often form a single H-bond. On the other hand, molecules with polar functionalities have a strong tendency to dimerize through the

formation of two H-bonds. Many solid state dimeric assemblies such as homo-dimers of carboxylic acids, amides, and ureas are examples of such dimers.[9] The presence of three H-bonds can be found in nucleic acid base pairs.[1,4] Usually four and more H-bonds are present in supramolecular complexes and polymers [5] Fig. 1.2 displays examples of systems with a different number of H-bonds. Bifurcation at both donor and acceptor atoms is also known.[2] (Fig. 1.3)

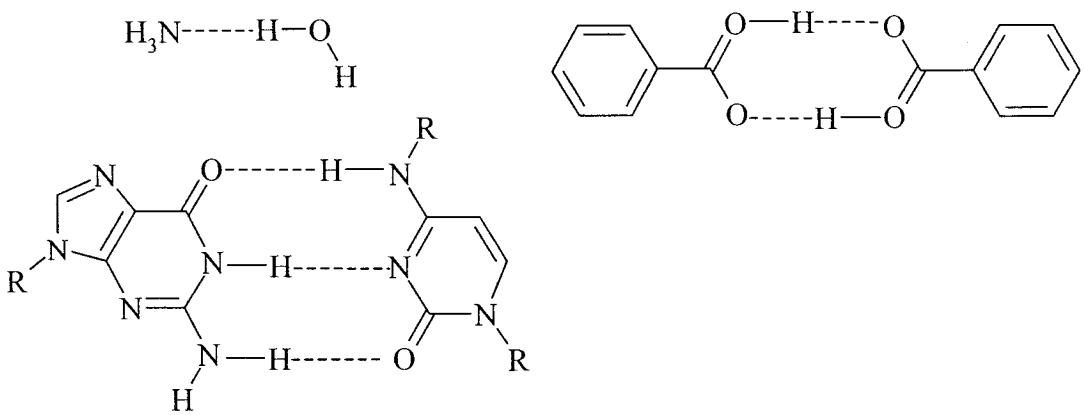

Fig. 1.2: Variation in the number of intermolecular H-bonds in different systems.

Fig. 1.3: Schematic H-bond pattern with (a) bifurcated donor and (b) bifurcated acceptor atoms.

1.1.2 The (improper blue shifting or) anti-hydrogen bond

Besides the conventional H-bonds, another kind of H-bond has been discovered recently that is known as an anti-hydrogen bond (abbreviated as anti-H bond) or improper, blue-shifting H-bond. Hobza et al. identified this novel kind of H-bond in the T-shaped benzene dimer (Fig. 1.4) and other benzene complexes with C-H donors.[10-12] The authors described the C-H---π interaction in the benzene dimer as an anti-H bond in which the C-H group is the proton donor and "π" represents the delocalized π-electrons as electron acceptor. The characterization of such an anti-H bond is based on the change in the C-H bond distance and of the frequency shift of its stretching vibration, both of which are opposite to those observed in conventional H-bonds involving C-H as proton donor (see Chapter 1.1.4).

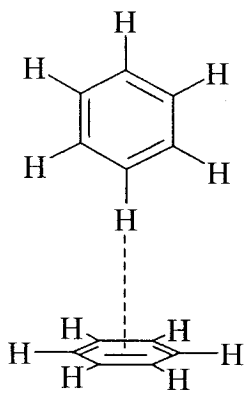

Fig. 1.4: Anti-H bond in the T-shaped benzene dimer.

The anti-H bond concept is not limited to the C-H---π interaction, and interactions involving proton acceptors such as oxygen and the halogens also exhibit this kind of

behaviour. C-H---O and C-H---F anti-H bonds have been reported in complexes such as ethylene oxide---fluoroform, methane---water, and in the difluoromethane dimer.[12]

1.1.3 Classification of hydrogen bonds

The classification of the H-bond as strong or weak was given by Jeffery and Saenger[3] in 1991 and was further refined as strong, moderate and weak by Jeffery in 1997.[1] H-bonds for electron deficient donor groups (O^+-H, -N^+-H) and for excess electron density acceptor groups (F^-, O^-) are termed strong H-bonds. These kinds of bonds are found in acid salts, HF complexes and in gas phase dimers with strong acids or strong bases.[1] Moderate hydrogen bonds are formed between neutral donor and acceptor groups (such as O-H, N-H), in which the donor atoms are more electronegative than the hydrogen atom and the acceptor atoms have unshared lone pair electrons. These moderate H-bonds are found in carboxylic acids, alcohols and phenols, to name a few, and so are considered "common" H-bonds. Weak H-bonds are formed between a hydrogen atom that is covalently bound to a slightly more electronegative atom, such as in C-H, and acceptor atoms with π electrons or with lone pairs. These H-bonds frequently occur in carbohydrates and peptides.[2] All H-bonds can be intramolecular or intermolecular.

1.1.4 Characterization of hydrogen and anti-hydrogen bonds

All H-bonds mentioned in 1.1.3 can be further classified based upon their energy, geometry and shift of the stretching frequency. The strength of a H-bond increases with an increase in the A-H bond dipole. Strong H-bonds exhibit an energy gain of 15-40 kcal/mol, moderate H-bonds 4-14 kcal/mol and weak H-bonds <4 kcal/mol.[1]

The geometrical characterization of a H-bond is based on the covalent bond distance of A-H, the hydrogen bond distance H---B, the heavy atom distance A---B and the A-H-B bond angle as illustrated in Table 1.1.

Table 1.1: Common distances (Å) and angle (degrees) of strong, moderate and weak hydrogen bonds.

	A-H---B interaction		
	Strong	Moderate	Weak
A-H	A-H ≈ H---B	A-H < H---B	A-H << H---B
H---B	~ 1.2 - 1.5	~ 1.5 - 2.2	2.2 - 3.2
A---B	2.2 - 2.5	2.5 - 3.2	3.2 - 4.0
A-H-B	175 - 180	130 - 180	90 - 150

Directionality is one of the important characteristics of H-bonds. Linear H-bonds are stronger than those with smaller H-bond angles A-H-B.[1] Small bond angles on hydrogen are believed to arise from van der Waals interactions, and a fundamental difference between weak H-bonds and van der Waals interactions is the directionality.[13]

Upon interaction, the A-H bond elongates due to a weakening of the bond. Conventional H-bonds with C, O, N and F as atoms A and B show this typical behaviour.[1] On the other hand, anti-H bonds show the opposite effect, i.e. upon interaction the A-H bond shortens.[10-12] This kind of behaviour was observed in the T-shaped benzene dimer and the other complexes listed in 1.1.2. In conventional hydrogen bonding, elongation of the A-H bond increases the dipole-dipole attraction between

proton donor and proton acceptor, and so the dominant contribution to the stabilization energy is the electrostatic interaction. In contrast, the London dispersion energy has been suggested to be the dominant stabilization energy in the anti-H bond.[12]

Such increases and decreases of A-H bond distances are associated with a change in frequency shift of the A-H bond. In conventional hydrogen bonding, the absorption bands of the H-bonded A-H stretching vibrations, ν(A-H), are shifted to lower frequencies with respect to that of the non-interacting A-H (red shift). In contrast, for an anti-H bond, the absorption bands of the H-bonded A-H stretching vibrations are shifted to higher frequency (blue shift). The first such blue shift was observed in the IR spectra of triformylmethane in chloroform in 1989 by Budesinsky et al.[12] The authors detected a sharp band close to the C-H stretch of chloroform but slightly shifted towards higher frequency.[12]

1.2 Computational methods

Computational methods have become reliable tools in the study of H-bonds. These methods are based on a quantum chemical approach.[14] Quantum chemical characterization provides information in terms of interaction energy, geometry, frequency shift, and electron density.[4]

A proper description of the energy and the geometry is necessary to predict various properties of the molecule. A geometry optimization is an iterative process performed on the molecule to find a stable atomic arrangement on a potential energy surface (PES). The PES is the mathematical relationship between the molecular geometries and their corresponding energies. A stable arrangement on PES is a point where the forces are zero and is called a stationary point. A geometry optimization does not indicate the nature of

the stationary point, that is, whether it is a minimum or a saddle point. For this purpose, a frequency calculation is performed on the optimized geometry, taking the second derivative of energy with respect to the atomic position. It determines whether the observed geometry is a minimum (no imaginary frequencies) or a transition state (one imaginary frequency). These frequency calculations are based on the harmonic oscillator approximation. Since molecules always have some vibrational motion even at zero temperature, it is necessary to add the zero-point vibrational energy (ZPVE) correction to the total energy of the optimized geometry. All these properties are predicted by performing calculations using different methods and basis sets.

A computational method that does not rely on experimental values is an ab initio method. The Hartree-Fock (HF) method is one of the simplest ab inito methods whose approximation is based on the wave function. This approximation considers the electron-electron interaction as an average interaction, i.e. an electron experiences all remaining electrons via an average field. As a result of this, HF is not accurate enough for some purposes. Another important approach that includes electronic interactions is known as density functional theory (DFT) method. In the DFT approximation, the energy of an electronic system is expressed in terms of the electron density.[14] B3LYP (Becke's three-parameter exchange functional[14,15] with the Lee-Yang-Parr correlation functional[16]) is one of the popular DFT methods and it has proven useful for the description of H-bonded molecules.[17-20]These methods are combinded with a basis set, the mathematical representation of the atomic orbitals. Special notations have been developed to denote these basis sets such as 6-31+G(d), 6-311+G(d,p).[14]

1.3 Substituent effects

In general, the introduction of substituents can lead to structural as well as reactivity changes in organic molecules. Substituents which are introduced near the reaction center and which are not directly involved in the considered reaction are capable of bringing about electronic perturbations in these molecules.[21] Similarly, substituents can have a substantial effect on the geometries and interaction energies of H-bonded molecules through changes in acidities and basicities of proton donor and proton acceptor atoms. These changes depend on the substituent's nature and position.

1.3.1 The Hammett substituent constant

The effect of the nature as well as the position of substituents on the reactivity of organic molecules was first observed in the ionization of meta (m-) and para (p-) substituted benzoic acid in water at 25°C.[21] On this basis, Hammett introduced an equation, expressed in Equation (1).

$$\log(\frac{K_X}{K_H}) = \rho\sigma_X \qquad (1)$$

K_H and K_X are equilibrium constants for the unsubstituted (or hydrogen substituted) (H) and substituted (X) systems, respectively, σ_X is the substituent constant and ρ is the reaction constant under a given set of conditions. This equation is known as the Hammett equation and is obeyed by a number of reactions which take place at or near a benzene ring on which substituents are located at meta and para positions. The sign and magnitude

of σ for a substituent group describe its capacity to perturb its electronic environment. Electron-donating groups (EDGs) are characterized by negative σ values whereas electron-withdrawing groups (EWGs) have positive values. But σ values also differ according to the position of the substituents on the aromatic ring. For example, for m-methoxy, σ_m = +0.10 (electron-withdrawing), for p-methoxy, σ_p = -0.12 (electron-donating). Depending on the system or reaction, other substituent constants have been proposed, e.g. σ+. This constant is employed for reactions where the X group can enter into direct resonance with the group that is the site of the reaction. Normally a substituent induces two different types of electronic effects, an inductive and a resonance effect.

Inductive effects occur due to the electronegativity of atoms and the dipoles of the functional groups. Substituents such as NO_2, CN and halogens are inductively electron-withdrawing whereas alkyl groups are inductively electron-donating.[22]

Resonance effects occur through p-orbital overlap with the π electrons of the aromatic ring. For many substituents this effect is greater when they are in para rather than in meta position. In substituents such as NO_2 and CN, aromatic π electrons can be delocalized onto the substituents. On the other hand, OH, OMe and NH_2 substituents activate the aromatic ring through electron donation.

Substituent constants have been widely used to interpret substituent effects in a variety of molecules.[23-25] In these studies, the constants are correlated with different parameters such as frequency shifts, bond distances and atomic charges to explain the effect of the substituent (X). In all cases, linear correlations were observed, which indicate the direct relationship between the nature of the substituent and the observed parameter.

For H-bonded molecules, several studies have shown the effect of substituents on the interaction energies of various molecular systems.[26-29] Kawahara et al. investigated the effect of substitution on H-bond energies of Watson-Crick type base pairs. The authors showed how the stabilities of the base pairs increased or decreased through the introduction of EDGs and EWGs. Ahn et al. have shown the effect of para and ortho substituents on hydrogen bonding in phenol-water complexes.[29] The authors found that in para substituted complexes, inductive and resonance effects influence the binding energy. In contrast, for ortho substituted complexes, a direct involvement of the substituent and a geometry change of the H-bond are responsible for the changes in binding energy. EWGs and EDGs show opposite trends.

1.3.2 The isodesmic reaction approach

An isodesmic reaction is a balanced chemical equation in which the number of formal chemical bonds of each type is conserved but the relationship between bonds is altered.[30] The energy difference from the isodesmic reaction can provide insight into stabilization or destabilization of the substituted molecules. An example of an isodesmic reaction is shown in Scheme 1.1.

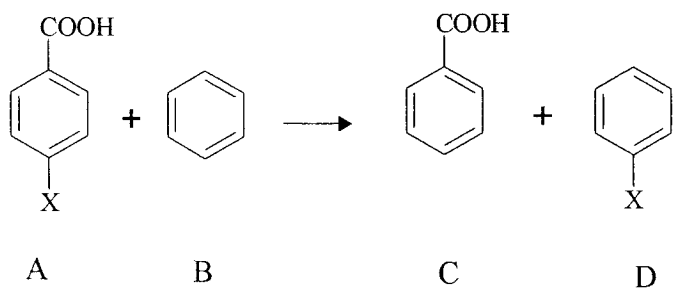

Scheme 1.1: Isodesmic reaction for p-substituted benzoic acids

From Scheme 1.1, the isodesmic reaction energy is calculated as the energy difference between products C and D and reactants A and B as illustrated in Equation 2.

$$\Delta E = [(E(C) + E(D)) - ((E(A) + E(B))] \quad (2)$$

Generally, if a substituted reactant of one type is more stable than the substituted product of another type, the isodesmic reaction is endothermic. On the other hand, if a substituted product of one type is more stable than the substituted reactant of another type, it is exothermic.

1.4 Methodologies

1.4.1 Supermolecular approach

The interaction between two molecules A and B leads to a complex A---B, which can be represented by Equation (3).

$$A + B \rightarrow A----B \quad (3)$$

In the supermolecular approach, the interaction energy (ΔE_{inter}) is calculated as the energy difference between the complex and the sum of the isolated individuals (Equation (4)).[4,14]

$$\Delta E_{inter} = E(A----B)_{(A---B)} - \left[E(A)_{(A)} + E(B)_{(B)}\right] \quad (4)$$

The interaction energy is determined by the strength of the H-bonds. It varies from 2-40 kcal/mol depending on the type of the H-bonds.[1] For most complexation reactions, the complex is more stable than the isolated monomers, so the process is exothermic and ΔE_{inter} is negative.[4] The main drawback of this approach is that computationally it suffers from the basis set superposition error (BSSE). A BSSE arises due to an artificial stabilization of the complex. An approximate way to evaluate this effect is to use the counterpoise method.[4,31] In this method, the calculation of $E(A)_{(A---B)}$ is carried out in the presence of the normal basis function of the complex but without the nuclei and electrons of B and same is true for B. Such functions are referred to as ghost orbitals. The BSSE is estimated as the difference between monomer energies with the regular basis and the energies calculated with the normal basis functions of the complex.[14] The BSSE is not important for sufficiently large basis sets.

1.4.2 Topological analysis of the electron density

The electron density $\rho(r)$ of a molecule provides information about the electronic distribution within the molecule, which allows for an understanding of all molecular properties. The quantum theory of "atoms in molecules" (AIM) analyses $\rho(r)$ in terms of its topology. The topology is described by the number and kinds of critical points.[32,33] Critical points (CP) are the points where the first derivative of $\rho(r)$ vanishes, ($\nabla\rho(r) = 0$), thus they determine the positions of extrema as maxima, minima or saddle points. Each CP is labeled by rank (ω) and signature (σ) as (ω, σ). A (3, -3) CP has three negative curvatures and it occurs at nuclear positions. A (3, -1) CP has two negative curvatures and one positive, is found between every pair of interacting nuclei and in a minimum geometry, is known as a bond critical point (BCP). Connecting all (3, -1) to their

respective (3, -3) CPs produces the molecular graph. Fig. 1.5 displays all the BCPs of ethene. A (3, +1) CP is a ring CP, has two positive curvatures and one negative, and is bounded by a ring of BCPs. Gradient vectors that terminate at a BCP span the interatomic surface. An atom is then defined as the unity of a (3, -3) CP and its basin, the area enclosed by the interatomic surfaces. Integration of $\rho(r)$ over a basin determines, e.g., an atom's volume, energy and charge.

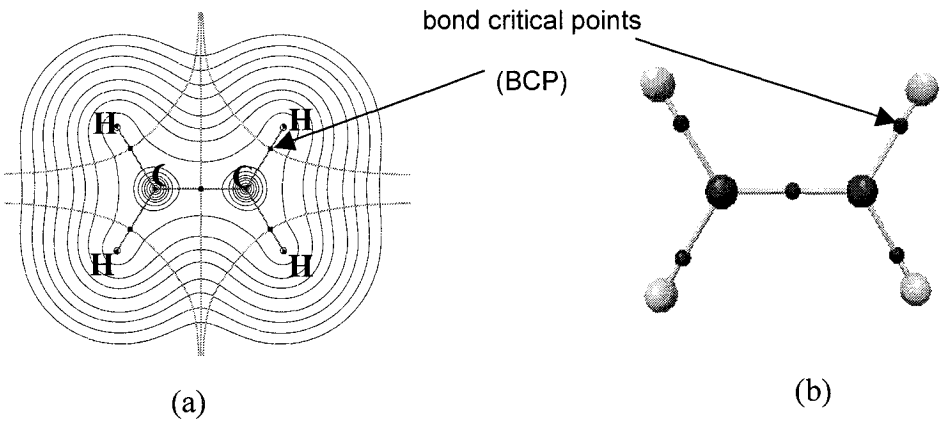

Fig. 1.5: Molecular graphs of ethene. (a) Contour plot of $\rho(r)$ with interatomic surfaces and bond paths, (b) AIM 2000 representation. Only one BCP is identified in each.

Within the framework of AIM, eight criteria have been proposed for the proper characterization of H-bonds.[32-34] (1) The presence of a bond critical point at the H---B. (2) The value of $\rho(r)$ at this BCP should lie in the range of 0.01 to 0.23 e/Å^3.[34] (3) The positive value of $\nabla^2\rho(r)$ should lie in the range of 0.58 to 3.35 e/Å^5. (4) A mutual penetration of the electron density of the hydrogen and acceptor atoms. The penetration is

defined as the difference between the non-bonded and bonded atomic radii ($\Delta r = r^0 - r$). It was found that the hydrogen is penetrated more if it belongs to a soft acidic group, such as C-H, compared with a hard one, such as F-H.[34,35] The range of penetration for both acceptor and donor atoms varies from 0.42-1.48 au.[35] Another set of criteria comprises the integrated atomic properties of the hydrogen atom involved in hydrogen bonding. (5) Loss of charge of the hydrogen atom upon formation of the hydrogen bond (from 0.003-0.075 au).[36,37] (6) Energetic destabilization of the hydrogen atom (from 0.003-0.039 au).[34] (7) Decrease in the dipolar polarization of the hydrogen atom (from 0.008-0.038 au).[35] (8) Decrease in the atomic volume of the hydrogen atom (from 2.45-13.03 au).[34,35]

1.4.3 Solvent effect

The study of solvent effects is important to understand solute-solvent interactions. It is well known that solute-solvent interactions can have substantial impact on the properties of molecules, especially on H-bonded systems.[38] SCRF (self-consistent reaction field) theory is one of the commonly used methods that models the solvent as a continuum of uniform dielectric constant ε, the reaction field.[14,39,40] The solute is treated as embedded in a cavity surrounded by the medium. SCRF approaches differ in how they define the cavity, the reaction field and the interaction between them.

The conductor-like screening model (COSMO) is one of the continuum methods which use a simple, approximate equation for the electrostatic interaction between the solvent and the solute. The optimization is based on the screening in conductors. COSMO was first described in detail at the semiempirical SCRF level by Klampt and Schuurmann in 1993.[41]

Chapter 2

Historical background to N-phenyl-N'-sulfinylhydrazine and objectives and organization of Chapters 3, 4 and 5

N-phenyl-N'-sulfinylhydrazine (PhNHNSO) was first synthesized in 1889 by Michaelis,[42] and substituted derivatives are used as pesticides and crop-control agents.[43] Only several decades after the first synthesis in 1977, the first X-ray structure analysis was carried out by Gieren and Dederer.[44] The compound was crystallized from anhydrous ethanol. It was revealed that PhNHNSO is roughly planar and in the crystalline state forms a dimer in which the two molecules are linked by two N-H---O=S hydrogen bonds. In addition, the presence of intramolecular H---O bonds was suggested. The hydrogen and oxygen atoms would thus act as two fold donors and acceptors, which would result in bifurcated H-bonds as shown in Fig. 2.1.

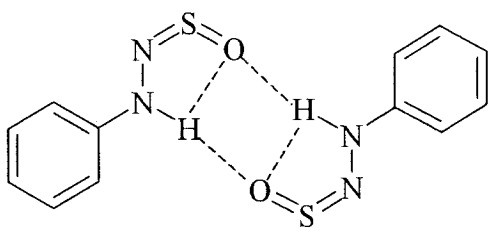

Fig. 2.1: Predicted H-bond network in PhNHNSO from X-ray and neutron diffraction studies.[44,45]

The reported inter- and intra-molecular H---O distances were 213 pm and 243 pm, respectively. In 1984, a neutron diffraction study was carried out by Schanda and Gieren that seemed to support the earlier results.[45] H-bond formation was confirmed in 2001 in a

spectroscopic study using Fourier Transform Infrared (FTIR) spectroscopy,[46] which showed a red shift of the frequency of the N-H stretching vibration upon dimerization. Upon introduction of a chloro substituent in the ortho position, no frequency shift was observed in a series of dilution spectra, which seemed to indicate that the o-chloro PhNHNSO did not dimerize.[46] On the other hand, introduction of a substituent in meta or para position led to a red shift of the frequency of the N-H stretching vibration.[47]

The experimental observations of the differences in dimerization behaviour for the unsubstituted and substituted PhNHNSO compounds raise questions about the existence and patterns of H-bonds in the PhNHNSO system. We took the opportunity to explore these compounds in detail computationally to find an explanation for the observed phenomena.

The overall objective of this study is to investigate the molecular geometry, structure and stability of PhNHNSO, its substituted derivatives, and their dimers. There are three main objectives.

The first objective is to investigate the possible configurations of the unsubstituted PhNHNSO monomer (Fig. 2.2) and its dimer with available computational methods, as well as to identify and characterize all weak interactions in the systems.

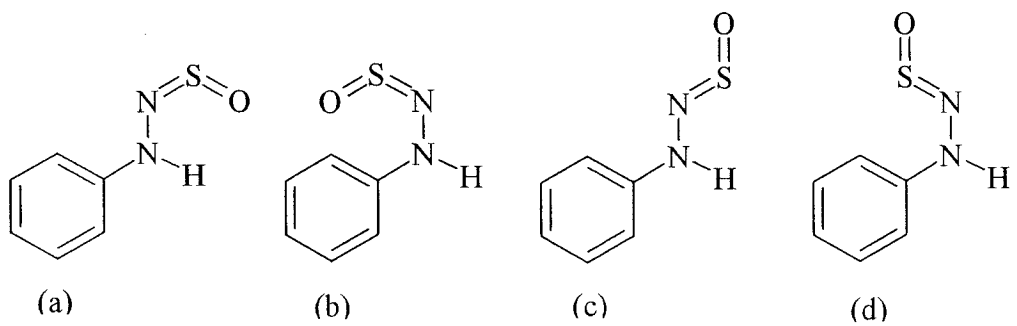

Fig. 2.2: (a) *Syn*, (b) *sickle*, (c) *anti1* and (d) *anti2* configurations of PhNHNSO.

The second objective is to investigate substituent effects on N-H, ortho C-H and S=O bonds in the substituted monomers. The substituted monomers to be investigated are given in Fig. 2.3.

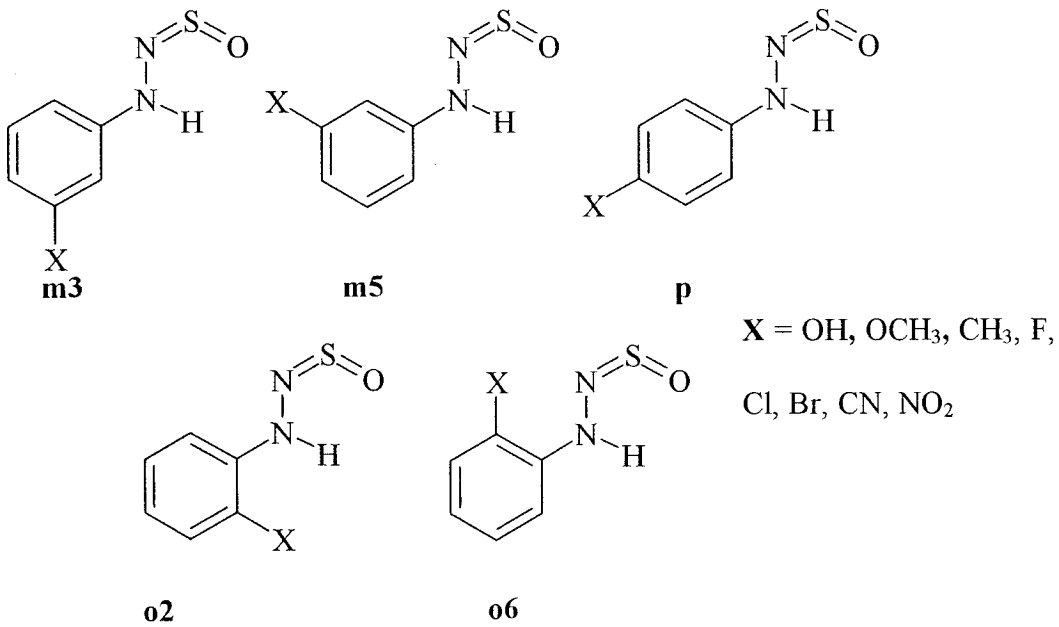

Fig. 2.3: Substituted PhNHNSO compounds to be studied and their notation.

The third objective is to analyze chloro and methyl substituted PhNHNSO dimers in terms of their relative stability and solvent effects onto such stabilities.

This thesis is based on three manuscripts, following the three objectives, which are described briefly in the following and compiled in Chapters 3, 4 and 5.

2.1 The hydrogen bonding network in the dimer of the syn-N-phenyl-N'-sulfinylhydrazine

To be submitted: Journal of Physical Chemistry A

Authors: Pratibha Malla and Heidi M. Muchall

Contribution by P.M.: Carried out all calculations and analyses of experimental and computational data, and wrote first draft of the manuscript

Other contributions: Synthesis and FTIR studies by D. Marion[46] and D. J. Zhang,[47] to be acknowledged in the manuscript

Summary:

N-phenyl-N'-sulfinylhydrazine (PhNHNSO) has been analyzed with spectroscopic and computational methods. Experimental infrared spectra show a red shift of the frequency of the N-H stretching vibration from monomer to dimer, confirming the presence of N-H---O hydrogen bonding interactions. Computational investigations of the monomer with HF and B3LYP methods and different basis sets revealed the preference of the *syn* configuration over *sickle* and *anti* forms. An electron density analysis within the framework of the quantum theory of atoms in molecules at the B3LYP/6-31+G(d) level revealed the presence of intramolecular N-H---O interactions in the *syn* configured monomer and intermolecular N-H---O and C-H---O interactions in the dimer. The intermolecular N-H---O and C-H---O interactions are identified as hydrogen and anti-hydrogen bonds, respectively.

2.2 The influence of substituents on hydrogen bond forming bonds in N-phenyl-N'-sulfinylhydrazine

To be submitted: Journal of Physical Chemistry A

Authors: Pratibha Malla and Heidi M. Muchall

Contribution by P.M.: Carried out all calculations and analyses of experimental and computational data, wrote first draft of the manuscript

Other contributions: Synthesis and FTIR studies by P. Napoli[48] and A. Bernardi[49] to be acknowledged in the manuscript

Summary:

For a series of substituted phenylsulfinylhydrazines PhNHNSO at the DFT (B3LYP) level, it was found that meta and para substituted compounds are more stable than their ortho substituted analogues. Substituents such as NO_2 and CN have a greater effect on geometries, frequencies, electron densities, atomic charges of N-H, ortho C-H and S=O than OCH_3 or OH substituents. The geometries, frequencies and electron densities of N-H, ortho C-H and S=O bonds are more affected by ortho than by meta or para substitution. The S=O bond length showed excellent linear correlation with both stretching frequency and electron density at the bond critical point. N-H and ortho C-H bonds, on the other hand, failed to show good correlation independent of basis set size (6-31+G(d), 6-311+G(2d,p), and cc-pVTZ). The strong electron-withdrawing substituents NO_2 and CN give shorter distances, larger frequencies and higher electron densities as compared to electron-donating substituents, and linear correlations with Hammett substituent constants for S=O and N-H bonds are revealed.

2.3 Chloro and methyl substituted N-phenyl-N'-sulfinylhydrazines: experimental and computational analyses

To be submitted: Journal of Physical Chemistry A

Authors: Pratibha Malla and Heidi M. Muchall

Contribution by P.M.: Carried out all calculations and analyses of experimental and computational data, wrote first draft of the manuscript

Other contributions: Synthesis and FTIR studies by P. Napoli[48] and A. Bernardi[49] to be acknowledged in the manuscript

Summary:

Experimental and computational analyses of chloro and methyl substituted PhNHNSO dimers were carried out. FTIR spectra suggested the presence of intermolecular interactions in meta and para substituted PhNHNSO dimers and their absence with ortho substituted monomers. An electron density analysis suggested the presence of intermolecular N-H---O and C-H---O interactions in all dimers, except for ortho2 substituted dimers which exhibit only N-H---O interactions. The N-H---O and C-H---O interactions are not greatly influenced by meta and para substituents. In contrast, ortho substituents greatly influence the N-H---O interactions, and ortho dimers show weaker intermolecular interactions than the other dimers. Based on the obtained data, it is evident that dimerization of ortho substituted PhNHNSO monomers is unfavourable, which is consistent with the experimental results.

Chapter 3

The hydrogen bonding network in the dimer of the syn N-phenyl-N'-sulfinylhydrazine

3.1 Introduction

The most prominent weak interaction, the hydrogen bond (H-bond), has been the subject of active research due to its key role in various chemical and biological systems.[1,3,4,50] A growing number of experimental and computational studies have focused on the classification of H-bonds.[51-54] The most well-known type is the conventional H-bond, defined as A-H---B where A and B are electronegative atoms such as nitrogen, oxygen or fluorine. Another type is the improper blue-shifting or anti-H bond, usually C-H----B, where B is either an electronegative atom carrying one or more electron lone pairs or a region of excess electron density (π electrons of an aromatic system).[10,36,55] The basis for the experimental detection of a conventional H-bond is the red shift (shift to smaller frequency) of the frequency of the A-H stretching vibration upon H-bond formation. A blue shift of the frequency of the C-H stretching vibration would allow the detection of an anti-H bond.[10,12,36]

N-phenyl-N'-sulfinylhydrazine (PhNHNSO) is known to form H-bonded dimers in the crystalline state. The first X-ray structure analysis of PhNHNSO by Gieren and Dederer revealed two monomers with *syn* configuration linked by two intermolecular N-H---O=S H-bonds (Fig. 3.1).[44] Each monomer was suggested to possess an additional intramolecular N-H---O bond (Fig. 3.1). In this structure, both hydrogen and oxygen atoms would thus act as two-fold donors and acceptors, resulting in bifurcated H-bonds and a four-membered ring structure. A later neutron diffraction study by Schanda and

Gieren seemed to support the earlier result.[45] In a recent study, we have shown that the SO bond in CH_3NHNSO is best described as a four electron bond and thus resembles the carbonyl C=O bond.[56] In this respect and with regard to possible H-bonding patterns, the NHNSO fragment might be treated as an extended NHCO, i.e. amide, fragment. While the cyclic amide dimer comprises an eight-membered ring structure, the cyclic sulfinylhydrazine dimer could simply form a ten-membered ring, without the need for bifurcation on the hydrogen atoms.

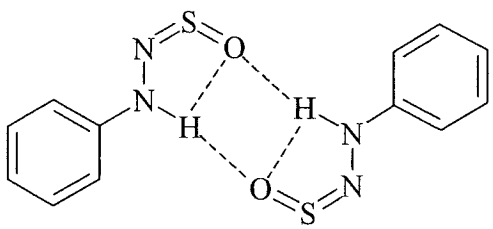

Fig. 3.1: H-bonding network in the PhNHNSO dimer as suggested from diffraction studies.[44,45]

The quantum theory of atoms in molecules (QTAIM) is a powerful method for the identification and characterization of H-bonds through a topological analysis of the electron density, $\rho(r)$ It has been used successfully for a variety of H-bonded systems.[55,34,35,37,57-60] Within the framework of AIM, eight criteria have been proposed for the detection and characterization of H-bonds.[32,34] These criteria comprise (1) the presence of a (3,-1) bond critical point (BCP) for the H---B pair and its associated bond path, (2) a low value of $\rho(r)$ at this BCP (3) a positive value of the Laplacian ($\nabla^2\rho(r)$) at the BCP, (4) the mutual penetration of the van der Waals envelop of both hydrogen and

acceptor (B) atom, (5) a loss of charge (q) of the hydrogen atom, (6) an energetic (E) destabilization of the hydrogen atom, (7) a decrease in the dipolar polarization (M) of the hydrogen atom, and (8) a decrease in the atomic volume (V) of the hydrogen atom. These criteria have been shown to hold for various H-bonds, anti-H bonds and dihydrogen bonds.[36,55,12,34,37,60,61]

The present study focuses on the detection and characterization of weak interactions in the PhNHNSO system using FTIR spectroscopy and density functional theory calculations, and topological analyses of the electron density within the quantum theory of atoms in molecules.[32,33] We show that not only was the proposed[44,45] H-bonding network in the dimer incorrect, but that bifurcation on oxygen leads to the formation of C-H---O anti-H bonds that play an important role in the overall stabilization of the dimer.

3.2 Experimental section

PhNHNSO was synthesized as described by Pearce et al.[62] The compound was recrystallized from ethanol and further purified by sublimation.

Infrared spectra were recorded at room temperature using a Nicolet-Impact 400 FTIR spectrophotometer. Solution studies were performed with a 0.1 mm spacer in a KBr liquid sample cell. At least 36 scans were collected in the 4000-400 cm^{-1} range.

3.3 Computational details

All calculations were performed using the Gaussian 98 package.[63] The different configurations of the monomer were optimized with Hartree-Fock (HF)[14] using 6-31+G(d) and 6-311+G(2d,p) basis sets. Electron correlation was taken into account with optimization at the density-functional theory (DFT) level using the Becke three-parameter exchange functional[14,15] with the Lee-Yang-Parr correlation functional[16]

(B3LYP) with 6-31+G(d) and 6-311+G(2d,p) basis sets. B3LYP has been shown to perform well in similar H-bonding studies.[17,19,64,65] All geometries were confirmed as true minima via vibrational frequency analyses. HF and DFT frequencies are reported scaled (see below). Based on the comparison of calculated and experimental frequencies of the N-H stretching vibration, and for computational feasibility, B3LYP/6-31+G(d) was chosen as an appropriate level of theory for the dimer investigation. The dimer was optimized without symmetry constraints. The interaction energy was calculated using the supermolecular approach, which determines the interaction energy as the energy difference between the dimer and the corresponding monomers.[14,50] The interaction energy thus obtained suffers from the basis set superposition error (BSSE). The BSSE was estimated by performing a single point calculation using the counterpoise method introduced by Boys and Bernardi.[31] Wave functions were obtained for the topological analysis of the electron density within the quantum theory of atoms in molecules (QTAIM).[32,33] All analyses were performed using AIMPAC,[66,67] the molecular graph of the dimer was plotted with AIM2000.[68] Single point calculations were performed with B3LYP/6-31+G(d) for solvent effects, employing the self-consistent reaction field theory (SCRF) method with COSMO (conductor like screening model).[41]

3.4 Results and discussion

3.4.1 Vibrational spectra

The IR spectrum of PhNHNSO was obtained neat in KBr and in three different organic solvents (CCl_4, $CHCl_3$, CH_2Cl_2) with different polarities. In the N-H stretching (ν(N-H)) region, the spectrum of the neat PhNHNSO shows only one broad absorption band at 3208 cm^{-1}, whereas all solution spectra exhibit two bands whose relative

intensities vary with the concentration and the solvent. The positions of the bands, given in Table 3.1, seem to be more or less unaffected by either concentration or solvent. As expected, while the band for the hydrogen bonded N-H stretch at 3211 cm^{-1} dominates in CCl_4 for a given concentration, it is the band from the non-hydrogen bonded N-H stretch at 3275 cm^{-1} that dominates the spectrum in CH_2Cl_2 at the same concentration. For $CHCl_3$ and CH_2Cl_2, the hydrogen bonded species is not detectable below concentrations of 0.01 mol/L. Similar dilution studies were performed earlier for the related N-ethylacetamide, which also forms dimers in the solid.[69] It was reported that in $CHCl_3$ and CH_2Cl_2, a hydrogen bonded ν(N-H) band is not detectable at a concentration of 0.04 mol/L, suggesting that the dimer of PhNHNSO is more stable than that of the amide. A possible reason is suggested from a change in the position of the H-bonded ν(N-H) band with both concentration of the amide solution and solvent. The band shift between H-bonded and non-bonded ν(N-H) in CCl_4 varied from 150 cm^{-1} for the more concentrated solution to 100 cm^{-1} at a higher dilution, suggesting more than one type of H-bonded network between amides in solution, such as cyclic and less stable acyclic species.[69] In contrast to N-ethylacetamide, in the case of γ-butyrolactam, the position of the hydrogen bonded ν(N-H) band remained constant over a range of concentrations, indicating only one type of H-bonded species.[69] As for the PhNHNSO system we also observe a more or less constant position for the H-bonded ν(N-H) band, we conclude the presence of only one kind of (cyclic) PhNHNSO dimer in the solid and in solution. This is in agreement with the cyclic dimer reported in diffraction studies.[44,45] While acyclic amides such as N-ethylacetamide exist in an E/Z equilibrium that allows for both cyclic and acyclic H-bonded dimers, γ-butyrolactam is fixed in its configuration and is thus predisposed to

form cyclic dimers. This would lead us to conclude that the acyclic PhNHNSO only has one configuration available at room temperature.

Table 3.1: Frequency (cm^{-1}) of the N-H stretching vibration of neat PhNHNSO and in CCl_4, $CHCl_3$ and CH_2Cl_2 solution. Concentration in mol/L.

	M	Free N-H	H-bonded N-H
Neat			3208
CH_2Cl_2	0.01	3275	-
	0.05	3275	3210
	0.1	3275	3211
	0.25	3275	3212
	0.5	3274	3212
	0.9	3274	3212
$CHCl_3$	0.01	3277	-
	0.05	3277	3210
	0.1	3277	3211
	0.25	3277	3212
	0.5	3277	3212
	0.9	3276	3212
CCl_4	0.01	3277	3212
	0.05	3277	3211
	0.1	3277	3211
	0.25	3276	3211

3.4.2 PhNHNSO Monomer

3.4.2.1 Energies and geometries

Four different configurations/conformations were considered for the PhNHNSO monomer, *syn*, *sickle*, *anti1* and *anti2* (Fig. 3.2), and all four proved to be minima.

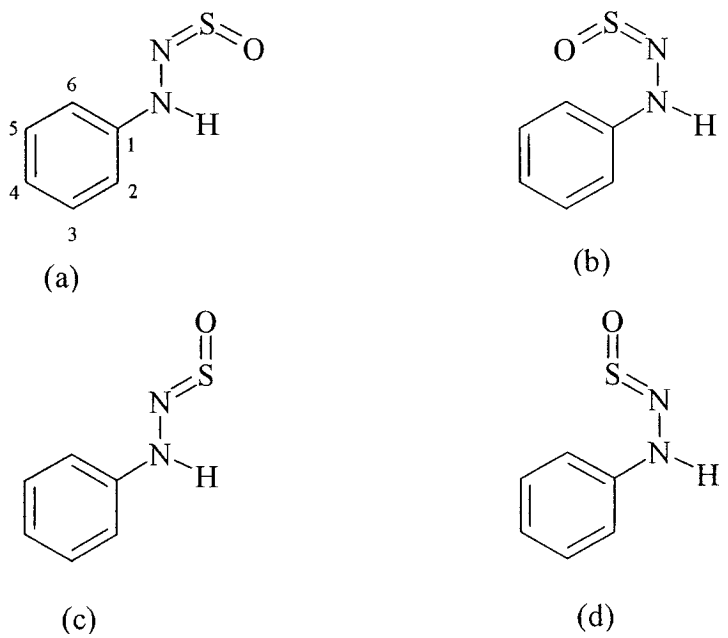

Fig.3.2: Configurations of the PhNHNSO monomer: (a) *syn*, (b) *sickle*, (c) *anti1*, (d) *anti2*.

The zero-point vibrational energy (ZPVE) corrected total energies and the relative energies of the four configurations/conformers of PhNHNSO are summarized in Table 3.2. As suggested from the diffraction studies of PhNHNSO in the solid,[44,45] *syn* is found to be by far the most stable configuration/conformer at all levels of theory. *Sickle* and *anti* forms have relative energies of 10 kcal/mol or more, and therefore are not populated in

contrast to the E/Z equilibrium found for amides[70] and in accord with our FTIR study.

Table 3.2: ZPVE corrected total energies (au) of four configurations of the PhNHNSO monomer. Relative energies (kcal/mol) are given in parentheses.

	syn	*sickle*	*anti1*	*anti2*
HF/6-31+G(d)	-811.761211	-811.742879	-811.738397	-811.731878
	(0)	(11.5)	(14.3)	(18.4)
HF/6-311+G(2d,p)	-811.907028	-811.890345	-811.886205	-811.880368
	(0)	(10.5)	(13.1)	(16.7)
B3LYP/6-31+G(d)	-815.004304	-814.986605	-814.982479	-814.978550
	(0)	(11.1)	(13.7)	(16.2)
B3LYP/6-311+G(2d,p)	-815.155494	-815.138855	-815.135058	-815.131698
	(0)	(10.4)	(12.8)	(14.9)

Table 3.3 presents selected geometrical parameters of *syn*, *sickle*, *anti1* and *anti2* at the B3LYP/6-31+G(d) level of theory; all are fully planar. As expected, changes in bond distances and bond angles between the configurations are observed but some bond angles change rather dramatically. The S=O and N-H bond lengths of the *syn* are longer than those of the other configurations, which is an indication of a possible intramolecular N-H---O interaction in *syn*, as suggested from diffraction studies of the dimer.[44,45] Such an interaction could be a weak H-bond, or simply an interaction between N-H and S=O bond dipoles. S=O and N=S bond lengths of the *syn* configuration are longer than those found in PhNSO[55] and the NSO bond angle is decreased by 10° (119.8° in PhNSO), all further indications for some possible intramolecular N-H---O interaction in *syn*.

Table 3.3: Selected geometrical parameters (distances in pm, angles in degrees) of four configurations of PhNHNSO from B3LYP/6-31+G(d).

	syn	*sickle*	*anti1*	*anti2*
S=O	151.7	150.4	149.6	149.6
N=S	160.8	157.8	160.4	160.0
N-N	131.4	131.9	132.5	132.6
N-H	102.6	101.4	102.0	101.3
N-C	140.4	141.7	140.5	140.3
C2-H	108.8	-	-	-
(N)H---O	215.7	-	-	-
(C)H---O	-	205.5	-	-
NSO	110	122	111	109
NNS	116	139	120	128
NNH	117	110	121	111
N-H---O	112	-	-	-
C-H---O	-	152	-	-
NNSO	0	0	180	180
CNNS	180	0	180	0

It is remarkable that a planar *sickle* configuration results upon torsion of the CNNS dihedral. In order to accommodate all atoms in plane, NSO and especially NNS bond angles open up significantly. This behaviour might point to the importance of π-conjugation in the monomer. It might also be attributed to the presence of a stabilizing C-

H---O interaction in the planar *sickle* (see below)[#]. *Anti1* and *anti2*, related through the same torsion of the CNNS dihedral, show only small changes in their geometries, with the possible exception again of the NNS bond angle. As in *sickle*, this is larger in *anti2*, exhibiting again the rather unexpected performance of a change in bond angle over a torsion. Geometrical parameters for *syn* at HF/6-31+G(d), HF/6-311+G(2d,p) and B3LYP/6-311+G(2d,p) can be found in Table A.1 (Appendix A). Noteworthy here is the larger (N)H---O distance of 222.6 pm with B3LYP/6-311+G(2d,p), whose implications are discussed below.

3.4.2.2 Frequencies

To select a model chemistry that would give reliable results for the PhNHNSO system at a reasonable cost, we compared the calculated, scaled frequencies for the N-H stretching vibration of the *syn*, *sickle*, *anti1* and *anti2* monomers with those obtained experimentally from a dilute sample in CH_2Cl_2.

We used mainly scaling factors from Scott and Radom,[71] even though only the one for HF/6-31+G(d) (0.8970) given in the paper fit our needs exactly. We decided that those for HF/6-311G(d,p) (0.9051) and B3LYP/6-31G(d) (0.9614) were adequate for our purposes, which thus were used for HF/6-311+G(2d,p) and B3LYP/6-31+G(d), respectively. For B3LYP/6-311+G(2d,p), we followed the suggestion from Andersson and Uvdal[72] and used a factor of 0.9679. The calculated N-H stretching frequency (Table 3.4) of *syn* is substantially lower than that of *sickle* or either of the *anti* configurations, independent of the level of theory. In fact, with B3LYP/6-31+G(d), the calculated wave number of 3281 cm^{-1} for *syn* shows an excellent agreement with the experimental value

[#] A full account of the stabilizing factors in a variety of RNSO compounds will be given elsewhere.

of 3275 cm^{-1}. Thus, the presence of *sickle* and *anti* configurations in our FTIR experiment is ruled out from the frequencies as well as from the energies already discussed. It is obvious that the experimental value is not reproduced by either of the HF calculations. B3LYP/6-311+G(2d,p) calculations also overestimate the experimental value somewhat. We therefore chose B3LYP/6-31+G(d) for both its (fortuitous) accuracy and low computational cost for the dimer study.

Table 3.4: Scaled frequency[a] (cm^{-1}) of the N-H stretching vibration in four configurations of the PhNHNSO monomer.

	syn	*sickle*	*anti1*	*anti2*	Experimental
HF/6-31+G(d)	3383	3450	3411	3481	
HF/6-311+G(2d,p)	3431	3441	3429	3509	3275[b]
B3LYP/6-31+G(d)	3281	3433	3336	3446	
B3LYP/6-311+G(2d,p)	3338	3463	3379	3469	

[a] See text for scaling factors; [b] In solution.

The rather low value of the N-H stretching frequency of *syn* can be attributed to the relative orientation of N-H and S=O bonds. Previous reports suggested the presence of intramolecular N-H---O interactions in the H-bonded monomers,[44,45] and these might also be present in the non-interacting monomers. However, the experimental detection of such an intramolecular N-H---O interaction in the monomer would only be possible if a configuration with a non-interacting N-H bond was available for comparison, which would exhibit a completely free ν(N-H) band upon dilution. This approach has been

taken for the detection of an intramolecular C-H---O interaction in 1-methoxy-2-(dimethylamino) ethane.[73] But, as discussed above, neither *sickle* nor *anti* configurations are available experimentally.

3.4.3 PhNHNSO Dimer

3.4.3.1 Energies and geometries

Upon dimer formation, the energy of the system is lowered. At the B3LYP/6-31+G(d) level of theory, the ZPVE corrected interaction energy is -11.40 kcal/mol. The BSSE is small, 2 kcal/mol. This interaction is thus found to be of comparable strength with those reported for the cyclic formamide dimer[60,61] and for substituted adenine-uracil base pairs.[74] The free energy of dimer formation for PhNHNSO is just negative with -0.65 kcal/mol.

Experimentally we probed dimer formation through an FTIR dilution study in different solvents, or to put it differently, the extent to which dissociation into the monomers occurs in solvents of differing polarity. Field effects on monomer and dimer have been assessed computationally by embedding the system of interest in a polarizable solvent cavity. Table 3.5 presents the solvation free energies ΔG_{solv} and their total electrostatic contributions ΔG_{el} obtained for the solvents CCl_4, $CHCl_3$ and CH_2Cl_2 with COSMO at the B3LYP/6-31+G(d) level of theory.

As expected both ΔG_{solv} and ΔG_{el} become more negative with an increasing polarity of the solvent. Changes in ΔG_{el} are more linear than those in ΔG_{solv}. The larger change in ΔG_{solv} from $CHCl_3$ to CH_2Cl_2 is the cause of a much more negative free energy of repulsion and dispersion in CH_2Cl_2 for both monomer and dimer, leading to a large and

negative total non-electrostatic contribution to ΔG_{solv}. The ΔG_{solv} values in $CHCl_3$ agree well with those for acetic acid and its cyclic dimer, reported at the B3LYP/6-31G(d,p) level of theory.[75]

Table 3.5: Free energies of solvation, ΔG_{solv}, and their electrostatic contributions, ΔG_{el} (kcal/mol) of the *syn* PhNHNSO monomer and dimer in three solvents.

	CCl_4		$CHCl_3$		CH_2Cl_2	
	ΔG_{solv}	ΔG_{el}	ΔG_{solv}	ΔG_{el}	ΔG_{solv}	ΔG_{el}
Dimer	1.46	-1.84	-0.15	-2.71	-6.35	-3.05
syn	-2.39	-2.38	-3.88	-3.53	-7.72	-3.98

For all solvents, the sum of the solvation energies of the two monomers is larger than the corresponding solvation energy of the dimer, suggesting a stronger interaction of the monomers with the solvent. The difference in solvation energies (dimer minus twice the monomer values) becomes increasingly larger as the solvent polarity is increased, which is in accord with our experimental findings presented above. Furthermore, the positive ΔG_{solv} for the dimer in CCl_4 reflects its poor solubility we found experimentally [Table 3.1].

Selected calculated and experimental geometrical parameters of the PhNHNSO dimer are reported in Table 3.6. The arrangement of the monomers in the dimer is shown in Fig. 3.1. Since the dimer consists of two equivalent, but not identical monomers, the reported bond distances and bond angles are averaged over the two H-bonded monomers. Not unexpectedly, the calculated bond distances are mostly comparatively longer than

those determined experimentally.[45,46] However, N-N and N-C bond distances show good agreement with experiment. Intramolecular and intermolecular (N)H---O distances are 7-12 pm longer and 22.2-6.5 pm shorter, respectively, compared to experiment. All bond angles are well reproduced.

A comparison between the geometrical parameters of the *syn* monomer and its dimer shows that the formation of the H-bonds causes substantial changes in bond distances and bond angles (see Table 3.3 for the monomer data). As expected, the H-bond donor N-H bond in the dimer is elongated by 0.6 pm, which is comparably lower than the reported value of 1.7 pm for the N-H bond elongation of formamide at the B3LYP/6-311++G(d,p) level.[61] In accord with the formation of an intermolecular H-bond, the S-O bond, which contains the H-bond acceptor atom, is also lengthened, by 0.8 pm. Changes are observed for N-C, S-N and N-N bond lengths and more importantly, for the ortho C-H bond distance (Table 3.6). Upon dimerization, in contrast to the N-H bond, the C-H bond is shortened by 0.3 pm. This decrease suggests an anti-H bond nature of a possible C-H----O interaction as was found in PhNSO.[55]

Table 3.6: Selected calculated and experimental geometrical parameters (distances in pm, bond angles in degrees) of the PhNHNSO dimer.

	B3LYP/6-31+G(d)	X-ray[44]	Neutron diffraction[45]
S=O	152.5	147.4	146.7
S=N	159.7	156.0	156.5
N-N	130.5	131.2	131.6
N-H	103.2	87.0	101.8
N-C	141.2	140.0	140.4
C2-H	108.6	95.0	109.0
(N)H---O(intra)[a]	250.0	243.0	238.0
(N)H---O(inter)[a]	190.8	213.0	197.3
(C)H---O(inter)[a]	237.2	-	-
NNH	121	120	120
NSO	114	114	114
NNS	122	120	119
NNC	121	121	120
N-H---O(intra)[a]	103	-	104
N-H---O(inter)[a]	160	-	158
C-H---O(inter)[a]	138	-	-

[a] Intra and inter refer to intramolecular and intermolecular, respectively, distances and angles.

A noticeable change is observed for the intramolecular (N)H---O distance, which increases by 34.3 pm upon dimer formation. This increase could be taken as further support for a possible weak intramolecular N-H---O interaction in the *syn* monomer, which is lost in the dimer to allow for a more favourable alignment of the two intermolecular N-H---O interactions. The loss of any intramolecular N-H---O interaction in the dimer is corroborated by the decrease in the intramolecular N-H---O angle to 103°, which corresponds well with the increase in the N-H---O distance.

3.4.3.2 Frequencies

The experimentally observed red-shift of the N-H stretching vibration of 67 cm^{-1} upon PhNHNSO dimerization is well reproduced computationally. The calculated, scaled frequency of the IR-active asymmetric stretching vibration for the two N-H bonds in the dimer is located at 3189 cm^{-1}, which is in very good agreement with the experimental value (3208 cm^{-1}) and gives a calculated red shift of the N-H stretching vibration of 92 cm^{-1}. This finally allows the conclusion that the intermolecular N-H---O interactions in the cyclic dimer of PhNHNSO that are present in the solid can be disrupted upon dissolution to give the *syn* configured monomers.

The scaled frequency of the asymmetric stretching vibration of the two ortho C-H bonds of the dimer that are directed at the respective other monomer is located at 3097 cm^{-1}. With a scaled ν(C-H) for the monomer of 3059 cm^{-1}, this leads to a blue shift of 38 cm^{-1}, and, in agreement with the shortening of the C-H bond, corroborates the presence of

C-H---O interaction with anti-H bond nature.* The magnitude and direction of the calculated shift are comparable with those of other C-H---O bonded systems.[12]

3.4.4 Identification and characterization of the weak interactions

Fig. 3.3 depicts the contour maps of the electron density for *syn* and *sickle* monomers and for the dimer from B3LYP/6-31+G(d) wave functions. As suspected, the topological analysis reveals the presence of a BCP for the intramolecular N-H---O interaction in *syn* (Fig. 3.3(a)) and for the C-H---O interaction in *sickle* (Fig. 3.3(b)). Both are indicated through arrows in Fig. 3.3. The distance to their respective ring critical points, 29 pm for N-H---O and 111 pm for C-H---O, reveals that, while the C-H---O interaction in *sickle* is topologically rather stable, the intramolecular N-H---O interaction in *syn* will be lost upon a slight increase in the N(H)---O distance, as bond and ring critical points will annihilate each other.[32] This is indeed observed, both upon dimer formation (Fig. 3.3(c)) as well as with the use of B3LYP/6-311+G(2d,p) for *syn*. Thus, the appearance of a saddle point in Fig. 3.3(a) and with it the intramolecular N-H---O interaction is not an artifact of the level of theory chosen, but rather an indication of the very weak nature of the interaction.

As the optimized dimer is not planar, only one monomer and the oxygen atom of the second monomer are plotted in the plane in Fig. 3.3(c). For clarity, the complete molecular graph for the dimer with all four weak interactions is given in Fig. 3.3(d). The presence of the BCPs for both intermolecular N-H---O and C-H---O interactions indicates the occurrence of bifurcated H-bonds on the acceptor atom.

---

*Both normal modes consist mainly of the vibrations of interest, with only small contributions from other C-H bonds.

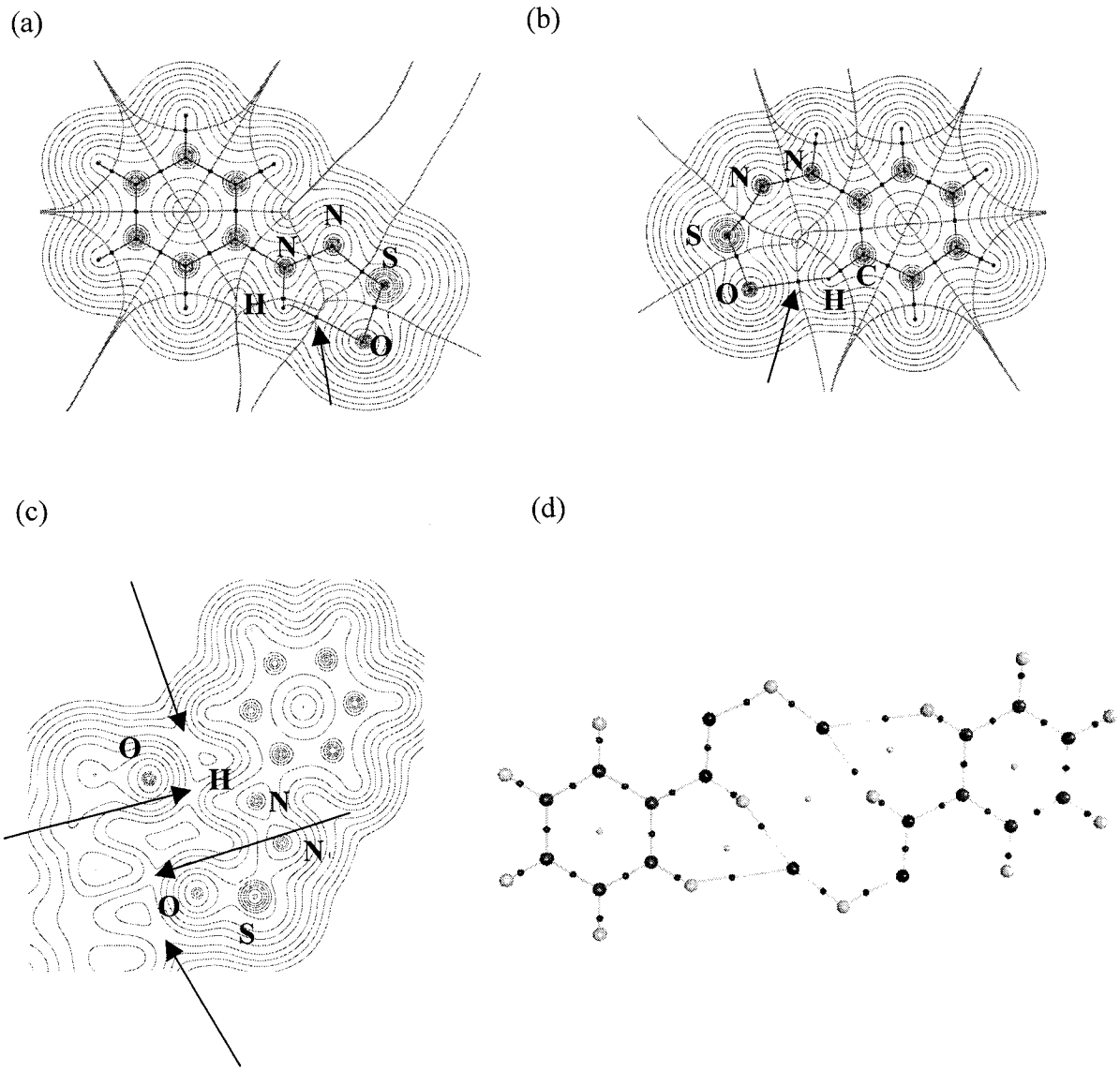

Fig. 3.3: Contour maps of the electron density of (a) the *syn* configuration, (b) the *sickle* configuration and (c) the dimer with only one monomer plus one oxygen atom from the second monomer in the plane of the plot. Saddle points for weak interactions are indicated by arrows. (d) Molecular graph of the dimer at the B3LYP/6-311+G(2d,p). The outermost contour in (a)-(c) is 0.001 au and the remaining contours increase in value in steps equal 2×10^n, 4×10^n, 8×10^n with n starting at -3 and increasing in steps of unity.

While the presence of the intermolecular N-H---O interactions corresponds to the conclusions from the earlier diffraction studies (Fig. 3.1), the absence of the intramolecular N-H---O interactions and presence of the intermolecular C-H---O interactions are in contradiction to what was suggested.[44,45]

The values of $\rho(r)$ and $\nabla^2\rho(r)$ at the BCPs of the intramolecular N-H---O interaction in the *syn* monomer and the intermolecular interactions within the dimer are presented in Table 3.7. As expected, the values of $\rho(r)$ and $\nabla^2\rho(r)$ for the N-H---O interaction within the monomer are quite small as compared to those for the dimer and correspond well with the geometrical parameters. In the dimer, the obtained values, averaged over the two like interactions, lie within their respective established ranges of 0.01 to 0.23 e/Å^3 and 0.58 - 3.35 e/Å^5 as was found for other H-bonded systems.[34,35]

Table 3.7: Electron density $\rho(r)$ (e/Å^3) and Laplacian $\nabla^2\rho(r)$ (e/Å^5) for BCPs of (N)H---O and (C)H---O interactions, and mutual penetrations[a] (pm) of H and O atoms of the PhNHNSO dimer from B3LYP/6-31+G(d).

	$\rho(r)$	$\nabla^2\rho(r)$	r^0_H	r_H	Δr_H	r^0_O	r_O	Δr_O
(N)H---O(intra)[b]	0.137	1.88	-	-	-	-	-	-
(N)H---O	0.172	2.21	123	71	52	176	120	56
(C)H---O	0.079	0.98	136	96	40	174	142	32

[a] Where r^0 are the non-bonded radii (pm) and r are the bond critical point radii (pm).

[b] For the *syn* monomer.

While naturally the density for the C-H---O interaction is smaller, it is sizable and significantly larger than the lower cut-off of 0.01 e/Å^3, which renders the C-H---O interaction non-negligible. Table 3.7 also shows the values for mutual penetration of both H and O atoms in the dimer, which is determined as the difference between a nonbonded atomic radius (r^0_H and r^0_O, the distance from the nucleus to the 0.001 au, or 6.7483 e/Å^3, density contour line) and the corresponding bonded atomic radius (r_H and r_O, the distance from the nucleus to the BCP).

The penetrations for both interactions are significant and of the same magnitude. The penetration for oxygen, Δr_O, is in fact comparable to that for oxygen in SO_2----HF (49 pm) and in H_2CO----HF (58 pm) complexes at the HF/6-311++G(d,p)//HF/6-31G(d,p) level,[35] corroborating our earlier findings that the SO bond in NSO species is better described as a four electron bond rather than through charge separation.[56] The penetration of hydrogen, Δr_H, in the C-H---O interaction is much greater than that in the comparable complex C_6H_6---OCH_2 (17 pm) obtained with HF/6-31G(d,p), even though the non-bonded radius for hydrogen in C_6H_6 with 132 pm is similar to the one reported in Table 3.7.[34] The larger penetration of the ortho hydrogen atom in the PhNHNSO dimer suggests a stronger interaction, and it is tempting to attribute this to a cooperativity caused by hydrogen bond bifurcation on oxygen.

The values of the integrated properties for the H atoms involved in weak interactions in the dimer along with the differences (Δ) from the *syn* monomer are given in Table 3.8. The positive Δ values for the atomic charges and energies of the H atoms indicate a loss of charge (more positive q) and a destabilization of the H atoms, respectively, upon the formation of the dimer. The negative Δvalues for dipolar

polarization and volume indicate a reduction in dipolar polarization and volume of the H atoms. These trends have been found to hold true for hydrogen atoms in a large number of H-bonding and anti-H bonding interactions.[33,35-37,55,60,61]

Table 3.8: Integrated properties[a] (au) of hydrogen atoms of interacting N-H and C-H bonds in the dimer and their differences from the *syn* monomer, with B3LYP/6-31+G(d).

		q	E	M	V
(N)H	dimer	0.512	-0.393894	0.135	17.47
	Δ	0.049	0.023692	-0.035	-7.41
(C)H	dimer	0.101	-0.579532	0.128	40.27
	Δ	0.050	0.014362	-0.027	-6.79

[a]Charge q, atomic energy E, dipolar polarization M and volume V.

The N-H---O Δ values of q, E, M and V are smaller compared to those for the N-H---O interactions in formamide dimerization (0.0789, 0.0412, -0.051, and -11.3 au) at the B3LYP/6-311++G(d,p) level.[61] In our case, the overall stability of the PhNHNSO dimer depends on each of two N-H---O and C-H---O interactions, and as a result, the N-H---O interactions show smaller Δ values than those in the formamide dimer with only two equivalent N-H---O interactions for a comparable dimer stabilization energy. The Δ values of E, M and V for the C-H---O interaction compare well with those of the C-H---O interactions in PhNSO at B3LYP/6-31+G(d) (ΔE 0.0086, ΔM -0.023, ΔV -6.17 au)[55] and in the C_6H_6---OCH_2 complex at HF/6-31(d,p) (ΔE 0.0136, ΔM -0.013 ΔV -13.03 au).[34]

Finally, the origin for the calculated blue shift for ν(C-H) in the C-H---O interaction is examined through an analysis of the electron density, ρ(r) of the ortho C2-H bond in the *syn* monomer and in the dimer. Table 3.9 shows the values of ρ(r), $\nabla^2\rho(r)$ and the distances from the BCP to the C and H nuclei. As expected, the calculated shortening of the C-H bond length upon dimerization is accompanied by an increase in ρ(r) and a more negative $\nabla^2\rho(r)$. While the distance from the BCP to the C nucleus increases, the distance to the H nucleus decreases, as is expected due to the loss of charge and decrease of volume of the H-bonded hydrogen atom, discussed above. Table 3.9 also shows that the decrease in the BCP---H distance is greater than the increase in the BCP---C distance, which leads to an overall shortening of the C-H bond and a classification of the C-H---O interaction as an anti-H bond.

Table 3.9: Bond critical point (BCP) data ρ(r) in e/Å^3 and $\nabla^2\rho(r)$ in e/Å^5 for the ortho C2-H bonds and distances (pm) from the BCP to the C and H nuclei in the PhNHNSO *syn* monomer and dimer.

	ρ(r)	$\nabla^2\rho(r)$	BCP---C	BCP---H
Monomer	1.860	-23.02	69.8	39.0
Dimer	1.887	-24.20	70.7	37.9
Δ	0.027	-1.18	0.9	-1.1

3.5 Conclusions

N-phenyl-N'-sulfinylhydrazine (PhNHNSO) has been analyzed using FTIR spectroscopy and computational methods. While in the solid only the ν(N-H) of the dimer is observed, dissociation equilibrium exists in dilute solutions, and both dimer and monomer ν(N-H) are detected. The position of the dimer ν(N-H) is not affected by solvent or concentration, suggesting only one dimeric species in solution and solid phases. B3LYP/6-31+G(d) calculations reveal a large energetic preference for a *syn* configured monomer over other configurations, as well as a good agreement between experimental and calculated red shifts of the ν(N-H). Analyses of the electron densities confirmed the presence of an intramolecular N-H---O interaction in the *syn* monomer and intermolecular N-H---O and C-H---O interactions in the dimer. Within the quantum theory of atoms in molecules, both types of intermolecular interactions in the dimer exhibit all necessary characteristics of H-bonds and, according to the changes calculated in ν(N-H) and ν(C-H) upon dimerization are identified as H-bonds and anti-H bonds, respectively. The present analysis suggests that both N-H---O and C-H---O interactions contribute significantly to the overall stabilization of the PhNHNSO dimer.

Chapter 4

The influence of substituents on hydrogen bond forming bonds in N-phenyl-N'-sulfinylhydrazine

4.1 Introduction

One of the fundamentals of organic chemistry is related to the effect of substituents on the structure and reactivity of organic compounds.[21,22] Substituent effects have been the subject of active research due to their important role in determining molecular behaviour, such as, enthalpies, acidities, geometries, electron densities, etc.[28,76-80] of the molecule. These studies are done to understand the effect that arises due to the position and the nature of the substituents and have revealed the different effects of electron-withdrawing and electron-donating substituents in different positions.[28,76-80] Earlier, Hammett has shown the influence of meta and para substitution on the acidity of benzoic acid.[21] The substituent effects are expressed by the Hammett substituent constants, σ, characterizing the electron-withdrawing and electron-donating behaviour of substituents.[21] Besides the reactivities, these constants have been successfully used to evaluate the substituent effect on various parameters,[78,23,81-83] such as atomic charges in disulfides and thiols,[81] the frequency of the carbonyl stretching vibration in thiazones[82] and N-H bond dissociation energies in aromatic amines, amides and hydrazines,[78] to name but a few. Conformational equilibria are also influenced by the introduction of substituents, and so Hammett substituent constants have also been used in conformational analysis, for example dihedral angles and barrier to cis-trans isomerization in acetanilides.[83] Finally, dimerization constants for phosphoric acid esters have been found

to correlate with σ .[84] The older literature is bursting with further examples ("voluminous and extensive" has been used as a description by Hansch , Leo and Taft).[85]

Previously we reported the importance of N-H, ortho C-H and S=O bonds in the dimerization of PhNHNSO.[86] The aim of the present study is to analyze the effects of substituents (OH, OCH_3, CH_3, F, Cl, Br, CN and NO_2) on these bonds in ortho, meta, para position. The different conformers of the substituted PhNHNSO compounds are studied using density functional theory calculations. The electron density analyses of the selected bonds are performed using the quantum theory of atoms in molecules (QTAIM).[32,33] Correlation analyses between different bond and atomic properties and Hammett substituent constants are investigated and discussed. Finally, the substituent effect is evaluated through the isodesmic reaction approach. We show that the ortho substitution has more influence on properties of N-H, ortho C-H and S=O bonds than meta or para substitution and the effect of electron-withdrawing substituents is greater than electron-donating substituents.

4.2 Computational details

All calculations were performed using the Gaussian 98 package.[63] The Becke three-parameter hybrid functional[15] with the Lee-Yang-Parr correlation functional[16] (B3LYP) and 6-31+G(d), 6-311+G(2d,p) and cc-pVTZ.[87] basis sets was employed to determine the energies and geometries of all compounds. All geometries were confirmed minima through vibrational frequency calculations. Calculated frequencies are reported unscaled, those for Cl- and CH_3-substituted species are also given scaled using the scaling factor of 0.9614[71] at the B3LYP/6-31+G(d) level. Barrier heights for conformational changes were calculated at the B3LYP/6-31+G(d) level. Wave functions were obtained at all levels of

theory for an analysis of the electron density within the quantum theory of atoms in molecules (QTAIM).[32] All analyses were performed using AIMPAC.[66,67] AIM integrated charges are reported. The relative stabilities of the substituted compounds were estimated using the isodesmic reaction approach at the B3LYP/6-31+G(d) level.

4.3 Results and discussion

Fig. 4.1 displays the numbering of the position of the substituted carbon atoms that have been used in the naming of the compounds to be descriptive.

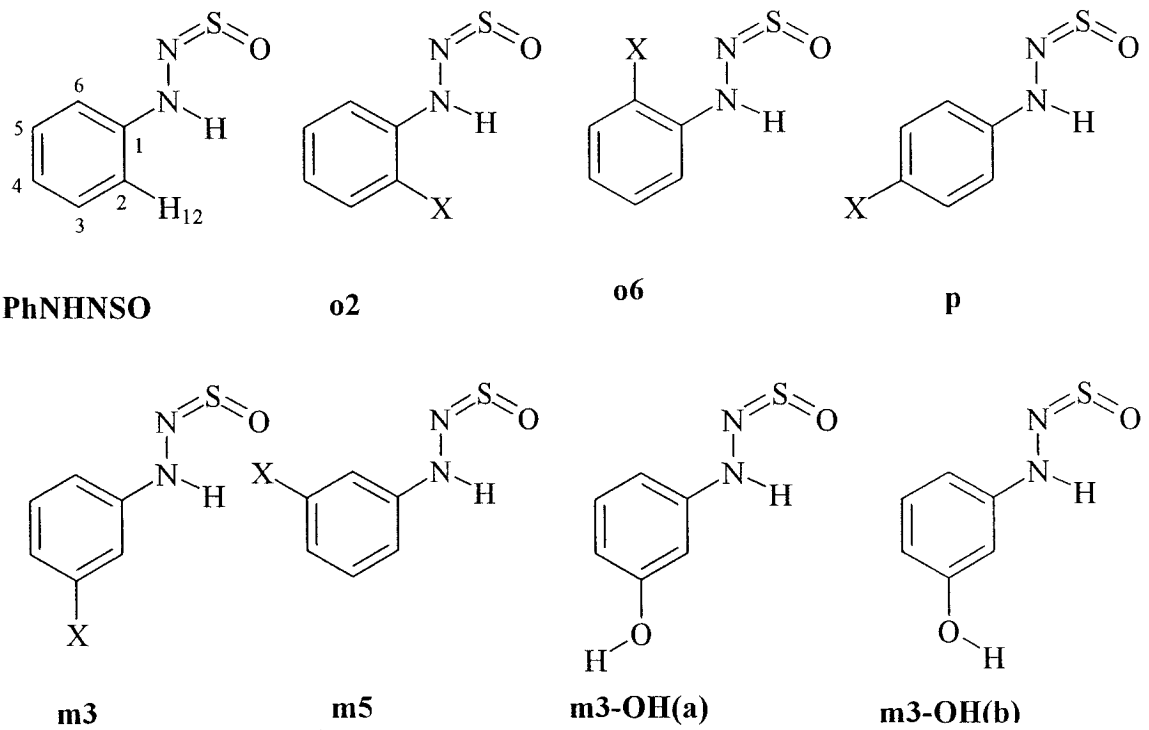

Fig. 4.1: Configurations/conformers of substituted PhNHNSO and numbering of compounds. (X= OH, OCH_3, CH_3, F, Cl, Br, CN and NO_2)

The substitution in the ortho position yields two possible conformers, **o2** (ortho2) and **o6** (ortho6), similarly substitution in meta position yields two conformers **m3** and **m5**. Compounds with substituent at position 4 are referred to as **p** (para). For OH and OMe substituents (we use Me for the CH_3 group), there are additional two possible orientation **a** and **b**. In conformer **a**, hydrogen atom or methyl group points away from the NHNSO group, while in conformer **b** they point towards the NHNSO group.

4.3.1 Energies

Table 4.1 summarizes the zero-point vibrational energy (ZPVE) corrected relative total energies of all substituted compounds. In general, **m3**, **m5** and **p** substituted compounds are within 2 kcal/mol of each other and are more stable than their **o2** and **o6** substituted analogues, except **o6-OH(b)**. There is little variation between the different levels of theory, with the possible exception of the hydroxyl species. The energy difference between conformers **m3** and **m5** is at most 0.7 kcal/mol, whereas that between **o2** and **o6** is around 1.0-8.0 kcal/mol. The observed larger difference for both **o2** and **o6** can be rationalized in terms of electronic and steric interactions that are known to occur for ortho substituents.[22,77] In general, substituted compounds **o2** are more stable than **o6**. For instance, **o2-OH(a)** is more stable than **o6-OH(a)** and the higher energy for the latter is due to a repulsive interaction between the oxygen of the hydroxyl group and the lone pair of nitrogen of the NSO group. Conformer **o6-OH(b)** in contrast, is exceptionally stable, due to a strong favorable interaction between the hydroxyl hydrogen and the NSO nitrogen group. Similarly, with the OMe substituent, the high energy of **o6-OMe(a)** and **o6-OMe(b)** is due to steric hindrance between methoxy methyl and the NSO group and a repulsive interaction between the methoxy oxygen and the NSO nitrogen lone pair,

respectively. Species **o2-OH(b)** and **o2-OMe(b)** are not observable at all the levels. All other substituents exhibit a similar pattern, **o6** being less stable than **o2**, and steric and or repulsion between lone pairs are responsible. The reason behind this energy difference is the repulsive interaction between the halo subsituents and NSO group. The extreme case is observed with NO_2 as substituent, the energy difference between **o2-NO_2** and **o6-NO_2** is found to be 7.8 kcal/mol. Both are strongly destabilize with respect to ortho and meta species, but the proportionally larger destabilization of **o6-NO_2** must be attributed to lone pair repulsion between the nitro oxygen atom and the NSO nitrogen. On the other hand, **o2-NO_2** should find some stabilization from the hydrogen bonding interaction between NH and the nitro groups. Further details on the influence of the substitutents on the geometries will be discussed in the next section. Overall, these analyses suggest that **o6**-substitution leads to high energy compounds (except for **o6-OH(b)**) and demonstrate a significant variation of the energies with the position of the substituent.

In view of the energy difference between the conformers, it is interesting to consider their equilibrium populations. Meta compounds for OH and OMe substituents contain four conformers and ortho compounds contain three conformers in the equilibrium. Meta and ortho compounds for all other substituents contain two conformers. The populations at room temperature are given in Table 4.2. It also includes para substituted compounds with OH and OMe substituents. It can be seen that the **m5** conformation is populated more than the **m3** conformation for OH, OMe, Me, F, Cl and Br substituents whereas the opposite is found for substituents CN and NO_2 But since the energy difference between **m3** and **m5** conformers is small, both conformers are populated to approximately equal amounts.

Table 4.1: Relative ZPVE corrected total energies[†a] (kcal/mol) of the substituted[†b] compounds PhNHNSO at the B3LYP level with three different basis sets.

	B3LYP/	m3		m5		p		o2		o6	
		a	**b**	**a**	**b**	**a**	**b**	**a**	**b**	**a**	**b**
OH	6-31+G(d)	0.9	1.2	0.8	0.6	1.5	1.6	1.2	-[†c]	6.9	0.0
	6-311+G(2d,p)	0.3	0.7	0.1	0	1.1	1.2	0.7	-[†c]	6.4	0.2
	cc-pVTZ	0.5	0.8	0.3	0.1	1.4	1.4	1.1	-[†c]	6.5	0.0
OMe	6-31+G(d)	0.5	0.5	0.4	0.0	1.1	1.0	0.5	-[†c]	6.9	8.2
	6-311+G(2d,p)	0.4	0.7	0.4	0.0	1.2	1.2	0.6	-[†c]	7.0	8.4
	cc-pVTZ	0.5	0.7	0.4	0.0	1.3	1.3	0.8	-[†c]	7.1	8.6
Me	6-31+G(d)	0.0		0.0		0.2		0.9		3.5	
	6-311+G(2d,p)	0.0		0.0		0.3		0.9		3.8	
	cc-pVTZ	0.1		0.0		0.3		0.9		3.7	
F	6-31+G(d)	0.3		0.0		0.6		1.7		5.8	
	6-311+G(2d,p)	0.3		0.0		0.8		1.6		5.7	
	cc-pVTZ	0.3		0		0.8		1.7		5.6	

(Continues to next page)

Table 4.1 (Continued)

	B3LYP/	**m3**	**m5**	**p**	**o2**	**o6**
Cl	6-31+G(d)	0.1	0.0	0.0	1.0	6.6
	6-311+G(2d,p)	0.1	0.0	0.1	0.8	6.5
	cc-pVTZ	0.1	0.0	0.1	0.8	6.7
Br	6-31+G(d)	0.1	0.0	0.1	0.4	6.1
	6-311+G(2d,p)	0.1	0.0	0.0	0.7	6.8
	cc-pVTZ	0.1	0.0	0.0	0.8	6.9
CN	6-31+G(d)	1.2	1.2	0.0	1.5	4.8
	6-311+G(2d,p)	1.2	1.2	0.0	1.3	4.8
	cc-pVTZ	1.3	1.3	0.0	1.3	4.7
NO_2	6-31+G(d)	1.5	1.7	0.0	2.2	10.0
	6-311+G(2d,p)	1.9	1.8	0.0	2.1	10.1
	cc-pVTZ	1.5	1.7	0.0	2.1	10.2

[†a] Total energies (ZPVE-corrected in au) for the most stable configuration is given in Table B.1 (Appendix B).

[†b] See Fig. 4.1 for a description of the numbering system.

[†c] Not a minimum.

The same is true for **p-OH** and as well as for **p-OMe(a)** and **p-OMe(b).** Ortho substituted systems behave differently. The **o2** conformers are found to be populated almost exclusively, the exception case being is **o6-OH**, where the **o6-OH(b)** conformer allows for H-bonding O-H---N.

Table 4.2: Equilibrium population (%) at room temperature of the substituted conformers from B3LYP/6-31+G(d).

	Substituents									
	OH(**a**)	OH(**b**)	OMe(**a**)	OMe(**b**)	Me	F	Cl	Br	CN	NO_2
m3	22	12	19	19	49	38	44	47	51	57
m5	27	39	21	41	51	62	56	53	49	43
p	53	47	49	51	-	-	-	-	-	-
o2	12	-[a]	100	-[a]	99	100	100	100	100	100
o6	0	88	0	0	1	0	0	0	0	0

[a] Not a minimum.

4.3.2 Barrier height

A conformational analysis is incomplete without a study of the rotational barrier.[70] Table 4.3 presents the calculated barrier heights for torsion of the C2-C-N-H dihedral angle in all substituted conformers and in the parent PhNHNSO. We did not consider a-b conversion for OH and OMe substituted compounds. The energy of the barrier is calculated from the most stable conformer to the transition state. All activation energies are remarkably similar and more or less centered around the value for the unsubstituted

PhNHNSO, 6.1 kcal/mol. Meta substituted species exhibit the smallest range of activation energies, followed by ortho with the exception of **o2-NO_2**, where NO_2 is hydrogen bonded to N-H and para species. The **p** substituted series shows a good correlation of activation energies with ν(N-H) (R^2=0.8184) and with the Hammett σ constant (R^2=0.9091), suggesting that the substituent effect is transmitted to the NHNSO head group. Plots are given in Fig. B.1 (Appendix B).

Table 4.3: Barrier heights (kcal/mol) from C2-C-N-H torsion for **o2-o6** and **m3-m5** conversion and in para and unsubstituted compounds PHNHNSO from B3LYP/6-31+G(d).

	H	OH(**a**)	OH(**b**)	OMe(**a**)	OMe(**b**)	Me	F	Cl	Br	CN	NO_2
	6.1										
m		6.4	6.6	6.2	6.5	5.8	6.6	6.3	6.3	6.4[a]	6.6[a]
p		5.3	5.2	5.2	5.2	5.8	5.6	6.1	6.2	7.4	8.1
o		7.0	-	6.9	-	4.9	6.5	6.7	6.5	7.2	10.0

[a] For **m3-m5** conversion.

4.3.3 Geometry and frequency

While substitution on the aromatic ring has an influence on all bonds and angles of the NHNSO headgroup, only N-H, C2-H (hereafter C-H) and S=O are discussed in the following, because they are paramount to H-bond formation. One more parameter that can be expected to play a role is the dihedral angle between the two π-systems, C2-C-N-H. All meta and para substituted compounds are fully planar, and Table 4.4 shows that this also holds for all **o2** and half of the **o6** species. A basis set effect is worth mentioning.

The intramolecular N-H---O distance is larger with larger basis sets, which leads to a change in structure of the monomers: the bond critical point in the electron density for an N-H---O interaction that is observed with B3LYP/6-31+G(d) disappears with larger basis sets. As discussed previously,[86] this is not an artifact of the level of theory, but rather an indication of the weak nature of this intramolecular interaction. The N-H---O interaction is not part of the discussion of this paper.

Table 4.4: Dihedral angles C2-C-N-H (degree) of **o2** and **o6** conformers from B3LYP/6-31+G(d).

	OH(**a**)	OMe(**a**)	Me	F	Cl	Br	CN	NO_2
o2	0	0	0	0	0	1	0	0
o6	11	17	0	1	20	0	0	22

4.3.3.1 N-H bond

The calculated N-H bond distances as well as the frequencies of the N-H stretching vibration of all substituted compounds with three different basis sets are presented in Table B.2 (Appendix B). The N-H bond distance is found in the range of 102.4-102.8 pm which decreases with increasing basis set as observed in a previous study.[55] In contrast to N-H bond distance, frequencies are larger with 6-311+G(2d,p) and smaller with the cc-pVTZ basis set. Compared to the unsubstituted PhNHNSO, the N-H bonds of **m3**, **m5** and **p** substituted compounds undergo 0.1pm change in their bond distances, which is not significant. On the other hand, **o2** and **o6** substituted compounds show bigger changes. It is found that **o2** conformers have shorter N-H bond distances compared to **o6** conformers.

Changes in frequency as a function of the bond distance are plotted in Fig. 4.2(a). The obtained correlation coefficients (R^2) for 6-31+G(d), 6-311+G(2d,p) and cc-pVTZ basis sets are 0.9484, 0.9473 and 0.959, respectively. Only the later is plotted. The correlation analysis shows the expected dependency, in that a shorter distance yields a higher frequency of the stretching vibration.

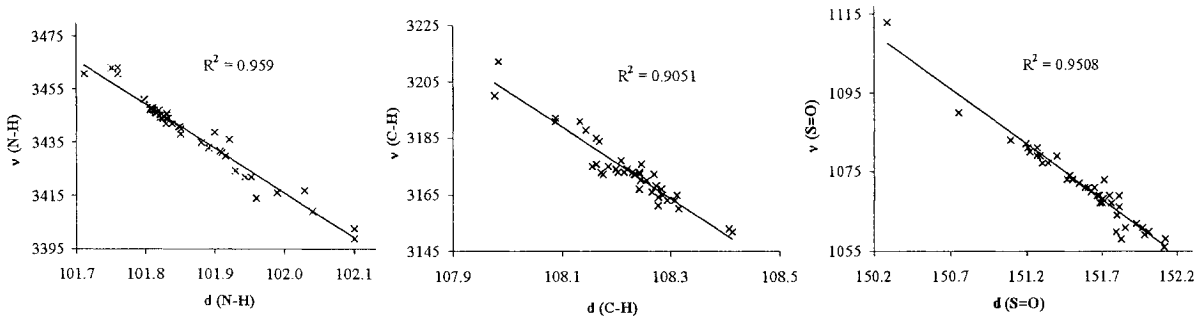

(a) (b) (c)

Fig. 4.2: Plots of bond distance (d, pm) and frequency (ν, cm^{-1}) for (a) N-H bond at the cc-pVTZ level, (b) ortho C-H bond at the cc-pVTZ level (c) S=O bond at the 6-31+G(d) level. All basis sets are for the B3LYP method.

Table 4.5 presents the calculated (scaled) and experimental frequencies of the N-H stretching vibration with Cl and Me substituents. Clearly, the calculated results are in good agreement with the experimental data.

Table 4.5: Experimental and calculated[a] N-H stretching frequencies (cm^{-1}) for Cl and Me substituted compounds.

		B3LYP/6-31+G(d)	Experimental[b]
Cl	**m3**	3284	
			3280
	m5	3286	
	p	3282	3277
	o2	3295	
			3280
	o6	3266	
Me	**m3**	3279	
			3276
	m5	3280	
	p	3277	3273
	o2	3300	
			3290
	o6	3247	

[a] Scaling factor 0.9614.

[b] Experimental frequencies are measured in $CHCl_3$ at 0.1 and 0.5 mol/L.

4.3.3.2 C-H bond

Table B.3 (Appendix B) presents the bond distances and frequencies of the ortho C-H (the C2-H) stretching vibration of **m3**, **m5**, **p** and **o6** substituted compounds. The C-H bond distance is found in the range of 108.4 pm to 108.9 pm which is close to the reported C-H bond distance of N-sulfinylamine at 6-31+G(d)[55] and of benzene.[36] As we observed for the N-H bond, the C-H bond distance also decreases with increasing basis set, but the frequencies are smaller with 6-311+G(2d,p) and larger with the cc-pVTZ

basis set. Substitution in **m3** position exhibit the largest effect on bond distance and frequency, which is understandable in terms of a neighboring effect (**m3** substitution is in ortho position to the C2-H bond). The R^2 obtained for the substituted compounds from 6-31+G(d), 6-311+G(2d,p) and cc-pVTZ basis sets are 0.8759, 0.7838 and 0.9051 respectively. The cc-pVTZ shows considerable improvement over 6-31+G(d) and 6-311+G(2d,p). Fig. 4.2(b) displays the frequency of the C-H stretch as a function of the bond distance for the cc-pVTZ basis set. The observed trend again is as expected, but the correlation is significantly worse than that for the N-H bond (Fig. 4.2(a)). Correlations for the individual series (**m3**, **m5**, **o6** and **p**) at cc-pVTZ, show that there is an excellent correlation for **m3** (R^2=0.9619) only. Analyzing all C-H stretching vibrations in the aromatic region, we found that this is due to the isolated nature of the C-H stretch in **m3**. ν(C-H) in **m5**, **o6** and **p** species shows varying degrees of coupling with the other C-H bonds and therefore poorer correlations. Plots are given in Fig. B.2 (Appendix B).

4.3.3.3 S=O bond

The calculated S=O bond distance and the frequency of the S=O bond stretching vibration with three different basis sets are presented in Table B.4 (Appendix B). The S=O bond distance is found in the range of 150.3 pm to 152.0 pm, which is longer than those previously reported at 6-31+G(d) for related systems.[55,88,89] Here also the same trend is observed with a change in basis set as the basis set increases, the bond distance decreases, but interestingly, the frequencies are larger with the larger basis set. The R^2 for frequency versus distance plots for all substituted compounds with 6-31+G(d), 6-311+G(2d,p) and cc-pVTZ basis sets are 0.9508, 0.8865 and 0.7242, respectively. The poorer value of R^2 for the cc-pVTZ basis set might be due to the occurrence of S=O/N=S

vibrational coupling due to the increase of basis set size, similar to what was discussed for the C-H bond above.

Fig. 4.2(c) shows the variation of bond distance and frequency of S=O bonds at the B3LYP/6-31+G(d) level. For individual **m3**, **m5**, **p**, **o2** and **o6** substituted compounds, R^2 are 0.9752, 0.919, 0.9979, 0.9735, and 0.8392, respectively, at the B3LYP/6-31+G(d) level. Among all of them, **m3**, **p** and **o2** substituted compounds show better correlations, suggesting that substituents in these positions have a greater effect than those in other positions. For **m3**, **p** and **o2** a noticeable change is observed with strong electron-withdrawing substituents, CN and NO_2. Species **m3-NO_2**, **m3-CN**, **p-NO_2**, **p-CN**, **o2-NO_2**, **o2-CN** have shorter S=O bonds and higher frequencies compared to the unsubstituted PhNHNSO. Similarly, **o2-F**, **o2-Cl** and **o2-Br** exhibit a pronounced shortening and higher frequency. Amongst the **o6** substituted compounds, OH, OMe, Me, F and Br substituents give longer bonds and lower frequencies. In contrast, CN and NO_2 give 0.3–0.4 pm shorter bonds and higher frequencies. Other geometrical parameters are presented in Table B.5 (Appendix B).

4.3.4 Electron densities

The quantum theory of atoms in molecules (QTAIM) is an important tool in the interpretation of either covalent or weak bonding interactions.[32] Within the framework of AIM, the presence of a (3,-1) or bond critical point (BCP), a point where the density attains its minimum value along the bond path, the line connecting the two nuclei is the necessary and sufficient criterion for two atoms to be bonded to one another. The information about the electronic distribution between two such interacting atoms is determined through an analysis of the properties of electron density at that BCP. For this

purpose, the hydrogen bond forming bonds of all substituted compounds are analyzed in terms of the electron density.

Table B.6 (Appendix B) presents the electron densities $\rho(r)$ at the bond critical point of the N-H bond with three different basis sets. As already observed for bond distance and frequency, the electron density also increases with the size of the basis set.

Fig. 4.3(a) presents plot for density at the BCP as a function of distance for the N-H bond at the B3LYP/cc-pVTZ level. With the obvious outlier of **o2-NO_2**, which forms a H-bond with N-H, we find decent polynomial second order trend, even though the correlation is not very good (R^2=0.7237). But the individual correlation for **o2** substituted compounds shows good linear trend (R^2= 0.8809) with NO_2, suggesting a bigger effect of **o2** substitution Similarly, for **p** and **o6** substituted compounds, R^2 are 0.7176 and 0.6588 and meta substituted compounds shows poor correlation. The cause of the poor correlation for meta substituted compounds has yet to be determined.

Electron densities at the C-H BCP are listed in Table B.7 (Appendix B). The plot of density versus distance (Fig. 4.3(b)) seems to be a scatter plot, against expectations. Because the situation was somewhat reminisce out of the frequency versus distance correlation for the C-H bond in Fig. 4.2(b), we again analyzed relationships for the individual substituted compounds (**m3**, **m5**, **o6**, and **p**) at cc-pVTZ. The plots are given in Fig B.3 (Appendix B). Briefly, except for **m3**, substitution, which causes an ortho-effect for the C2-H bond, all correlations are good, with R^2>0.8. As both **p** and **o6** are in meta position with respect to C2-H, they have only a small spread of C2-H distances. Substitution in **m5**, which is para with respect to C2-H, has a bigger effect, and, while the C-H distance is invariant when the substituent is an electron-donor, the slope of the

density versus distance relationship shows the wrong sign for electron-acceptors. The origin of this effect has yet to be determined.

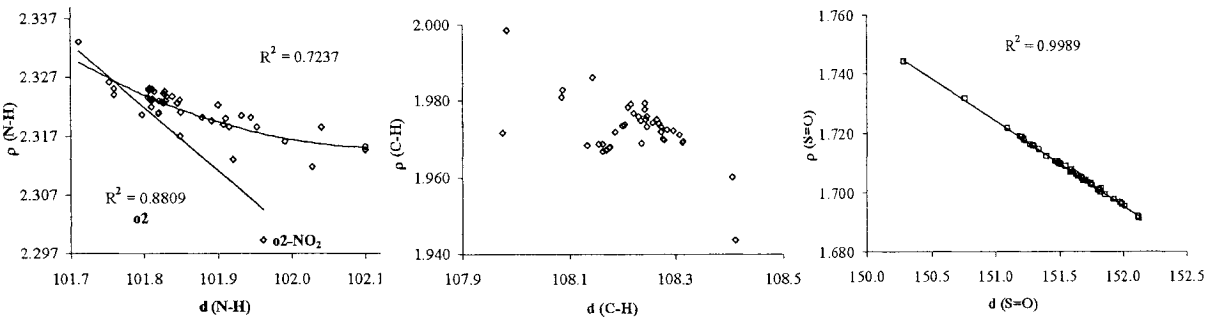

(a) (b) (c)

Fig. 4.3: Plots of bond distance (d, pm) and electron density (ρ, e/Å^3) for (a) N-H bond at the cc-pVTZ level, (b) ortho C-H bond at the cc-pVTZ level (c) S=O bond at the 6-31+G(d) level. All basis sets are for the B3LYP method. See text for the correlations.

Table B.8 (Appendix B) presents the electron densities of the S=O bond with three basis sets. The electron density at the bond critical point of the S=O bond is found in the range of 1.691 - 1.744 e/Å^3, which is lower that the previously reported values for SO_2, CH_3-NSO and CH_3NHNSO.[56] The plot of frequency versus distance, shown in Fig. 4.3(c), reveals an excellent linear correlation (R^2 of 0.9989). The largest variation is found for **o2** substituted compound, and substituents NO_2 and CN have a larger effect than OH and OMe.

From these analyses it seems, that substitution in **o2** position has a large effect. In order to be able to assess effects due to **m3**, **m5**, and **p** substitution we carried out analyses with the Hammett substituent constant.

4.3.5 Hammett correlations

4.3.5.1 Bond distances, frequencies and electron densities

Correlation with standard Hammett substituent constants σ, taken from Hansch, Leo and Taft[85] reflects the effects of substituents on observable properties such as bond distances, frequencies etc. In general, these constants are applicable only to meta and para substituted compounds, and ortho substituted compounds are ruled out from the following discussion.

Fig. 4.4 shows the linear dependency of bond distances, frequencies and electron densities of the S=O bond with the substituent constant (σ: σ_m for meta substitution, σ_p for meta substitution) for the 6-31+G(d) basis set. The R^2 for all **m3**, **m5** and **p** substituted compounds are found to be 0.9537, 0.9177 and 0.9524 for the three properties. The **p** substituted compounds seem to correlate better but in general, the substituents effects are similar for all. Fig. 4.4(a) shows a decrease in bond distance with an increasing electron-withdrawing capability of the substituent. The good overall correlation for σ_m and σ_p suggest a predominantly inductive effect of the substitution on the remote S=O bond.

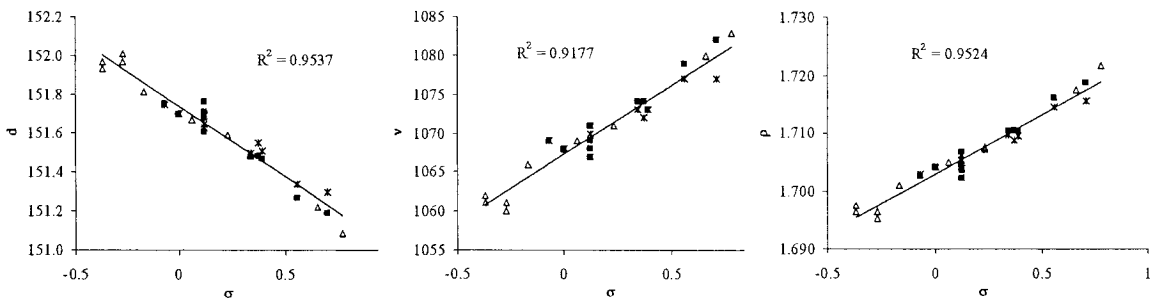

Fig. 4.4: Dependencies for the S=O bond: (a) bond distance (d, pm) (b) frequency (ν, cm^{-1}) and (c) electron density (ρ, e/$Å^3$) versus. σ from B3LYP/6-31+G(d). (Δ**p**, ▪ **m3**, * **m5** substitution).

In accord with the distance versus σ correlation, Fig. 4.4(b) shows that the slope of frequency versus σ correlation has the opposite sign, and strong electron-withdrawing substituent lead to high frequency of the S=O stretching vibration. The larger scatter for the basis set used in Fig. 4.4(b) was discussed above. Finally, Fig. 4.4(c) shows the density versus σ correlation. The positive slope, indicating high values of electron density for electron-withdrawing substituents, is in accord with Figs. 4.4(a) and (b).

As might be expected from above discussions, the story is not as uniform for N-H and C-H bonds. Good correlations for N-H bond are only found for para substituted compounds, and these are presented in Fig. 4.5. Plots for the variations of bond distances, frequencies and electron densities are correlated with σ^+ constants, as it was found that σ^+

is more suitable than σ, suggesting that for para substituted compounds, the resonance effect is more important than the inductive effect, which is different from the S=O bond.

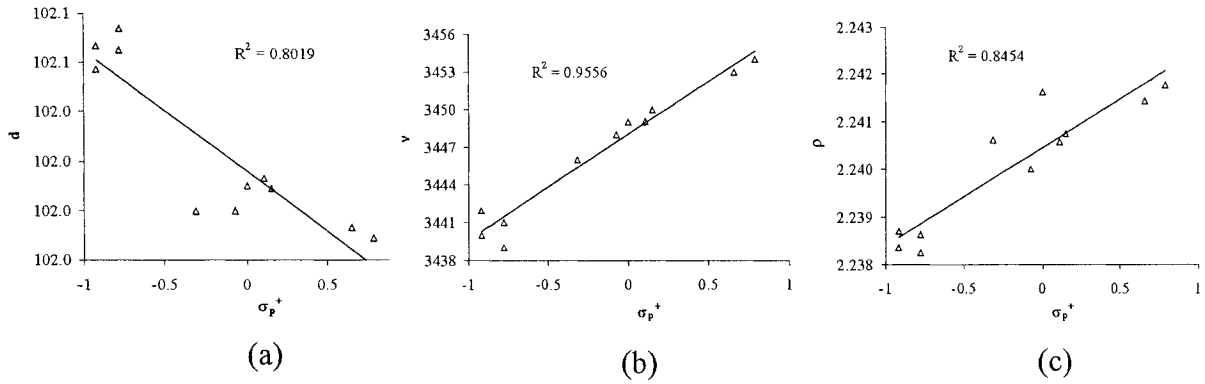

(a) (b) (c)

Fig. 4.5: Dependencies for the N-H bond of para substituted compounds: (a) bond distance (d, pm) (b) frequency (ν, cm^{-1}) and (c) electron density (ρ, e/$Å^3$). and σ_p^+ from B3LYP/6-311+G(2d,p).

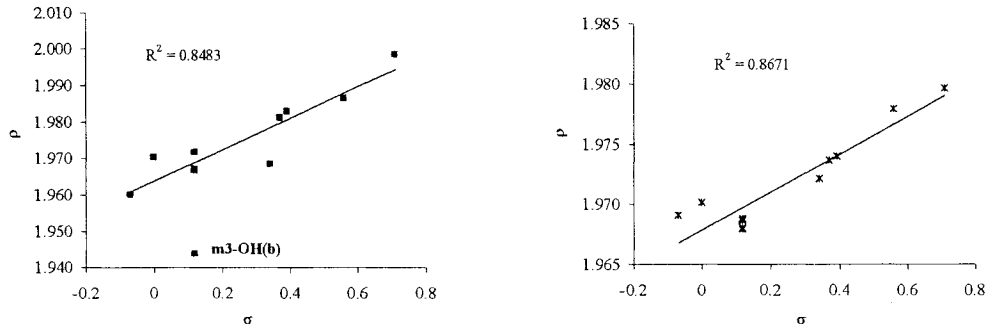

(a) (b)

Fig. 4.6: Correlations for the ortho C-H between electron density (ρ, e/$Å^3$) and σ for (a) **m3** (b) **m5** from B3LYP/cc-pVTZ. (▪ **m3**, ∗ **m5** substitution).

Aside from this, the trends for S=O and N-H bond properties are similar as is evident from the signs of the slopes of the correlation lines, indicating that para substituents have the same effect on S=O and N-H bonds.

For the ortho C-H bond, only **m3** and **m5** substituted compounds show a reasonable relationship between the electron density and the σ constants, whereas **p** substituted compounds show no trend and these are presented in Fig. 4.6. As mentioned earlier, this is not unexpected, because **m3** is ortho to C2-H and **m5** is para to C2-H.

Based on the above correlations, it is found that changes in the S=O bond of **m3**, **m5** and **p** substituted compounds are dependent on the nature of the substituent whereas only the N-H bond of **p** compounds show a dependence. In contrast, **m3** and **m5** substituted compounds show dependence for the ortho C-H bond. Resonance and inductive effects are responsible for the behaviour of the different substituents.

4.3.5.2 Atomic charges on hydrogen and oxygen atoms

A study of the atomic charges can be very useful in the determination of the influence of a substituent on a particular atom. Table 4.6 presents the atomic charges on oxygen of the S=O bond and on hydrogen of N-H and ortho C-H bonds of meta and para substituted compounds. Even though changes in the charges are small, as is expected from remote substituent, it can be seen that the atomic charge on oxygen decreases (becomes less negative) as the substituent's electron-withdrawing nature increases.

Fig. 4.7(a) displays the plot of a variation of the atomic charge on oxygen with σ. A decent linear correlation is observed (R^2=0.8794) whose R^2 value is worsened through mOH data points. The obtained values of R^2 for individual **m3**, **m5** and **p** are 0.9295,

0.9202 and 0.9536, respectively. Electron-withdrawing groups exhibit the same effect, a loss of charge, on the hydrogen atoms of N-H and C-H bonds

Table 4.6: AIM integrated atomic charges (au) from B3LYP/6-31+G(d).

		O	H(N-H)	H(C-H)
H		-1.198	0.463	0.051
OH	**m3(a)**	-1.198	0.462	0.041
	m3(b)	-1.197	0.464	0.073
	m5(a)	-1.198	0.464	0.051
	m5(b)	-1.197	0.465	0.051
	p(a)	-1.199	0.464	0.056
	p(b)	-1.200	0.463	0.055
OMe	**m3(a)**	-1.198	0.463	0.071
	m3(b)	-1.199	0.461	0.049
	m5(a)	-1.199	0.463	0.050
	m5(b)	-1.198	0.464	0.050
	p(a)	-1.200	0.463	0.054
	p(b)	-1.200	0.463	0.052
Me	**m3e**	-1.199	0.462	0.043
	m5e	-1.198	0.462	0.050
	p	-1.199	0.463	0.050

(Continues to next page)

Table 4.6 (Continued)

		O	H(N-H)	H(C-H)
F	**m3**	-1.195	0.465	0.082
	m5	-1.196	0.465	0.055
	p	-1.197	0.465	0.060
Cl	**m3**	-1.195	0.465	0.075
	m5	-1.195	0.465	0.057
	p	-1.196	0.465	0.060
Br	**m3**	-1.195	0.465	0.075
	m5	-1.196	0.465	0.075
	p	-1.196	0.465	0.060
CN	**m3**	-1.192	0.467	0.078
	m5	-1.193	0.466	0.062
	p	-1.191	0.466	0.063
NO2	**m3**	-1.191	0.468	0.116
	m5	-1.193	0.466	0.065
	p	-1.189	0.467	0.066

The correlation for the N-H hydrogen with σ is not linear, but shows curvature (Fig. 4.7(b)). Again, **m3-OH** either falls off the correlation, or is part of a second trend with negative slope for electron-donating substituents. This will warrant further analysis. The individual R^2 for **m3**, **m5** and **p** are 0.8167, 0.8488 and 0.8444, respectively.

For the ortho C-H hydrogen, **m3** substituted compound show larger effect than **m5** and **p** (Fig. 4.7(c)). The obtained individual R^2 for **m3**, **m5** and **p** are 0.7234, 0.9435 and 0.6761, suggesting the better correlation for **m5**. Overall, a better correlation is observed with σ than with σ^+ constants, suggesting that resonance effects are not predominant.

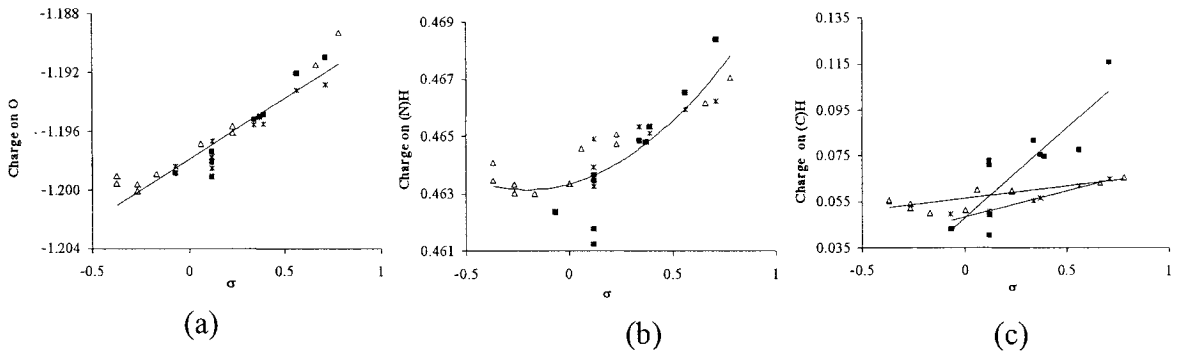

Fig. 4.7: Correlation between atomic charges (au) and σ for (a) the oxygen atom of the S=O bond (b) the hydrogen atom of the N-H bond and (c) the hydrogen atom of the C-H bond from B3LYP/6-31+G(d).(Δ **p**, ▪ **m3**, * **m5** substitution)

4.3.6 Stability of substituted compounds

The relative stabilities of the substituted PhNHNSO are determined by means of the isodesmic reaction given in Scheme 4.1:

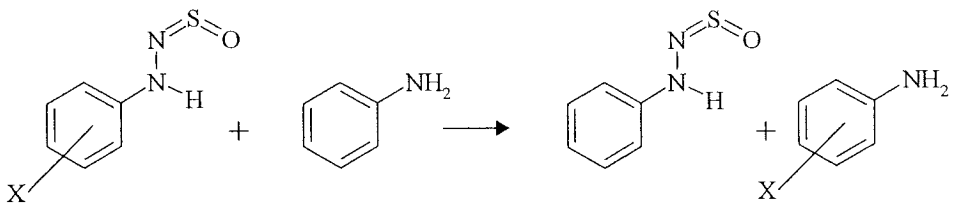

Scheme 4.1: Isodesmic reaction for the substituted PhNHNSO and aniline.

Table 4.7 reports the isodesmic reaction energies of the substituted compounds Electron-donating substituents OMe(**a**), OMe(**b**) and Me in **m3** and **m5** and **p** position (with the exception of **m3-OH**) lead to an endothermic reaction, i.e. they stabilize PhNHNSO. On the other hand, electron-withdrawing substituents F, Cl, Br, CN and NO_2 lead to exothermic reactions, destabilizing PhNHNSO.

Table 4.7: Calculated isodesmic reaction energies (ΔE) from B3LYP/6-31+G(d).

	OH(**a**)	OH(**b**)	OMe(**a**)	OMe(**b**)	Me	F	Cl	Br	CN	NO_2
m3	-0.03	-0.38	0.24	0.09	0.33	-1.33	-1.32	-0.34	-2.24	-2.55
m5	0.08	0.30	0.29	0.70	0.36	-1.05	-1.18	-0.28	-2.26	-2.70
p	1.33	1.26	1.51	1.54	0.71	-0.12	-0.65	-0.06	-2.71	-3.59
o2	-0.12	-	0.30	-	-0.18	-1.93	-2.32	-1.37	-4.67	-6.17
o6	-5.81	1.06	-5.74	-6.91	-2.81	-6.01	-7.89	-7.04	-7.94	-13.95

For **o2** substitution, only **o2-OMe(a)** and **o6-OH(b)** lead to endothermic reactions and therefore reveal stabilized reactants. Fig. 4.8 displays plots of isodesmic reaction energies versus σ for (a) **m3** and **m5** and (b) **p** substituted species. Good linear trends are observed. Overall it is clear from these analyses that the stability of PhNHNSO is sensitive to the nature and position of the substituents, and strong electron-withdrawing groups destabilize PhNHNSO in all positions. In contrast, electron-donating groups in general stabilize when in meta or para positions.

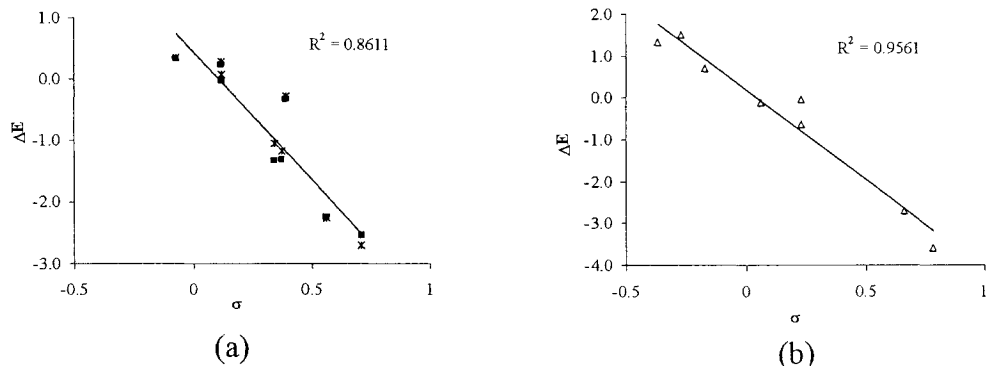

Fig. 4.8: Correlation between isodesmic reaction energies (ΔE) (kcal/mol) and σ for (a) meta and (b) para substituted compounds from B3LYP/6-31+G(d). (Δ **p**, ▪ **m3**, ∗ **m5** substitution).

4.4 Conclusions

A series of substituted PhNHNSO compounds was investigated using B3LYP with three different basis sets 6-31+G(d), 6-311+G(2d,p) and cc-pVTZ. The data obtained in this work show that, while 6-31+G(d) basis set can provide useful results, larger basis sets 6-311+G(2d,p) and cc-pVTZ often show some improvement. It is found that the energy of the substituted compounds is sensitive towards the nature and position of the substituents. The ortho substituted compounds are less stable compared to their meta and para substituted analogues. Geometries and frequencies of N-H and S=O bonds are more affected by ortho substitution than by meta or para substitution. The extent of changes in geometries and frequencies of N-H and ortho C-H is smaller compared to those of the S=O bond, despite its remoteness.

Correlation analyses show the mostly linear relation between bond distances, frequencies and electron densities. The S=O bond has shown excellent correlations throughout, unlike compared to N-H and ortho C-H bonds. Linear correlations with Hammett substituent constant for S=O and N-H bonds reflect the direct influence of the nature of the substituents. Strong electron-withdrawing substituents NO_2 and CN give shorter distances, higher frequencies and higher electron densities compared to electron-donating substituents OMe and OH. It is obvious that the stability of the PhNHNSOs is substituent dependent. Stabilization is observed for substitution in meta position by electron-donating substituents, whereas destabilization is observed for the substitution in any positions by electron-withdrawing substituents.

Chapter 5

Chloro and methyl substituted N-phenyl-N'-sulfinylhydrazines: experimental and computational analyses

5.1 Introduction

The hydrogen bond (H-bond) interaction plays an important role in molecular association in chemical and biological systems.[1,2,4] It is known that the strength of H-bond interactions is influenced by the position and the nature of substituents.[26,29,90] Electron-donating and electron-withdrawing substituents can have different effects on the H-bond properties of a molecule. Kawahara et al. have shown that the introduction of an electron-withdrawing group into the uracil ring of the Watson-Crick adenine-uracil base pair resulted in stronger stable hydrogen bonding.[26] Similar study of adenine-thymine and cytosine-guanine base pairs revealed that fluoro and nitro substituents have a greater effect on the stabilization energy compared to other substituents.[90] Ahn et al. have shown the effect of para and ortho substituents on hydrogen bonding in phenol-water complexes.[29] It was found that in para substituted complexes, electron-withdrawing groups and electron-donating groups have opposite trends on the changes in binding energy. In contrast, for ortho substituted complexes, a geometry change of the H-bond due to a direct involvement of the substituent was observed.

Our previous work has focused on the unsubstituted PhNHNSO monomer and the dimer[44] using FTIR spectroscopy and density functional theory calculations.[86] We have confirmed that PhNHNSO exists as a dimer in the solid, and shown that in solution both dimeric and monomeric forms exist in equilibrium, based on an observed red shift in the frequency of the N-H stretching vibration upon dimer formation. A pattern of acceptor

bifurcated H-bonds with intermolecular N-H---O and C-H---O interactions has been revealed through an analysis of the electron density. The interactions have been identified as H-bond and anti-H bond, respectively, and both contribute significantly to the overall stabilization of the dimer. Upon the introduction of substituents in different positions on the aromatic ring of the PhNHNSO monomer, it has been shown that the hydrogen bond forming N-H and S=O bonds are more influenced by electron-withdrawing than by electron-donating substituents.[91] We find that while meta and para substituted PhNHNSO monomers dimerize, ortho substituted monomers do not.

A topological analysis of the electron density $\rho(r)$ is crucial for the identification and characterization of H-bonds. The quantum theory of atoms in molecules (QTAIM)[32,33] is a powerful method for topological analysis of the electron density. It has been used successfully for a variety of H-bonded systems.[55,34,35,37,57-60] Within the framework of AIM, eight proposed criteria,[32,34] comprise (1) the presence of a (3,-1) bond critical point (BCP) for the H---B pair and its associated bond path, (2) a low value of $\rho(r)$ at this BCP (3) a positive value of the Laplacian ($\nabla^2\rho(r)$) at the BCP, (4) the mutual penetration of the van der Waals envelop of both hydrogen and acceptor (B) atom, (5) a loss of charge (q) of the hydrogen atom, (6) an energetic (E) destabilization of the hydrogen atom, (7) a decrease in the dipolar polarization (M) of the hydrogen atom, and (8) a decrease in the atomic volume (V) of the hydrogen atom. These criteria have been shown to applicable successfully to various H-bonds, anti-H bonds and dihydrogen bonds.[33,36,55,61]

With respect to the different dimerization behaviour of the monomers, the aim of the present study is to investigate the effect of the nature and position of the substituent

on the intermolecular interactions in the PhNHNSO dimer (Fig. 5.1) using FTIR spectroscopy, density functional theory calculations, and topological analyses of the electron density.[32,33]

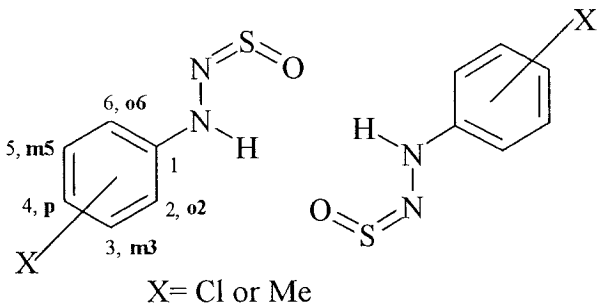

Fig. 5.1: Notation of the substituted PhNHNSO dimers and numbering of the ring carbon atoms.

5.2 Experimental section

Chloro and methyl substituted PhNHNSO were synthesized as described by Pearce et al.[62] The compound was recrystallized from ethanol and further purified by sublimation. Infrared spectra were recorded at room temperature using a Nicolet-Impact 400 FTIR spectrophotometer. Solution studies were performed with a 0.1 mm spacer in a KBr liquid sample cell. At least 36 scans were collected in the 4000-400 cm^{-1} range.

5.3 Computational details

All calculations were performed using the Gaussian 98 package.[63] Geometry optimization, and frequency analyses used the Becke three-parameter exchange functional[15] with the Lee-Yang-Parr correlation functional[16] (B3LYP) and the 6-31+G(d) basis set. All geometries were confirmed as true minima via vibrational frequency

analyses. Vibrational frequencies are scaled using a scaling factor of 0.9614.[71] The interaction energy was calculated as the energy difference between the dimer and the corresponding monomers using the supermolecular approach.[4,14] The BSSE was estimated by performing a single point calculation using the counterpoise method introduced by Boys and Bernardi.[31] Wave functions were obtained at the same level of theory for the topological analyses of the electron density within the quantum theory of atoms in molecules (QTAIM).[32,33] All analyses were performed using AIMPAC[66,67] and the molecular graph of the dimer was plotted with AIM2000.[92] Single point calculations were performed with B3LYP/6-31+G(d) for solvent effects, employing the self-consistent reaction field theory (SCRF) method with COSMO (conductor like screening model).[41]

5.4 Results and discussion

5.4.1 Vibrational spectra

The FTIR spectra of chloro and methyl substituted PhNHNSO were recorded in chloroform at a concentration of 0.1 and 0.5 M. The band positions for both chloro and methyl substituted PhNHNSOs are given in Table 5.1. In the N-H stretching (ν(N-H)) region, both meta and para substituted PhNHNSO show two absorption bands, one corresponding to the non hydrogen bonded N-H and the other to the hydrogen bonded N-H similar to PhNHNSO itself,[86] suggesting the presence of both monomer and dimer in the solution. In contrast, ortho substituted PhNHNSOs exhibit only one absorption band corresponding to the non hydrogen bonded N-H. The absence of the H-bonded ortho dimers might point to the significance of the bifurcated H-bonding network in the PhNHNSO dimer. It was revealed that the C-H---O interactions play an important role in the overall stability of the dimer, and any replacement of an ortho H atom by a

substituent could eliminate the possibility of such interactions. For chloro substituted PhNHNSO, frequencies of the N-H stretching vibration of meta and para substituted monomers are located at 3280 cm^{-1} and 3277 cm^{-1} and those of the asymmetric N-H stretch in the dimers are located at 3211 cm^{-1} and 3209 cm^{-1}. For the ortho substituted monomer, ν(N-H) frequency is located at 3280 cm^{-1}. With methyl substitution, ν(N-H) frequencies for meta and para substituted monomers are located at 3276 cm^{-1} and 3273 cm^{-1} and those of the dimers are located at 3209 cm^{-1} and 3207 cm^{-1}. The ortho methyl substituted PhNHNSO has the largest ν(N-H) frequency of 3290 cm^{-1}. As expected, frequencies vary with the position and the nature of the substituent.

Table 5.1: Frequency (cm^{-1}) of the N-H stretching vibrations of chloro and methyl substituted PhNHNSOs in $CHCl_3$ solution at concentration of 0.1 and 0.5 mol/L.

	Free N-H	H-bonded N-H
mCl	3280	3211
pCl	3277	3209
oCl	3280	-
mMe	3276	3209
pMe	3273	3207
oMe	3290	-

Compared to the unsubstituted PhNHNSO,[86] in meta and para substituted PhNHNSO monomers, ν(N-H) increases with Cl substitution and decreases with Me substitution. As the meta substituted PhNHNSOs show a 2 cm^{-1} increase in values of H-

bonded ν(N-H) compared to their para substituted analogues, this stresses the importance of electronic and inductive effects that we investigated in the monomers computationally.[91] Earlier similar studies were performed with meta, para and ortho substituted benzoic acid in CCl_4 and it was reported that the ν(C=O) frequency varies with the nature of the substituent, e.g., it increases with Cl substitution and decreases with Me substitution and a larger effect is observed with meta than with para substitution.[93] The different behaviour of the substituted PhNHNSO monomers with respect to dimerization is discussed in the remainder of this paper.

5.4.2 Energies

Table 5.2 presents the zero-point vibrational energy (ZPVE) corrected relative energies, ΔE, of the chloro and methyl substituted PhNHNSO dimers. The designation of the substituent positions on the aromatic ring is given in Fig. 5.1. Among the chloro substituted dimers, the para substitution leads to the most stable dimer, ortho substitution to the least stable. The high energy of the ortho substituted dimers might arise from the conformations of the individual ortho substituted monomers. Our previous study showed that **oCl2** and **oCl6** monomers have higher energies than meta and para substituted analogues,[91] and association of such two monomers consequently leads to high energy dimers. On the other hand, meta and para substituted monomers have almost equal energies,[91] as a result their corresponding dimers are almost equally stable. The hetero-dimers, **mCl3-5** and **oCl2-6**, show similar stabilities to their respective homo-dimers.

Table 5.2: ZPVE corrected relative energies ΔE^{a}, interaction energies ΔE_{inter} and free energies of dimerization ΔG (kcal/mol) of chloro and methyl substituted PhNHNSO dimers.

	Substituent					
	Cl			Me		
positions	ΔE	ΔE_{inter}	ΔG	ΔE	ΔE_{inter}	ΔG
m3	0.3	-12.2	-1.4	0	-11.2	0.3
m5	0.3	-11.9	-0.9	0	-11.2	-0.4
p	0	-12.2	-1.4	0.2	-11.3	0.3
o2	9.9	-4.3	6.6	6.9	-6.1	4.8
o6	13.2	-12.2	-1.0	7.9	-10.3	0.7
m3-5	0.3	-12.1	-1.3	0	-11.2	0.5
o2-6	11.9	-7.9	2.9	6.9	-8.6	2.3

[a] ZPVE corrected total energies of the global minimum: **pCl** -2549.236490 au, **mMe3** -1708.609310 au.

The situation for methyl substituted dimers is very similar. Again, meta and para substituted dimers are low in energy, with all meta species as global minima. The destabilization of **oMe2**, **oMe6** and **oMe2-6** is less than for chloro substitution.

Table 5.2 also presents the interaction energies and free energy of dimerization of all substituted PhNHNSO dimers. The BSSE is similar for all (around 2 kcal/mol). In accord with our experimental findings, **o2** and **o2-6** substituted dimers have small negative interaction energies and large positive free energy differences, suggesting that

association involving **o2** monomers is unfavourable. Surprisingly, and in seemingly contrast with experiment, the **o6** dimer exhibits interaction values similar to those of meta and para substituted dimers.

A possible reason is supplied in a population analysis of the substituted PhNHNSO monomers.[91] It was revealed that the equilibrium lies almost completely on the **o2** side, suggesting that **o6** monomers are simply unavailable for dimerization. As a result, it is impossible to observe either ortho chloro or ortho methyl dimers experimentally. Interaction and free energies for the meta and para substituted dimers are similar to those for the unsubstituted dimer (ΔE_{inter} 11.4 kcal/mol, ΔG 0.7 kcal/mol). Values for chloro substitution are slightly lower (more negative) and therefore more favourable than those for methyl substitution.

From the above observations, it is evident that the association of two **o2** monomers as homo-dimer and one **o2** and one **o6** monomers as hetero-dimer is highly unfavourable and the association of two o6 monomers is as favourable as **m3**, **m5** and **p** monomers. But even though the favourable dimerization **o6** monomers, **o6** dimers are failed to observe experimentally.

It is well known that solvent-solute interactions can have a substantial impact on the properties of H-bonded molecules.[38,94-96]A computational assessment of the effect of different solvents was carried out by embedding the system of interest in a polarizable solvent cavity. Tables 5.3 and 5.4 present the solvation free energies, ΔG_{solv}, and their total electrostatic contributions, ΔG_{el}, obtained for the solvents CCl_4, $CHCl_3$ and CH_2Cl_2 with COSMO for the chloro and methyl substituted PhNHNSOs.

Table 5.3: Free energies of solvation, ΔG_{solv}, and their electrostatic contributions, ΔG_{el} (kcal/mol) of the methyl substituted PhNHNSO monomers and dimers in three solvents.

		CCl_4		$CHCl_3$		CH_2Cl_2	
		ΔG_{solv}	ΔG_{el}	ΔG_{solv}	ΔG_{el}	ΔG_{solv}	ΔG_{el}
mCl3	Dimer	3.66	-1.77	1.95	-2.61	-4.63	-2.95
	Monomer	-1.36	-2.35	-2.89	-3.48	-6.95	-3.91
mCl5	Dimer	3.57	-1.74	1.85	-2.58	-4.82	-2.90
	Monomer	-1.35	-2.39	-2.94	-3.57	-7.01	-4.03
pCl	Dimer	2.93	-1.97	1.14	-2.91	-5.63	-3.28
	Monomer	-1.68	-2.54	-3.31	-3.76	-7.45	-4.25
oCl2	Dimer	4.46	-2.24	2.48	-3.35	-3.83	-3.78
	Monomer	-0.15	-1.66	-1.40	-2.49	-5.23	-2.82
oCl6	Dimer	4.21	-1.89	2.41	-2.83	-3.95	-3.20
	Monomer	-0.90	-2.35	-2.46	-3.51	-6.41	-3.96
mCl3-5	Dimer	3.51	-1.75	1.80	-2.60	-4.81	-2.93
	Monomer	-1.36	-2.37	-2.92	-3.53	-6.98	-3.97
oCl2-6	Dimer	4.61	-2.07	2.71	-3.09	-3.58	-3.09
	Monomer	-0.53	-2.01	-1.93	-3.00	-5.82	-3.39

Table 5.4: Free energies of solvation, ΔG_{solv}, and their electrostatic contributions, ΔG_{el} (kcal/mol) of the methyl substituted PhNHNSO monomers and dimers in three solvents.

		CCl_4		$CHCl_3$		CH_2Cl_2	
		ΔG_{solv}	ΔG_{el}	ΔG_{solv}	ΔG_{el}	ΔG_{solv}	ΔG_{el}
mMe3	Dimer	3.18	-1.68	1.50	-2.49	-5.23	-2.81
	Monomer	-1.85	-2.32	-3.36	-3.44	-7.53	-3.88
mMe5	Dimer	2.67	-1.73	0.98	-2.57	-5.87	-2.90
	Monomer	-1.79	-2.29	-3.29	-3.39	-7.43	-3.82
pMe	Dimer	3.34	-1.53	1.74	-2.27	-4.98	-2.56
	Monomer	-1.43	-2.20	-2.91	-3.28	-7.01	-3.70
oMe2	Dimer	2.67	-2.27	0.74	-3.36	-5.87	-3.79
	Monomer	-1.16	-1.82	-2.43	-2.70	-6.41	-3.04
oMe6	Dimer	3.57	-1.55	1.98	-2.30	-4.48	-2.59
	Monomer	-1.04	-1.97	-2.4	-2.93	-6.36	-3.31
mMe3-5	Dimer	2.95	-1.73	1.26	-2.56	-5.52	-2.89
	Monomer	-1.82	-2.31	-3.33	-3.42	-7.48	-3.85
oMe2-6	Dimer	3.28	-1.76	1.60	-2.61	-4.9	-2.94
	Monomer	-1.10	-1.90	-2.42	-2.82	-6.39	-3.18

As expected, for both chloro and methyl substitution, ΔG_{solv} and ΔG_{el} become more negative with an increasing polarity of the solvent as observed for PhNHNSO itself.[86] For the unsubstituted system, it had been found that changes in ΔG_{el} are more linear than those in ΔG_{solv}, and that the larger change in ΔG_{solv} from $CHCl_3$ to CH_2Cl_2 was the cause

of a much more negative free energy of repulsion and dispersion in CH_2Cl_2 for both monomers and dimers. This is also observed for the substituted PhNHNSOs.

5.4.3 Geometries

The geometry is one of the many molecular properties affected by the formation of intermolecular interaction. Table 5.5 presents the bond distances, averaged over the two H-bonded monomers, of hydrogen bond forming N-H, ortho C-H and S=O bonds of all substituted PhNHNSO monomers and dimers. Other selected geometrical parameters are given in Table C.1 (Appendix C).

A comparison between the geometrical parameters of the isolated monomers[91] and the respective dimers show that the formation of intermolecular interactions causes the expected changes in bond distances and bond angles. Upon dimerization, N-H and S=O bonds elongate while the C-H bond involved in the interaction shortens. In chloro substituted dimers, the N-H bond elongates by 0.7 – 0.8 pm and the S=O bond by 0.6 – 0.9 pm, whereas the ortho C-H bond shortens by 0.1 – 0.3 pm. Similarly, in the methyl substituted dimers, the N-H bond elongates by 0.6 – 0.8 pm and the S=O bond by 0.6 – 0.8 pm, while the C-H bond shortens by 0.2 - 0.3 pm. An elongation of the N-H bond is treated as evidence for the existence of a hydrogen bonding interaction.[97-99]

Table 5.5: Distances (pm) of the N-H, ortho C-H and S=O bonds involved in intermolecular interactions in PhNHNSO dimers and their difference from the respective monomers.

	N-H		C-H		S=O	
	Dimer	Δ	Dimer	Δ	Dimer	Δ
mCl3	103.2	0.7	108.5	-0.1	152.4	0.9
mCl5	103.3	0.8	108.5	-0.2	152.4	0.9
pCl	103.2	0.6	108.5	-0.2	152.5	0.9
oCl2	103.2	0.7	-	-	151.8	0.6
oCl6	103.3	0.7	108.6	-0.1	152.6	0.9
mCl3-5	103.2	0.7[a]	108.5	-0.2[a]	152.4	0.9[a]
oCl2-6	103.2	0.7[b]	108.5	-0.3	152.1	0.6[b]
mMe3	103.2	0.6	108.6	-0.3	152.5	0.7
mMe5	103.3	0.7	108.5	-0.3	152.5	0.8
pMe	103.3	0.7	108.6	-0.2	152.6	0.8
oMe2	103.2	0.8	-	-	152.4	0.6
oMe6	103.4	0.6	108.6	-0.2	152.6	0.6
mMe3-5	103.3	0.7[a]	108.6	-0.2[a]	152.5	0.7[a]
oMe2-6	103.2	0.6[b]	108.5	-0.3	152.6	0.7[b]

[a] Difference to the average value for **m3** and **m5** monomers.

[b] Difference to the average value for **o2** and **o6** monomers

Similarly, a shortening of the ortho C-H bond upon dimerization is treated as evidence for the presence of a hydrogen bonding interaction.[12,36] Table 5.6 presents the intermolecular H-bond distance and angles of N-H---O and C-H---O interactions of all dimers.

The results show that in the substituted dimers, large changes from the values for the unsubstituted dimer are only found with ortho substitution. For **o2** and **o2-6** dimers, the longer distance and smaller angle of the N-H---O interaction suggest a weaker intermolecular interaction. The **o6** dimers show a smaller variation from that of the PhNHNSO dimer values, so their N-H---O interactions are comparatively stronger than those in **oCl2** and **oCl2-6** dimers.

For the C-H---O intermolecular interaction, large changes from the unsubstituted dimer are observed only with chloro substitution. Again, the (C)H---O distance is largest for ortho substitution. Changes with methyl substitution show a much smaller spread, indicating a smaller influence of methyl substitution. Other geometrical parameters are reported in the appendix C.

Larger differences for (N)H---O and (C)H---O distances in the ortho dimers might be due to more dramatic changes in the overall geometry of these dimers, in particular torsions. Table 5.7 presents the CCNN dihedral angle of the dimers. Like PhNHNSO itself, the planar meta and para substituted monomers[91] do not twist upon dimerization, whereas the planar **o2** monomers exhibit a significant distortions as the dimer is formed. Even **oCl6**, which is a monomer already has a dihedral angle of 30°, is further twisted by 11° upon dimerization. These changes explain the shorter and longer N-H---O and C-H---

O distance, respectively as well as the relative (loss of conjugation) and the interaction energies.

Table 5.6: H-bond distances (pm) and bond angles on hydrogen (degrees) of all PhNHNSO dimers.

	(N)H---O	N-H-O	(C)H---O	C-H-O
PhNHNSO	190.8	160	237.2	138
mCl3	190.8	160	234.6	138
mCl5	190.7	160	237.6	138
pCl	190.9	159	235.4	138
oCl2	194.1	146	-	-
oCl6	189.0	157	240.1	133
mCl3-5	190.5	160	235.8	138
oCl2-6	193.9	150	244.8	131
mMe3	191.1	161	237.4	139
mMe5	190.9	161	238.3	137
pMe	190.5	160	237.5	137
oMe2	192.8	154	-	-
oMe6	191.5	162	236.1	137
mMe3-5	190.6	161	237.9	138
oMe2-6	197.0	153	237.2	136

Table 5.7: CCNN dihedral angle (degree) of the substituted PhNHNSO dimers.

	m3	**m5**	**p**	**o2**	**o6**	**m3-5**	**o2-6**
Cl	1	1	1	20	41	1	22[a]
Me	1	1	1	24	21	1	21

[a] Individual dihedral angles in the dimer are 13° for the **o2** and 31° for the **o6** fragment.

5.4.4 Frequencies

The scaled asymmetric N-H stretching vibrations of the substituted PhNHNSO dimers as well as the experimental and calculated red shifts are presented in Table 5.8. Frequencies of the N-H stretching vibrations in chloro and methyl monomers have been reported.[91] As was found for the unsubstituted PhNHNSO, experimental and calculated red shifts are in reasonably good agreement. Both **o2-6** dimers show a much larger values of the ν(N-H) than any of the other dimers, in keeping with their larger (N)H---O distances and their small interaction energies and free energies of dimerization. We would have expected the **o2** monomers to follow this trend, but as Table 5.8 shows, here the red shifts are greatest, indicating relatively stronger N-H---O interaction.

Table 5.8 also reports the scaled calculated frequencies of the C-H stretching vibration of the dimers. The blue shift of the C-H stretching vibration for chloro and methyl substituted dimers ranges from 22 to 34 cm^{-1} and from 39 to 45 cm^{-1}, respectively. The observed blue shift is in good agreement with the shortening of the C-H bond, suggesting the anti-H bond nature of the C-H---O interactions.

In a previous study of a series of substituted PhNHNSO monomers, we showed a significant ortho effect for the parameters of the N-H bond as well as a poor overall

Table 5.8: Scaled frequency (cm^{-1}) of the N-H and the C-H stretching vibration of the PhNHNSO dimers and their shift from the respective monomers.

	N-H			C-H	
	dimer	$\Delta\nu$[a]	Expt ($\Delta\nu$)	dimer	$\Delta\nu$
mCl3	3196	-88	-69	3106	22
mCl5	3194	-92		3089	21
mCl3-5	3196	-89		3101	25
pCl	3196	-86	-68	3091	25
oCl2	3186	-109	-[b]	-	-
oCl6	3169	-97		3096	33
oCl2-6	3219	-62		3096	34
mMe3	3191	-88	-67	3084	39
mMe5	3187	-93		3098	34
mMe3-5	3186	-94		3099	45
pMe	3186	-91	-66	3095	41
oMe2	3185	-115	-[b]	-	-
oMe6	3168	-79		3095	42
oMe2-6	3247	-26		3096	43

[a] Values for ν(N-H) for the monomers are given in Table 4.5.

[b] Experimentally not observed.

correlation for ν(C-H) due to vibrational coupling. The calculated frequencies in Table 5.8 should therefore not be over interpreted.

5.4.5 Identification and characterization of the weak interactions

Fig. 5.2 displays the contour maps of the electron density and the molecular graph for two of the selected dimers, **mCl3** and **oCl2**. Since the optimized dimers are not planar, only certain atoms involved in the interactions are plotted in the plane of Fig. 5.2(a). As expected from the PhNHNSO dimer, the topological analysis reveals the presence of bond critical points (BCP) for the N-H---O and C-H---O interactions (indicated by arrows in Fig. 5.2(a) suggesting the presence of bifurcated H-bonds on the acceptor atom in the **mCl3** dimer. A representation of the molecular graph for **mCl3** (Fig. 5.2(b)) shows the bifurcation on oxygen even more clearly. Similar H-bonding patterns are revealed for all other **m3**, **m5**, **p** and **o6** dimers. For the **oCl2** dimer naturally, only N-H---O interactions are found (Fig. 5.2(c)). In addition, though, the molecular graphs for **oCl2** (Fig. 5.2(d)) and **oMe2** dimers exhibit contacts between oxygen atoms of one monomer and **o2**-substituted of the other monomer, as well as O-O contacts. Table 5.9 presents the values of $\rho(r)$ and $\nabla^2\rho(r)$ at the BCPs of the N-H---O interactions of all the substituted dimers.

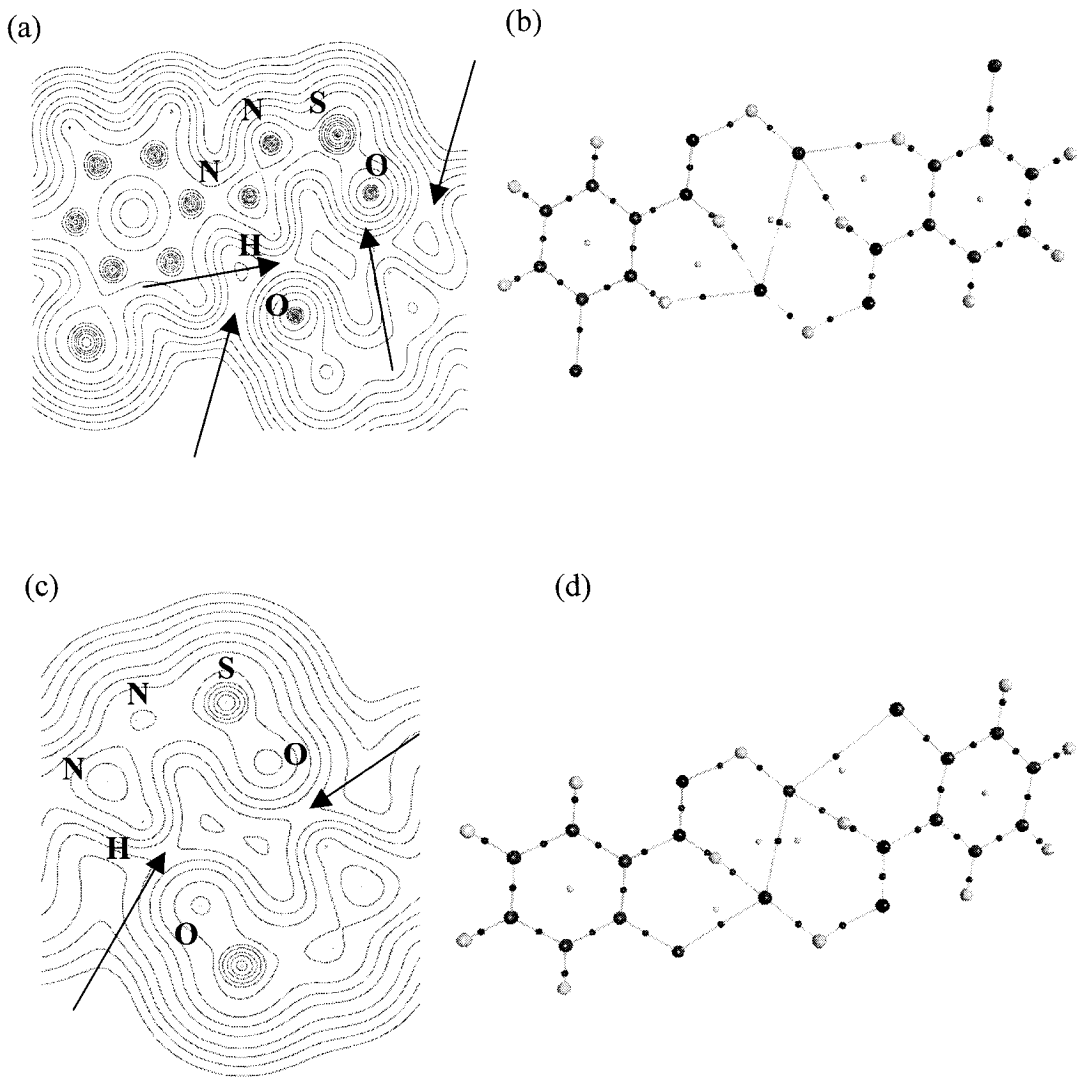

Fig. 5.2: Contour maps of the electron density of (a) the **mCl3** dimer with only one monomer plus one oxygen atom from the second monomer in the plane of the plot and (c) the **oCl2** dimer with S atoms of two monomers in the plane of the plot. Saddle points for weak interactions are indicated by arrows. The outermost contour is 0.001 au and the remaining contours increase in value in steps equal 2×10^n, 4×10^n, 8×10^n with n starting at -3 and increasing in steps of unity. (c) and (d) show the molecular graphs for the **mCl3** and **oCl2** dimers, respectively.

Table 5.9: Electron density $\rho(r)$ (e/Å^3) and Laplacian ($\nabla^2\rho$) (e/Å^5) for BCPs of (N)H---O and (C)H---O interactions of chloro and methyl substituted dimers.

	(N)H---O		(C)H---O	
	$\rho(r)$	$\nabla^2\rho(r)$	$\rho(r)$	$\nabla^2\rho(r)$
PhNHNSO	0.172	2.21	0.079	0.98
mCl3	0.171	2.22	0.081	1.02
mCl5	0.172	2.22	0.078	0.97
pCl	0.170	2.22	0.081	1.01
oCl2	0.169	2.07	-	-
oCl6	0.182	2.31	0.073	0.94
mCl3-5	0.173	2.23	0.080	1.00
oCl2-6	0.167	2.10	0.066	0.86
mMe3	0.170	2.19	0.078	0.97
mMe5	0.172	2.20	0.077	0.96
pMe	0.173	2.23	0.078	0.98
oMe2	0.168	2.10	-	-
oMe6	0.171	2.16	0.081	1.01
mMe3-5	0.173	2.22	0.078	0.97
OMe2-6	0.156	1.97	0.078	0.99

In the chloro substituted dimers, the obtained values of $\rho(r)$ and $\nabla^2\rho(r)$, averaged over the two like N-H---O interactions, lie within the respective established ranges of

0.01 to 0.23 e/Å^3 and 0.58 to 3.35 e/Å^5.[33] Individual values are given in Table C.2 (Appendix C). While the values of $\rho(r)$ and $\nabla^2\rho(r)$ in meta and para substituted dimers show little variation and they are only 0.001-0.002 e/Å^3 and 0.01-0.02 e/Å^5 larger than those for the PhNHNSO dimer,[86] comparatively larger changes are observed with **oCl2** and **oCl2-6** dimers whose N-H---O interactions carry less electron density at the BCP. The values of $\rho(r)$ and $\nabla^2\rho(r)$ are 0.003 to 0.005 e/Å^3 and 0.14 to 0.11 e/Å^5 smaller that those for the PhNHNSO. The largest changes are obtained for the **oCl6** dimer whose N-H---O interaction possess the largest density at the BCP in the chloro series, in accord with its short (N)H---O distance and small value of its ν(N-H), suggesting a comparatively strong interactions. In the methyl substituted dimers, similar trends are observed, with the exception of **oMe6** whose N-H---O BCP does not carry an enlarged density, which again is in accord with (N)H---O distance and N-H stretching frequency.

Table 5.9 also reports average values of $\rho(r)$ and $\nabla^2\rho(r)$ at the BCPs of the C-H---O interactions. Individual values are given in Table C.3 (Appendix C). All values are much smaller than those of the N-H---O interactions but still lie within the expected range of H-bond interactions.[33] The observed values are also comparable with those of other C-H---O interactions.[36,55] Among all the dimers, **oCl6** and **oCl2-6** have the smallest values of $\rho(r)$ and $\nabla^2\rho(r)$. Density variation within the methyl series is small, in accord with the frequency of the C-H stretch.

The mutual penetration of both H and O atoms is determined as the difference between a nonbonded atomic radius (r^0_H and r^0_O, the distance from the nucleus to the 0.001 au density contour line (6.7483 e/Å^3)) and the corresponding bonded atomic radius (r_H and r_O, the distance from the nucleus to the BCP). Table 5.10 shows the values for

mutual penetration of both H and O atoms in the dimers. In all cases, for the N-H---O interaction, the penetration of the oxygen atom is greater than that of the hydrogen atom, as was observed for Base---HF complexes.[35] The exceptional cases are **oCl2**, **oMe2**, and **oMe2-6** in which the hydrogen atom is penetrated more than the oxygen atom, and **oCl2-6** with similar penetrations of both H and O, suggesting weaker N-H---O interactions in these dimers, and supporting conclusions drawn from values of $\rho(r)$. In contrast, for C-H---O interactions, the hydrogen atom is penetrated more similar to PhNHNSO, and the penetration is much greater than that in other complexes,[33] suggesting a comparatively stronger nature of the C-H---O interactions.

Table 5.10: Mutual penetration of nonbonded (r^0) and bonded (r) radii (pm) of H and O atoms of all dimers.

		(N)H	(C)H	(NH)---O	(CH)---O			(N)H	(C)H	(NH)---O	(CH)--- O
mCl3	r^0	123	133	181	176	**mMe3**	r^0	128	139	181	176
	r	71	94	120	140		r	71	96	120	142
	Δ	52	39	62	36		Δ	57	43	61	34
mCl5	r^0	123	133	181	176	**mMe5**	r^0	123	139	181	176
	r	71	96	120	142		r	71	96	120	142
	Δ	52	37	62	34		Δ	52	43	61	34
pCl	r^0	122	136	180	174	**pMe**	r^0	128	139	180	176
	r	71	95	120	141		r	71	96	120	142
	Δ	51	41	60	33		Δ	57	43	60	34
oCl2	r^0	136		175		**oMe2**	r^0	151		175	
	r	72		122			r	72		121	
	Δ	64		53			Δ	79		54	
oCl6	r^0	123	137	181	176	**oMe6**	r^0	128	133	180	176
	r	70	98	119	142		r	71	96	120	141
	Δ	53	39	62	34		Δ	57	37	60	35

(continues on next page)

Table 5.10 (Continued)

		(N)H	(C)H	(NH)---O	(CH)---O			(N)H	(C)H	(NH)---O	(CH)---O
mCl3-5	r^0	123	133	181	176	**mMe3-5**	r^0	123	139	181	176
	r	71	95	120	141		r	71	96	120	142
	Δ	52	38	62	35		Δ	55	43	61	34
oCl2-6	r^0	130	139	178	176	**oMe2-6**	r^0	140	133	178	176
	r	73	100	121	145		r	74	96	123	141
	Δ	57	39	57	31		Δ	66	37	55	35

[a] Where r^0 are the non-bonded radii (pm) and r are the bond critical point radii (pm).

The values of the integrated properties for the H atoms involved in weak interactions in the dimers along with the differences (Δ) from the respective monomers are given in Tables 5.11 and 5.12.

The positive Δ values for the atomic charges suggest a loss of charge (more positive q) upon dimerization. In both dimer series, for the N-H---O interaction only the H atoms of **o2** and **o2-6** show significantly less loss of charge than those in the PhNHNSO dimer. A small loss of charge is also found for the H atoms of the C-H---O interactions in **mCl3-5** and **oCl2-6**. Because a loss of charge is associated with an energetic destabilization, the energies of the H atoms (Table 5.11) reflect the above changes in q, in that a smaller destabilization is found for H atoms in N-H---O for both **o2** and **o2-6** dimers, and for H atoms in C-H---O for **mCl3-5** and **oCl2-6**.

Table 5.11: Integrated atomic properties[a] (au) of hydrogen atoms of interacting N-H and C-H bonds of chloro substituted dimers and their difference from the respective monomers.

			q	E	M	V
mCl3	(N)H	Dimer	0.512	-0.393097	0.135	17.44
		Δ	0.047	0.023110	-0.034	-7.40
	(C)H	Dimer	0.124	-0.568846	0.125	38.92
		Δ	0.049	0.014993	-0.025	-6.69
mCl5	(N)H	Dimer	0.513	-0.392772	0.135	17.44
		Δ	0.048	0.023431	-0.034	-7.43
	(C)H	Dimer	0.105	-0.576784	0.128	40.12
		Δ	0.048	0.014375	-0.025	-6.46
pCl	(N)H	Dimer	0.513	-0.393101	0.135	17.47
		Δ	0.048	0.023300	-0.035	-7.37
	(C)H	Dimer	0.110	-0.574988	0.126	39.68
		Δ	0.050	0.015088	-0.026	-6.75
oCl2	(N)H	Dimer	0.514	-0.391085	0.139	17.09
		Δ	0.036	0.017311	-0.027	-6.15

(continues on next page)

Table 5.11 (Continued)

			q	E	M	V
oCl6	(N)H	Dimer	0.512	-0.392882	0.135	17.22
		Δ	0.049	0.024751	-0.035	-7.46
	(C)H	Dimer	0.108	-0.576280	0.129	39.94
		Δ	0.049	0.015119	-0.023	-6.20
mCl3-5	(N)H	Dimer	0.513	-0.392905	0.135	17.44
		Δ	0.048	0.023300	-0.034	-7.42
	(C)H	Dimer	0.105	-0.576773	0.127	40.04
		Δ	0.039	0.010726	-0.025	-6.06
oCl2-6	(N)H	Dimer	0.510	-0.394318	0.140	17.40
		Δ	0.039	0.018697	-0.028	-6.56
	(C)H	Dimer	0.099	-0.579925	0.132	40.64
		Δ	0.040	0.011474	-0.020	-5.50

[a] Charge q, atomic energy E, dipolar polarization M and volume V.

The negative Δ values for the dipolar polarization and the volume of the atoms indicate a reduction in dipolar polarization and volume in accord with the above changes of the H atoms. In general, the magnitude of the change of the H atom of **o2** and **o2-6** dimers is smaller compared to those of the other dimers.

Table 5.12: Integrated atomic properties[a] (au) of hydrogen atoms of interacting N-H and C-H bonds of methyl substituted dimers and their difference from the respective monomers.

			q	E	M	V
mMe-3	(N)H	Dimer	0.511	-0.394131	0.135	17.59
		Δ	0.049	0.024026	-0.035	-7.37
	(C)H	Dimer	0.093	-0.582988	0.129	40.61
		Δ	0.050	0.014075	-0.028	-7.21
mMe-5	(N)H	Dimer	0.511	-0.394059	0.135	17.52
		Δ	0.049	0.024022	-0.035	-7.44
	(C)H	Dimer	0.099	-0.579950	0.129	40.53
		Δ	0.049	0.014309	-0.026	-6.60
pMe	(N)H	Dimer	0.512	-0.393751	0.135	17.48
		Δ	0.049	0.024196	-0.035	-7.44
	(C)H	Dimer	0.101	-0.579602	0.128	40.39
		Δ	0.051	0.014813	-0.027	-6.72
oMe-2	(N)H	Dimer	0.509	-0.395661	0.138	17.36
		Δ	0.044	0.023480	-0.028	-6.01

(Continues to next page)

Table 5.12 (Continued)

			q	E	M	V
oMe-6	(N)H	Dimer	0.508	-0.395800	0.136	17.37
		Δ	0.047	0.023966	-0.034	-7.03
	(C)H	Dimer	0.100	-0.581137	0.128	39.81
		Δ	0.052	0.015272	-0.026	-6.88
mMe3-5	(N)H	Dimer	0.512	-0.393964	0.135	17.50
		Δ	0.050	0.024155	-0.035	-7.46
	(C)H	Dimer	0.096	-0.581398	0.129	40.62
		Δ	0.050	0.014263	-0.027	-6.85
oMe2-6	(N)H	Dimer	0.505	-0.398164	0.140	17.71
		Δ	0.042	0.021290	-0.028	-6.18
	(C)H	Dimer	0.098	-0.581887	0.129	40.03
		Δ	0.050	0.014522	-0.025	-6.66

[a] Charge q, atomic energy E, dipolar polarization M and volume V.

From the above discussion, it is clear that all the integrated properties reveal a loss of charge, destabilization of energy, decrease in dipolar polarization, and decrease in atomic volume of the hydrogen atom involved in the interactions upon dimerization. These observations obviously provide the evidence for the existence of N-H---O and C-H---O interactions in the dimers. However, considering the values of $\rho(r)$, $\nabla^2\rho(r)$ and a comparatively small properties of the H atoms of both N-H---O and C-H---O interactions of the **o2** and **o2-6** dimers, these computationally observed interactions have to be

interpreted as being weaker, which is in accord with their higher relative energies and the fact that these dimers are not observed experimentally.

5.5 Conclusion

Mono-chloro and mono-methyl substituted N-phenyl-N'-sulfinylhydrazine (PhNHNSO) dimers have been analyzed using FTIR spectroscopy and computational methods. The experimental IR spectra revealed a red shift of the frequency of the N-H stretching vibration for meta and para substituted PhNHNSOs, suggesting the presence of dimers. On the other hand, ortho substituted PhNHNSOs show no shift in the frequency of the N-H stretching vibration, indicating the absence of hydrogen bonding interactions. B3LYP/6-31+G calculations reveal a good agreement with the experimental red shift in meta and para substituted PhNHNSOs. Computational analyses of energies, geometries and electron densities revealed that bifurcated N-H---O and C-H---O interactions in meta and para substituted dimers contribute towards the stability of the dimers, and are characterized as H-bond and anti-H bond, respectively. In the ortho substituted dimers, the observed N-H---O interactions are identified as comparatively weaker and the dimerization of two ortho monomers is considered unfavourable, which is in good agreement with the experimental findings. Ortho-substituted monomers with an ortho hydrogen in the correct position for the formation of bifurcated H-bonds would yield dimers with comparable stability to meta and para dimers, but are not populated.

Chapter 6

Conclusions and future work

This study was prompted by experimental observations in the dimerization behaviour of N-phenyl-N'-sulfinylhydrazines (PhNHNSO) made in this group. From FTIR studies it was obvious that PhNHNSO dimerized through H-bond formation in the solution. Such behaviour was altered upon the introduction of a substituent (chloro or methyl) in the ortho position of the aromatic ring and dimerization did not occur, whereas meta and para substitution did not affect the dimerization. The large effect of the substituent position in the ortho case suggested a change in the H-bonding pattern. It also pointed to a possible involvement of the ortho hydrogen atoms in the H-bonding network. A much smaller substituent effect was observed for meta and para substituted PhNHNSOs. This research was thus directed to the proper understanding of H-bonding interactions in unsubstituted and substituted PhNHNSOs, as well as to the influence of substituents on dimerization in order to explain the observed experimental behaviour. For the most part, B3LYP calculations with various basis sets were carried out to provide energies, frequencies and geometries of monomers and dimers, and wave functions for electron densities. The latter were analyzed within the quantum theory of atoms in molecules.

The first part of this research focused on the unsubstituted PhNHNSO monomer and dimer. Four possible configurations *syn*, *sickle*, *anti1* and *anti2* were considered and the *syn* configuration was found to be by far energetically favoured. The comparison of geometries of the *syn* monomer and its dimer revealed a lengthening of the N-H and shortening of an ortho C-H bond upon the formation of the dimer. A corresponding red

shift of the frequency of the N-H stretching vibration was found to be in good agreement with the experimental data. Patterns of H-bonding interactions in the *syn* monomer and its dimer were investigated using the quantum theory of atoms in molecules. Analyses of the electron densities confirmed the presence of an intramolecular N-H---O interaction in the monomer and intermolecular N-H---O and C-H---O interactions in the dimer. According to established criteria in the electron density, both intermolecular interactions can be characterized as hydrogen bonds. A blue shift of the frequency of the C-H stretching vibration further classifies the C-H----O interaction as an anti-hydrogen bond. The observed bifurcated H-bonding interactions provide evidence for the involvement of the ortho C-H bond in the dimerization.

The second part of this research focused on the investigation of substituted PhNHNSO monomers. The substituents covered all five available aromatic positions in mono-substitution. Among the five different substituted monomers for a given substituents, ortho substituted compounds were found to be least stable. Amongst the two possible ortho positions, ortho2 was the energetically much more favoured rotamer. The effect of position and nature of the substituent on three important (because hydrogen bond forming) bonds, N-H, ortho C-H and S=O, was investigated. It was found that geometries, frequencies and electron densities of N-H and S=O bonds are more affected by ortho than by meta and para substitution. Electron withdrawing substituents NO_2 and CN generally have a greater effect than electron donating substituents OCH_3 and OH. Correlation analyses between bond distances, frequencies and electron densities revealed that, in general, the S=O bond gives better correlations than N-H and ortho C-H bonds. Linear correlations with Hammett substituent constants are observed for all three bonds.

The strong electron-withdrawing substituents NO_2 and CN give shorter distances, and higher electron densities, frequencies and atomic charges compared to electron-donating substituents OCH_3 and OH. Even though N-H and ortho C-H bonds show less satisfying correlations, similar trends are observed for all three bonds, suggesting similar effects of electron-withdrawing or electron-donating substituents on all bonds. It is clear from Hammett correlations that for N-H bonds, a better correlation is obtained for para substitution. For ortho C-H bonds, **m5** substitution shows the best correlation, which is in line with the **m5** position being para to the C-H bond. The higher electron densities in these bonds induced by the electron withdrawing substituents suggest that these compounds can form stronger H-bonds.

The third part of this research focused on the chloro and methyl substituted PhNHNSO dimers. Calculations showed that ortho substituted dimers are less stable compared to meta and para substituted dimers, and chloro substituted dimers show stronger interaction and free energies of dimerization than methyl substituted dimers. The bifurcated nature of the H-bonding pattern of intermolecular N-H---O and C-H---O interactions that was present in the unsubstituted dimer persists with meta and para substitution and in ortho substituted compounds that have an ortho C-H bond available. The exceptional cases are dimers with substituent in ortho2 position, as these can only exhibit N-H---O interactions. Meta and para substituted dimers have stronger N-H---O and C-H---O interactions than ortho substituted dimers. Considering the values of $\rho(r)$, $\nabla^2\rho(r)$ and all integrated properties, we conclude that N-H---O interactions of dimers involving ortho2 substituted monomers are comparatively weak in nature. This seems to be due to the highly twisted geometries of the ortho-substituted dimers, induced through

unfovourable atomic interactions, for example between Cl and O (in ortho2) or N (in ortho6).

A rather intriguing story thus has a quite simple explanation in the end. A bifurcated hydrogen bonding network is necessary to properly stabilize PhNHNSO dimers. One ortho substituted rotamer (ortho2) does not allow for this, the other (ortho6) is too unstable and therefore not available for dimer formation. Substituents effects for meta and para substitution are much smaller. In the present study, we chose methyl and chloro substituents for experimental convenience. Because these have similar Hammett σ constants, the observed substituent effects for meta and para substitution were rather small. Future studies should focus on substituents that have vastly different Hammett σ constants, such as NO_2 and OCH_3, to amplify the already observed effects on dimerization energy.

The FTIR spectra of chloro and methyl substituted dimers did not allow an evaluation of differences in dimer strength in terms of observed red shift. We expect to observe experimentally different amounts of red shift with the use of substituents such as NO_2 and OCH_3. Furthermore, FTIR spectroscopy is not an ideal technique to demonstrate the ortho C-H involvement in the hydrogen bonding network. Proton NMR studies should be much more suited. Especially for substituted compounds, we expect to be able to observe chemical shift difference in dilution studies for ortho C-H nucleus only. NMR studies might also allow determining dimer strengths quantitatively for comparison with our calculated values.

References

(1) Jeffrey, G. A. *An introduction to hydrogen bonding*; Oxford University Press: Oxford, U. K., 1997.

(2) Desiraju, G. R.; Steiner, T. *The weak hydrogen bond: in structural chemistry and biology*; Oxford University Press Inc., New York, 1999.

(3) Jeffrey, G. A.; Saenger, W. *Hydrogen bonding in biological structures*; Springer-Verlag: Berlin, New York, 1991.

(4) Scheiner, S. *Hydrogen bonding: a theoretical perspective*; Oxford University Press: New York; Oxford, 1997.

(5) Steed, J. W. *Supramolecular chemistry*; John Wiley: England, 2000.

(6) Latimer, W. M.; Rodebush, W. H. *J. Am. Chem. Soc.* **1920**, 42, 1419.

(7) Pauling, L. *J. Am. Chem. Soc.* **1931**, 53, 1367.

(8) Tewari, K. S.; Mehrota, S. N.; Vishnoi, N. K. *A textbook of organic chemistry*; Vikas Publishing House Pvt. Ltd.: New Delhi, 1992.

(9) Prins, L. J.; Reinhoudt, D. N.; Timmerman, P. *Angew. Chem. Int. Ed. Engl.* **2001**, 40, 2382.

(10) Hobza, P.; Špirko, V.; Selzle, H. L.; Schlag, E. W. *J. Phys. Chem. A* **1998**, 102, 2501.

(11) Hobza, P.; Špirko, V.; Havlas, Z.; Buchhold, K.; Reimann, B.; Barth, H. D.; Brutschy, B. *Chem. Phys. Lett.* **1999**, 299, 180.

(12) Hobza, P.; Havlas, Z. *Chem. Rev.* **2000**, 100, 4253.

(13) Steiner, T.; Desiraju, G. R. *Chem. Commun.* **1998**, 891.

(14) Jensen, F. *Introduction to computational chemistry*; John Wiley & Sons Ltd.: Baffins Lane, 1999.

(15) Becke, A. D. *J. Chem. Phys.* **1993**, 98, 5648.

(16) Lee, C.; Yang, W.; Parr, R. G. *Phys. Rev. B* **1988**, 37, 785.

(17) Novoa, J. J.; Sosa, C. *J. Phys. Chem. A* **1995**, 99, 15837.

(18) Georgievaa, I.; Binev, D.; Trendafilova, N.; Bauer, G. *Chem. Phys.* **2003**, 286, 205.

(19) Latajka, Z.; Bouteiller, Y. *J. Chem. Phys.* **1994**, 101, 9793.

(20) Lu, J.; Zhou, Z.; Wu, Q.; Zhao, G. *J. Mol. Struc. (Theochem)* **2005**, 724, 107.

(21) Isaacs, N. S. *Physical organic chemistry*, Harlow, Essex, England: Longman Scientific & Technical; New York: Wiley, 1987.

(22) Mcmurry, J. *Organic chemistry*; Brooks/Cole Publishing Company: California, 1984.

(23) Sengar, R. S.; Nemykin, V. N.; Basu, P. *New J. Chem.* **2003**, 27, 1115.

(24) Bueno, W. A.; Lucisano, Y. M. *Spec. Acta, Part A: Mol. and Biomol. Spec.* **1979**, 35A, 381.

(25) Drago, R. S.; Epley, T. D. *J. Am. Chem. Soc.* **1969**, 91, 2883.

(26) Kawahara, S.; Wada, T.; Kawauchi, S.; Uchimaru, T.; Sekine, M. *J. Phys. Chem. A* **1999**, 103, 8516.

(27) Kawahara, S.; Uchimaru, T. *Eur. J. Org. Chem.* **2003**, 2577.

(28) Vaschetto, M. E.; Retamal, B. A.; Monkman, A. P. *J. Mol. Struct. (Theochem)* **1999**, 468, 209.

(29) Ahn, D.; Park, S.; Lee, S. *J. Phys. Chem. A* **2003**, 107, 131.

(30) http://www.iupac.org/reports/1999/7110minkin/i.html.

(31) Boys, S. F.; Bernardi, F. *Mol. Phys.* **1970**, 19, 553.

(32) Bader, R. F. W. *Atoms in Molecules: a quantum theory*; Clarendon: Oxford, UK, 1990.

(33) Popelier, P. *Atoms in Molecules: an introduction.*; Prentice-Hall, Harlow, 2000.

(34) Koch, U.; Popelier, P. L. A. *J. Phys. Chem. A* **1995**, 99, 9747.

(35) Carroll, M. T.; Bader, R. F. W. *Mol. Phys.* **1988**, 65, 695.

(36) Cubero, E.; Orozco, M.; Hobza, P.; Luque, F. J. *J. Phys. Chem. A* **1999**, 103, 6394.

(37) Gàlvez, O.; Gómez, P. C.; Pacios, L. F. *J. Chem. Phys.* **2001**, 115, 11166.

(38) Reichardt, C. *Solvents and solvent effects in organic chemistry*; Weinheim, Federal Republic of Germany; New York, NY, USA: VCH., 1988.

(39) Foresman, J. B. *Exploring chemistry with electronic structure methods*, Second Edition ed.; Gaussian, Inc.: Pittsburgh, PA.

(40) Cramer, C. J. *Essentials of computational chemistry*; John Wiley: New York, 2002.

(41) Klamt, A.; Schuurmann, G. *J. Chem. Soc. Perkin Trans.2* **1993**, 799.

(42) Michaelis, A. *Ber.* **1889**, 22, 2228.

(43) Wegler, R.; Unterstenhofer, G. Sulfur-containing arylhydrazines as pesticides. In *US 2898265 (Patent language unavailable)* USA, 1959.

(44) Gieren, A.; Dederer, B. *Angew. Chem. Int. Ed. Engl.* **1977**, 16, 179.

(45) Schanda, F.; Gieren, A. *Acta Cryst.* **1984**, C40, 306.

(46) Marion, D. *419 Thesis*; Concordia University, Montreal, 2001.

(47) Zhang, D. J. *450 Thesis*; Concordia University, Montreal, 2004.

(48) Napoli, P. *450 Thesis*; Concordia University, Montreal, 2002.

(49) Bernardi, A. *419 Thesis*; Concordia University, Montreal, 2004.

(50) Hadzi, D. *Theoretical treatments of hydrogen bonding*; John Wiley & Sons Ltd.: Chichester, 1997.

(51) Pawlukojc, A.; Leciejewicz, J. *Chem. Phys.* **2004**, 299, 39.

(52) Dubis, A. T.; Grabowski, S. J. *J. Phys. Chem. A* **2003**, 107, 8723.

(53) Wang, B.; Hinton, J. F.; Pulay, P. *J. Phys. Chem. A* **2003**, 107, 4683.

(54) Dubis, A. T.; Grabowski, S. J.; Romanowska, D. B.; Misiazek, T.; Leszczynski, J. *J. Phys. Chem. A* **2002**, 106, 10613.

(55) Muchall, H. M. *J. Phys. Chem. A* **2001**, 105, 632.

(56) Muchall, H. M. (http://www.arkat-sa.org/ark/journal/Volume2/Part3 /Tee/OT-304C/304.htm).

(57) Grabowski, S. J. *J. Mol. Struct.* **2002**, 615, 239.

(58) Kolandaivel, P.; Nirmala, V. *J. Mol. Struct.* **2004**, 694, 33.

(59) Wojtulewski, S.; Grabowski, S. J. *J. Mol. Struct.* **2003**, 645, 287.

(60) Cheeseman, J. R.; Carroll, M. T.; Bader, R. F. W. *Chem Phys. Lett.* **1988**, 143, 450.

(61) Gàlvez, O.; Gómez, P. C.; Pacios, L. F. *J. Chem. Phys.* **2003**, 118, 4878.

(62) Pearce, L. B.; Feingold, M. H.; Cerny, K. F.; Anselme, J.-P. *J. Org. Chem.* **1979**, 44, 1881.

(63) Frisch, M. J.; Trucks, G. W.; Schlegel, H. B.; Scuseria, G. E.; A., R. M.; Cheeseman, J. R.; Zakrzewski, V. G.; Montgomery, J. A., Jr.; Stratmann, R. E.; Burant, J. C.; Dapprich, S.; Millam, J. M.; Daniels, A. D.; Kudin, K. N.; Strain, M. C.; Farkas, O.; Tomasi, J.; Barone, V.; Cossi, M.; Cammi, R.; Mennucci, B.; Pomelli, C.; Adamo, C.; Clifford, S.; Ochterski, J.; Petersson, G. A.; Ayala, P. Y.; Cui, Q.; Morokuma, K.; Malick, D. K.; Rabuck, A. D.; Raghavachari, K.; Foresman, J. B.; Cioslowski, J.; Ortiz, J. V.; Stefanov, B. B.; Liu, G.; Liashenko, A.; Piskorz, P.; Komaromi, I.; Gomperts, R.; Martin, R. L.; Fox, D. J.; Keith, T.; Al-Laham, M. A.; Peng, C. Y.; Nanayakkara, A.; Gonzalez, C.; Challacombe, M.; Gill, P. M. W.; Johnson, B. G.; Chen, W.; Wong, M. W.; Andres, J. L.; Head-Gordon, M.; Replogle, E. S.; Pople, J. A. *Gaussian 98, Revision A.7*; Gaussian, Inc.: Pittsburgh, PA, 1998.

(64) Bertran, J.; Oliva, A.; Rodriguez-Santiago, L.; Sodupe, M. *J. Am. Chem. Soc.* **1998**, 120, 8159.

(65) Sim, F.; St-Amant, A.; Papai, I.; Salahub, D. R. *J. Am. Chem. Soc.* **1992**, 114, 4391.

(66) Biegler-Koenig, F. W.; Bader, R. F. W.; Tang, T. J. *J. Comput. Chem.* **1982**, 3, 317.

(67) The AIMPAC suite of programs is available from Professor R. F. W. Bader, McMaster University, Hamilton, ON L8S 4M1, Canada and from the AIMPAC website (www.chemistry.mcmaster.ca/aimpac).

(68) Biegler-König, F. *AIM2000*; University of Applied Sciences: Bielefeld, Germany.

(69) Klemperer, W.; Cronyn, M. W.; Maki, A. H.; Pimental, G. C. *J. Am. Chem. Soc.* **1954**, 76, 5846.

(70) Eliel, E. L.; Wilen, S. H.; Mander, L. N. *Stereochemistry of organic compounds*; Wiley & Sons Ltd.: New York, 1994.

(71) Scott, A. P.; Radom, L. *J. Phys. Chem. A* **1996**, 100, 16502.

(72) Andersson, M. P.; Uvdal, P. *J. Phys. Chem. A* **2005**, 109, 2937.

(73) Matsuura, H.; Yoshida, H.; Hieda, M.; Yamanaka, S.; Harada, T.; Shin-Ya, K.; Ohno, K. *J. Am. Chem. Soc.* **2003**, 125, 13910.

(74) Kawahara, S.; Uchimaru, T.; Taira, K.; Sekine, M. *J. Phys. Chem. A* **2001**, 105, 3894.

(75) Chocholoušová, J.; Vacek, J.; Hobza, P. *J. Phys. Chem. A* **2003**, 107, 3086.

(76) Wiberg, K. B. *J. Org. Chem.* **2002**, 67, 4787.

(77) Bohm, S.; Fiedler, P.; Exner, O. *New J. Chem.* **2004**, 28, 67.

(78) Li, Z.; Cheng, J. *J. Org. Chem.* **2003**, 68, 7350.

(79) Arulmozhiraja, S.; Sato, T.; Yabe, A. *J. Org. Chem.* **2003**, 68, 5084.

(80) Wiberg, K. B.; Breneman, C. M. *J. Am. Chem. Soc.* **1990**, 8765.

(81) Chandra, A. K.; Nam, P.; Nguyen, M. T. *J. Phys. Chem. A* **2003**, 107, 9182.

(82) Pihlaja, K.; Ovcharenko, V.; Kolehmainen, E.; Laihia, K.; Fabian, W. M. F.; Dehne, H.; Perjessy, A.; Kleist, M.; Teller, J.; Sustekova, Z. *J. Chem. Soc. Perkin Trans.2* **2002**, 329.

(83) Ilieva, S.; Hadjieva, B.; Galabov, B. *J. Org. Chem.* **2002**, 67, 6210.

(84) Deford, J.; Chu, F.; Anslyn, E. V. *Tetrahedron Lett.* **1996**, 37, 1925.

(85) Hansch, C.; Leo, A.; Taft, R. W. *Chem. Rev.* **1991**, 91, 165.

(86) Malla, P.; Muchall, M. H. *J. Phys. Chem. A* **To be submitted**.

(87) Woon, D. E.; Dunning, T. H., Jr. *J. Chem. Phys.* **1993**, 98, 1358.

(88) Remko, M. *J. Phys. Chem. A* **2003**, 107, 720.

(89) Romano, R. M.; Della Vedova, C. O.; Boese, R.; Hildebrandt, P. *Phys. Chem. Chem. Phys.* **1999**, 1, 2551.

(90) Meng, F.; Liu, C.; Xu, W. *Chem. Phys. Lett.* **2003**, 373, 72.

(91) Malla, P.; Muchall, H. M. *J. Phys. Chem. A* **To be submitted**.

(92) Biegler-Koenig, F. *AIM2000*; University of Applied Sciences: Bielefeld, Germany.

(93) Avram, M. *Infrared spectroscopy applications in organic chemistry*; New York, Wiley-Interscience, 1972.

(94) Aquino, A. J. A.; Tunega, D.; Haberhauer, G.; Gerzabeck, M. H.; Lischka, H. *J. Phys. Chem. A* **2002**, 106, 1862.

(95) Colominas, C.; Teixidó, J.; Cemeli, J.; Luque, F. J.; Orozco, M. *J. Phys. Chem. B* **1998**, 102, 2269.

(96) Yekeler, H. *J. Computer-Aided Molecular Design* **2001**, 15, 287.

(97) Grabowski, S. J. *J. Phys. Chem. A* **2001**, 105, 10739.

(98) Ichikawa, M. *Acta Cryst.* **1978**, B34, 2074.

(99) Grabowski, S. *J. Phys. Chem. A* **2000**, 104, 5551.

Appendix A: Supplemental information related to Chapter 3

Table A.1: Selected geometrical parameters (distances in pm, angles in degrees) of *syn* monomer at different levels of theory.

	HF/6-31+G(d)	HF/6-311+G(2d,p)	B3LYP/6-311+G(2d,p)
S=O	146.9	144.7	149.6
N=S	154.0	152.0	158.5
N-N	129.6	130.2	131.5
N-H	100.3	99.8	102.0
N-C	140.2	139.7	140.0
C2-H	107.6	107.5	108.4
(N)H---O	224.0	231.4	222.6
NSO	111	113	112
NNS	119	121	117
NNH	118	118	117
N-H---O	108	106	110
NNSO	0	0	0
CNNS	180	180	180

Appendix B: Supplemental information related to Chapter 4

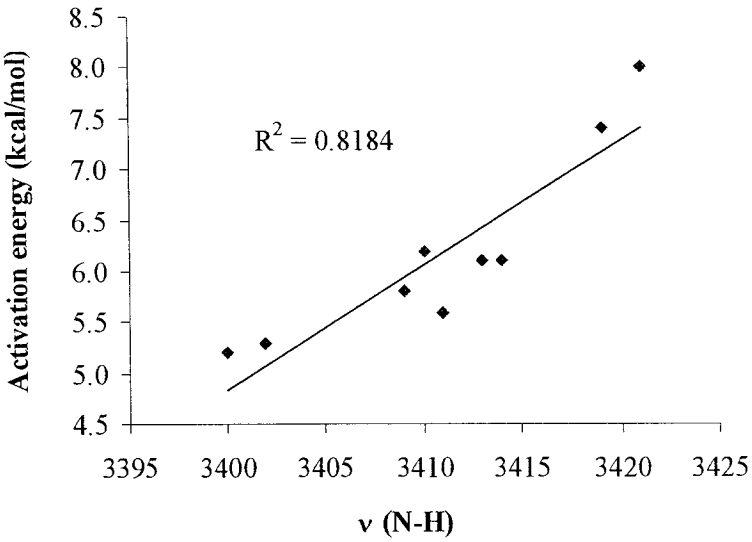

(a)

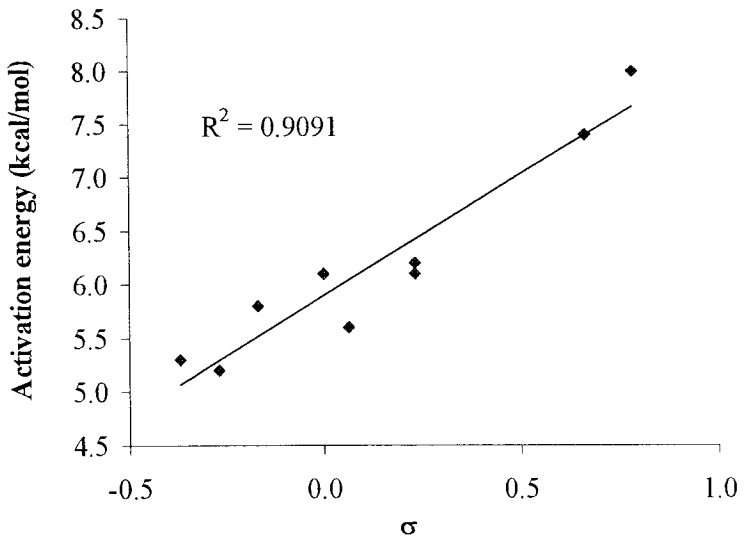

(b)

Fig. B.1: Plots of activation energy with (a) frequency (ν, cm^{-1}) and (b) Hammett substituent constant (σ) for the N-H bond of para substituted compounds from B3LYP/6-31+G(d).

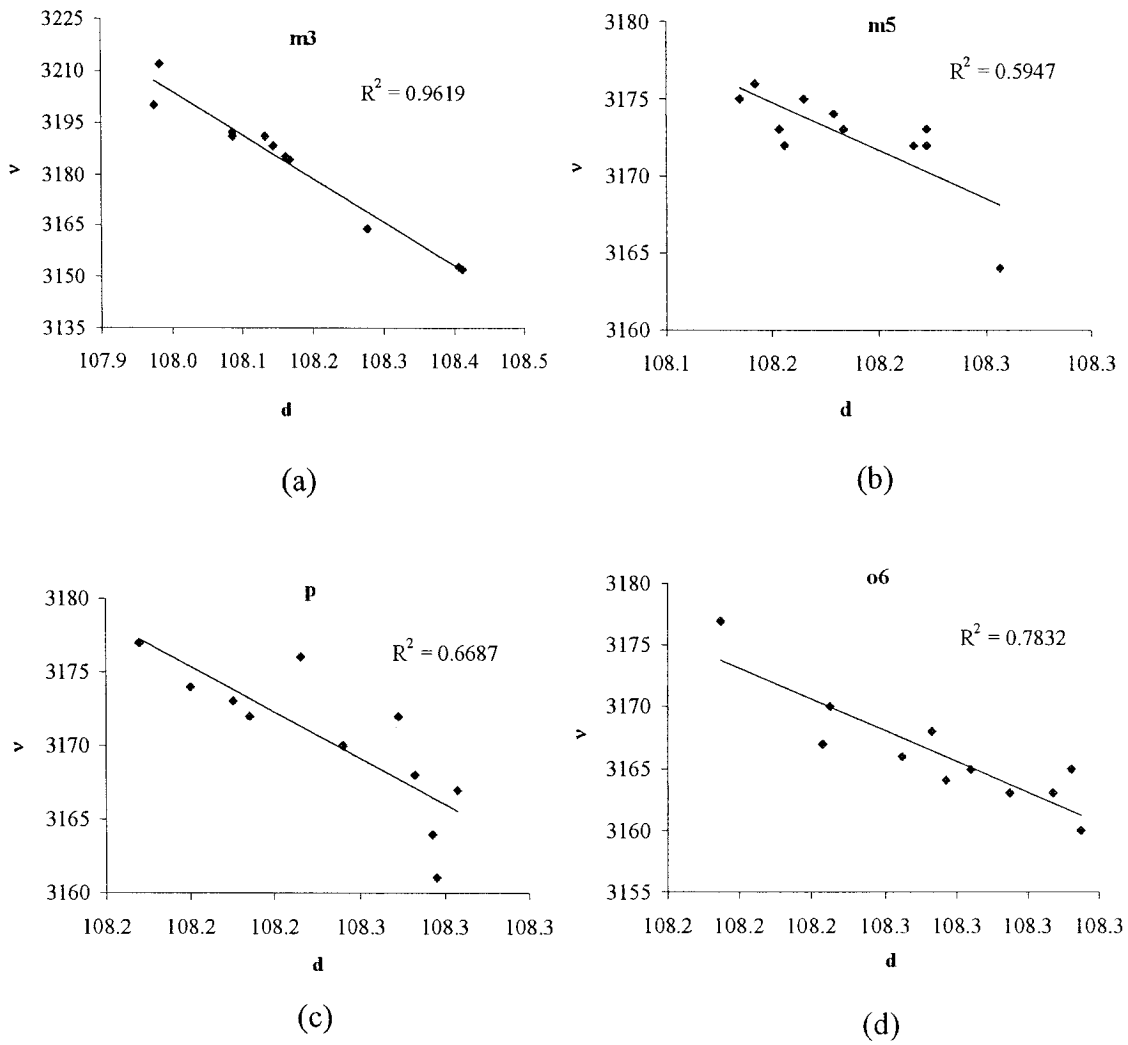

Fig. B.2: Plots of bond distance (d, pm) and frequency (ν, cm^{-1}) for the ortho C-H bond (a) **m3** (b) **m5** (c) **p** (d) **o6** from B3LYP/cc-pVTZ.

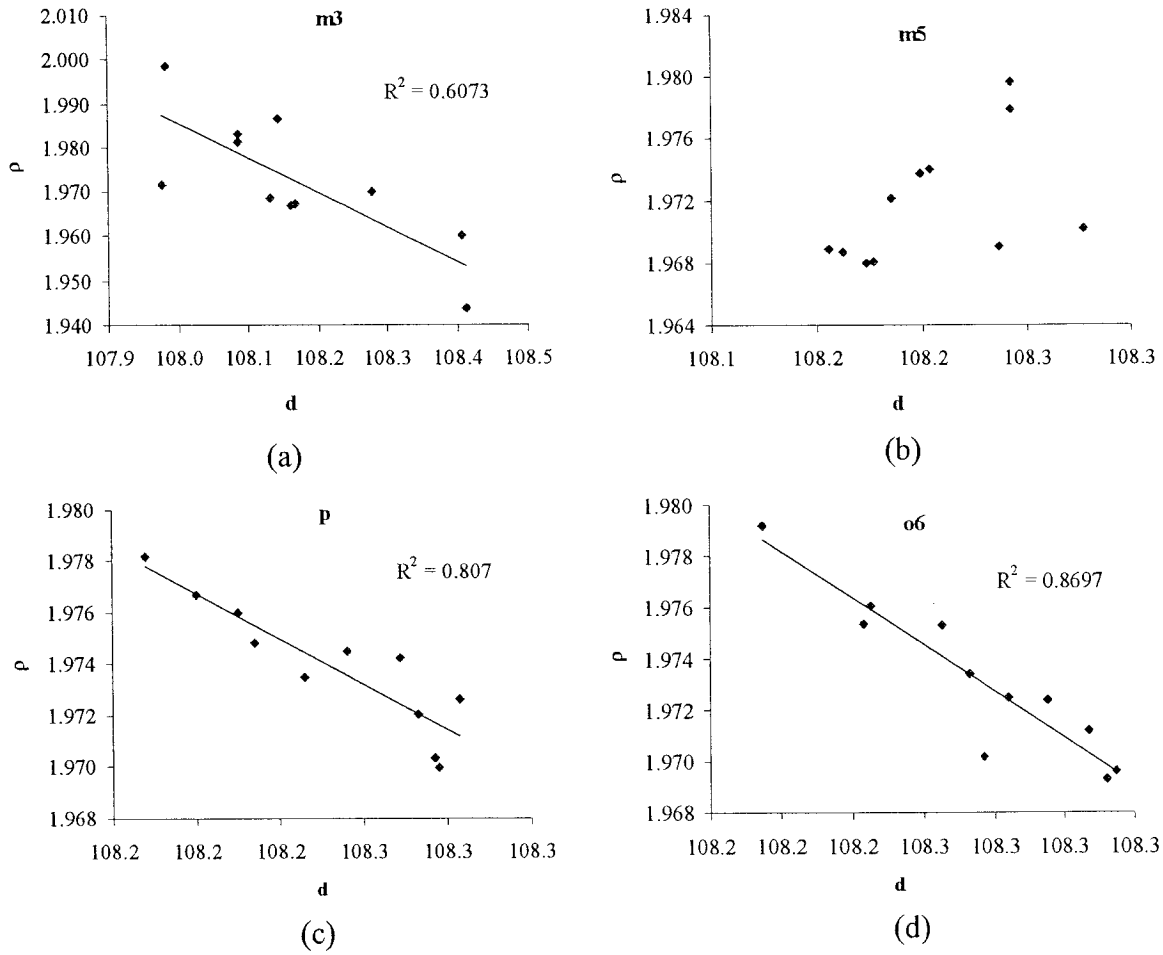

Fig. B.3: Plots of bond distance (d, pm) and electron density (ρ, e/Å^3) for the ortho C-H bond (a) **m3** (b) **m5** (c) **p** (d) **o6** from B3LYP/cc-pVTZ.

Table B.1: Total energies (ZPVE- corrected in au) for the most stable configurations at the B3LYP level with three different basis sets.

	B3LYP/	Configurations	E_{total}
OH	6-31+G(d)	**o6(b)**	-890.223247
	6-311+G(2d,p)		-890.401104
	cc-pVTZ		-890.434379
OMe	6-31+G(d)	**m5(b)**	-929.499186
	6-311+G(2d,p)		-929.683797
	cc-pVTZ		-929.720028
Me	6-31+G(d)	**m5**	-854.295758
	6-311+G(2d,p)		-854.457433
	cc-pVTZ		-854.489775
F	6-31+G(d)	**m5**	-914.25385
	6-311+G(2d,p)		-914.43444
	cc-pVTZ		-914.46819

(Continues on next page)

Table B.1 (Continued)

	B3LYP/	Configurations	E_{total}
Cl	6-31+G(d)	**m5**	-1274.608533
	6-311+G(2d,p)		-1274.789004
	cc-pVTZ		-1274.825681
Br	6-31+G(d)	**m5**	-3386.14060
	6-311+G(2d,p)		-3388.70334
	cc-pVTZ		-3388.82003
CN	6-31+G(d)	**p**	-907.251208
	6-311+G(2d,p)		-907.425208
	cc-pVTZ		-907.459928
NO_2	6-31+G(d)	**p**	-1019.512267
	6-311+G(2d,p)		-1019.722805
	cc-pVTZ		-1019.761122

Table B.2: Bond distances (pm) and frequencies (cm^{-1}) of the N-H stretching vibration of substituted compounds from B3LYP with three different basis sets.

		6-31+G(d)		6-311+G(2d,p)		cc-pVTZ	
		Distance	Frequency	Distance	Frequency	Distance	Frequency
H		102.6	3413	102.0	3449	101.8	3441
OH	**m3(a)**	102.5	3418	102.0	3453	101.8	3446
	m3(b)	102.6	3410	102.0	3449	101.8	3442
	m5(a)	102.5	3418	102.0	3453	101.8	3447
	m5(b)	102.5	3418	102.0	3453	101.8	3448
	p(a)	102.6	3402	102.1	3442	101.9	3435
	p(b)	102.6	3401	102.1	3440	101.9	3433
	o2(a)	102.5	3434	102.0	3466	101.8	3463
	o6(a)	102.8	3370	102.2	3415	102.1	3403
	o6(b)	102.8	3384	102.2	3426	102.0	3417
OMe	**m3(a)**	102.5	3415	102.0	3450	101.8	3444
	m3(b)	102.6	3411	102.0	3447	101.8	3442
	m5(a)	102.5	3417	102.0	3454	101.8	3447
	m5(b)	102.5	3415	102.0	3452	101.8	3444
	p(a)	102.6	3402	102.1	3441	101.9	3432
	p(b)	102.6	3400	102.1	3439	101.9	3430

(continues on next page)

Table B.2 (Continued)

		6-31+G(d)		6-311+G(2d,p)		cc-pVTZ	
		Distance	Frequency	Distance	Frequency	Distance	Frequency
	o2(a)	102.5	3436	101.9	3468	101.8	3463
	o6(a)	102.7	3378	102.2	3421	102.1	3399
	o6(b)	102.6	3398	102.1	3434	102.0	3422
Me	**m3**	102.6	3411	102.0	3448	101.8	3442
	m5	102.6	3412	102.0	3448	101.8	3441
	p	102.6	3409	102.0	3446	101.9	3439
	o2	102.4	3433	101.9	3468	101.7	3461
	o6	102.8	3384	102.2	3419	102.0	3409
F	**m3**	102.5	3417	102.0	3453	101.8	3445
	m5	102.5	3419	102.0	3454	101.8	3447
	p	102.6	3411	102.0	3448	101.9	3440
	o2	102.4	3436	101.9	3468	101.8	3461
	o6	102.7	3383	102.2	3425	102.0	3416
Cl	**m3**	102.5	3416	102.0	3451	101.8	3444
	m5	102.5	3418	102.0	3453	101.8	3447
	p	102.5	3414	102.0	3449	101.8	3444
	o2	102.5	3426	102.0	3457	101.8	3451
	o6	102.6	3396	102.1	3436	101.9	3422

(continues on next page)

Table B.2 (Continued)

		6-31+G(d)		6-311+G(2d,p)		cc-pVTZ	
		Distance	Frequency	Distance	Frequency	Distance	Frequency
Br	**m3**	102.5	3415	102.0	3453	101.8	3446
	m5	102.5	3417	102.0	3453	101.8	3447
	p	102.6	3410	102.0	3450	101.8	3444
	o2	102.5	3411	102.0	3442	101.8	3438
	o6	102.7	3377	102.0	3440	101.9	3424
CN	**m3**	102.5	3417	102.0	3452	101.8	3445
	m5	102.5	3419	102.0	3455	101.8	3447
	p	102.5	3419	102.0	3453	101.8	3446
	o2	102.6	3413	102.1	3440	101.9	3436
	o6	102.6	3401	102.1	3438	101.9	3431
NO_2	**m3**	102.5	3422	102.5	3394	101.8	3447
	m5	102.5	3421	102.0	3455	101.8	3448
	p	102.5	3421	102.0	3454	101.8	3447
	o2	102.6	3407	102.2	3417	102.0	3414
	o6	102.5	3419	102.0	3452	101.8	3444

Table B.3: Bond distances (pm) and frequencies (cm^{-1}) of the ortho C-H stretching vibration of substituted compounds from B3LYP with three different basis sets.

		6-31+G(d)		6-311+G(2d,p)		cc-pVTZ	
		Distance	Frequency	Distance	Frequency	Distance	Frequency
H		108.8	3182	108.4	3161	108.3	3164
OH	**m3(a)**	108.6	3204	108.4	3180	108.2	3185
	m3(b)	108.9	3167	108.6	3148	108.4	3152
	m5(a)	108.7	3192	108.3	3173	108.2	3176
	m5(b)	108.7	3190	108.3	3171	108.2	3175
	p(a)	108.7	3187	108.4	3166	108.3	3170
	p(b)	108.7	3192	108.4	3172	108.2	3176
	o6(a)	108.8	3181	108.5	3162	108.3	3163
	o6(b)	108.8	3183	108.5	3172	108.3	3165
OMe	**m3(a)**	108.7	3201	108.4	3179	108.2	3184
	m3(b)	108.5	3215	108.2	3195	108.0	3200
	m5(a)	108.7	3189	108.4	3169	108.2	3172
	m5(b)	108.7	3190	108.3	3170	108.2	3173
	p(a)	108.8	3185	108.5	3164	108.3	3167
	p(b)	108.8	3186	108.4	3165	108.3	3168
	o6(a)	108.8	3182	108.5	3163	108.3	3163
	o6(b)	108.8	3183	108.4	3163	108.3	3165

(continues on next page)

Table B.3 (Continued)

		6-31+G(d)		6-311+G(2d,p)		cc-pVTZ	
		Distance	Frequency	Distance	Distance	Frequency	Distance
Me	**m3**	108.9	3167	108.6	3148	108.4	3153
	m5	108.8	3187	108.4	3168	108.2	3172
	p	108.8	3177	108.5	3157	108.3	3161
	o6	108.8	3176	108.5	3157	108.3	3160
F	**m3**	108.6	3211	108.3	3187	108.1	3191
	m5	108.7	3192	108.4	3172	108.2	3175
	p	108.7	3191	108.4	3170	108.2	3173
	o6	108.8	3185	108.5	3164	108.3	3168
Cl	**m3**	108.6	3208	108.3	3187	108.1	3192
	m5	108.7	3191	108.4	3170	108.2	3174
	p	108.7	3189	108.4	3169	108.2	3172
	o6	108.8	3186	108.4	3165	108.3	3166
Br	**m3**	108.6	3209	108.3	3186	108.1	3191
	m5	108.7	3190	108.4	3170	108.2	3173
	p	108.7	3189	108.4	3168	108.3	3172
	o6	108.8	3180	108.4	3167	108.2	3167

(continues on next page)

Table B.3 (Continued)

		6-31+G(d)		6-311+G(2d,p)		cc-pVTZ	
		Frequency	Distance	Distance	Frequency	Distance	Distance
CN	**m3**	108.6	3183	108.3	3183	108.1	3188
	m5	108.7	3189	108.4	3168	108.2	3172
	p	108.7	3192	108.4	3171	108.2	3174
	o6	108.7	3187	108.4	3167	108.2	3170
NO_2	**m3**	108.4	3232	108.4	3184	108.0	3212
	m5	108.7	3192	108.4	3170	108.2	3173
	p	108.7	3195	108.4	3174	108.2	3177
	o6	108.7	3192	108.4	3171	108.2	3173

Table B.4: Bond distances (pm) and frequencies (cm^{-1}) of the S=O stretching vibration of substituted compounds from B3LYP with three different basis sets.

		6-31+G(d)		6-311+G(2d,p)		cc-pVTZ	
		Distance	Frequency	Distance	Frequency	Distance	Frequency
H		151.7	1068	149.5	1083	149.8	1098
OH	**m3(a)**	151.6	1071	149.5	1087	149.7	1103
	m3(b)	151.7	1068	149.6	1086	149.8	1110
	m5(a)	151.7	1071	149.5	1086	149.7	1101
	m5(b)	151.6	1070	149.5	1084	149.7	1115
	p(a)	151.9	1062	149.8	1080	150.0	1097
	p(b)	152.0	1061	149.8	1080	150.0	1097
	o2(a)	151.5	1074	149.4	1089	149.6	1104
	o6(a)	152.1	1056	149.7	1078	149.9	1099
	o6(b)	151.8	1058	150.0	1083	150.2	1094
OMe	**m3(a)**	151.7	1069	149.6	1088	149.8	1105
	m3(b)	151.8	1067	149.7	1086	149.8	1101
	m5(a)	151.7	1067	149.6	1085	149.8	1102
	m5(b)	151.7	1067	149.6	1084	149.8	1098
	p(a)	152.0	1061	149.9	1079	150.0	1098
	p(b)	152.0	1060	149.9	1078	150.1	1097

(continues on next page)

Table B.4 (Continued)

		6-31+G(d)		6-311+G(2d,p)		cc-pVTZ	
		Distance	Frequency	Distance	Distance	Frequency	Distance
	o2(a)	151.6	1071	149.5	1087	149.7	1104
	o6(a)	152.1	1058	149.8	1081	150.2	1095
	o6(b)	151.9	1061	150.0	1082	149.9	1099
Me	**m3**	151.8	1069	149.7	1086	149.8	1105
	m5	151.7	1069	149.7	1084	149.8	1101
	p	151.8	1066	149.7	1084	149.9	1102
	o2	151.8	1064	149.7	1083	149.9	1100
	o6	152.0	1059	149.9	1086	150.0	1101
F	**m3**	151.5	1074	149.4	1090	149.6	1112
	m5	151.5	1073	149.4	1086	149.6	1114
	p	151.7	1069	149.6	1084	149.8	1102
	o2	151.3	1079	149.2	1092	149.4	1108
	o6	151.8	1060	149.7	1080	149.9	1100
Cl	**m3**	151.5	1074	149.5	1087	149.6	1105
	m5	151.5	1072	149.4	1086	149.6	1105
	p	151.6	1071	149.5	1087	149.7	1101
	o2	151.2	1081	149.2	1094	149.3	1111
	o6	151.7	1073	149.6	1088	149.8	1104

(continues on next page)

Table B.4 (Continued)

		6-31+G(d)		6-311+G(2d,p)		cc-pVTZ	
		Distance	Frequency	Distance	Distance	Frequency	Distance
Br	**m3**	151.5	1073	149.4	1092	149.6	1105
	m5	151.5	1073	149.4	1091	149.6	1104
	P	151.6	1071	149.5	1091	149.6	1106
	o2	151.2	1080	149.1	1094	149.3	1111
	o6	151.8	1069	149.6	1087	149.8	1103
CN	**m3**	151.2	1079	149.2	1095	149.4	1109
	m5	151.3	1077	149.2	1091	149.4	1106
	p	151.2	1080	149.1	1096	149.3	1112
	o2	150.8	1090	148.7	1100	148.9	1113
	o6	151.4	1079	149.3	1093	149.5	1109
NO_2	**m3**	151.2	1082	151.2	1035	149.4	1119
	m5	151.3	1077	149.3	1088	149.4	1120
	p	151.1	1083	149.0	1097	149.3	1112
	o2	150.3	1113	148.3	1118	148.5	1129
	o6	151.3	1081	149.2	1094	149.4	1109

B.5 Discussion of other geometrical parameters

In **m3** position, N=N bond distance of **m3-OMe(a)**, **m3-OMe(b)** and **m3-Cl** compounds remain same as the unsubstituted PhNHNSO. But slight increase in bond distance of 0.1 pm is observed for N=S and C-N bonds. Species like **m3-OH(a)** and **m3-OH(b)** shows the changes in bond distance within the range of 0.1- 0.2 pm. Similarly, **m3-F**, **m3-Cl** and **m3-Br** have 0.3 pm longer N=N bond distances and 0.2 pm shorter N=S and C-N bonds. Bond angles change by 0.1 degree. More changes in bond angle is found with **m3-NO_2** which has longer N=N and shorter N=S and C-N bonds. The bond distance of N=N bond is 132.0 pm which is 0.6 pm longer than the PhNHNSO whereas N=S and C-N bonds are 0.5 and 0.4 pm shorter. There are some changes in bond angles, NNH, NNS and NSO angles are increased by 0.3, 0.1 and 0.4 degrees. For **m3-CN,** 0.5 pm longer N=N bond and 0.4 and 0.3 pm shorter N=S and C-N bonds are observed. Compared to electron withdrawing substituents, electron donating substituents give smaller change in geometries.

In **m5** position, no noticeable difference is observed and changes are the same as **m3** position. Substitution in **p** position tends to give more changes in geometries compared to **m3** and **m5** positions. Species like **p-CN** and **p-NO_2** have 0.6 pm and 0.8 pm longer N=N bonds and 0.5-0.9 pm shorter N=S and C-N bonds. Similarly, **p-F**, **p-Cl** and **p-Br**, also show small change in bond distances by about 0.1 to 0.2 pm.

A noticeable change is observed in **o2** position where CN and NO_2 substituents give significant changes in bond distances from 0.9 pm to 1.5 pm for N=N, N=S and C-N bonds. Bond angles are also changed by 0.8 degrees to 3.4 degrees. Among other substituents, F, Cl and Br substituents give changes in bond distance from 0.1 pm to 0.5

pm and in bond angle of 0.6 degrees to 1 degree. Comparatively, changes in bond distance with OH(**a**), OMe(**a**) and Cl substituents are small around 0.1 pm to 0.2 pm.

In **o6** position, **o6-OH(b)** has the longest N=S bond distance of 162.3 pm which is 1.5 pm longer than the unsubstituted PhNHNSO compound. Here again, the changes due to electron withdrawing groups are more significant than electron donating groups.

Finally, for the O---H bond distance, **o2** substitution has greater influence. As can be seen from the Table B.5, NO_2 substituent significantly elongates the O---H bond by 18.2 pm which is possibly due to the strong attractive interaction between the oxygen of NO_2 group and the hydrogen atom. The observed bond distance between the hydrogen of NH group and the oxygen of nitro group is 188.3 pm, suggesting that the hydrogen atom is pushed back to the side of oxygen atom of NO_2 without elongating the N-H bond. But the other substituents, F, Cl, Br and CN do not elongate the O---H bond as significantly as NO_2. They elongate O---H bond by 3.5 pm to 7.5 pm whereas Me shorten the O---H bond distance by 1.9 pm. This is due to the steric hindrance between methyl group and the hydrogen of the N-H bond. Upon comparison of geometries of all compounds, it is found that strong electron withdrawing substituents, CN and NO_2 are capable of giving substantial change when in **o2** and **o6** positions compared to electron donating substituents. Among all the substituted compounds, **o2** and **o6** substituted compounds experienced the most significant changes in their geometries compared to **m3**, **m5** and **p** substituted compounds.

Table B.5: Comparison of selected distances (pm) and bond angles (degrees) of the substituted compounds from B3LYP/6-31+G(d).

	N-N	N=S	C1-N	O---H	NNH	NNS	NSO
PhNHNSO	131.4	160.8	140.4	215.7	117.2	115.6	110.2
m3-OH(a)	131.5	160.7	140.4	216.5	117.2	115.7	110.3
m3-OH(b)	131.5	160.8	140.4	214.8	117.0	115.4	110.1
m3-OMe(a)	131.4	160.8	140.4	216.4	117.2	115.7	110.3
m3-OMe(b)	131.4	160.9	140.5	215.3	117.1	115.5	110.2
m3-Me	131.4	160.9	140.5	215.4	117.3	115.6	110.3
m3-F	131.7	160.6	140.2	216.3	117.3	115.6	110.3
m3-Cl	131.7	160.6	140.2	216.3	117.3	115.6	110.3
m3-Br	131.7	160.6	140.2	216.0	117.3	115.6	110.3
m3-CN	131.9	160.4	140.1	216.7	117.4	115.6	110.4
m3-NO_2	132.0	160.3	140.0	217.7	117.5	115.7	110.6
m5-OH(a)	131.5	160.7	140.3	216.3	117.3	115.6	110.3
m5-OH(b)	131.5	160.9	140.3	216.3	117.3	115.7	110.2
m5-OMe(a)	131.4	160.8	140.4	216.2	117.2	115.7	110.3
m5-OMe(b)	131.4	160.9	140.4	216.1	117.2	115.6	110.2
m5-Me	131.4	160.9	140.5	215.7	117.2	115.6	110.3

(continues on next page)

Table B.5 (Continued)

	N-N	N=S	C1-N	O---H	NNH	NNS	NSO
m5-F	131.7	160.6	140.1	216.4	117.3	115.6	110.3
m5-Cl	131.7	160.6	140.2	216.1	117.2	115.6	110.3
m5-Br	131.7	160.6	140.1	215.9	117.3	115.6	110.2
m5-CN	131.9	160.4	140.0	216.4	117.3	115.6	110.4
m5-NO_2	131.9	160.3	140.0	216.4	117.4	115.6	110.4
p-OH(a)	131.2	161.3	140.5	213.8	117.0	115.3	109.8
p-OH(b)	131.2	161.3	140.5	213.4	117.0	115.3	109.7
p-OMe(a)	131.2	161.3	140.5	213.9	117.0	115.3	109.8
p-OMe(b)	131.2	161.3	140.5	213.4	117.0	115.3	109.7
p-Me	131.3	160.0	140.4	215.2	117.2	115.5	110.2
p-F	131.5	160.9	140.4	215.0	117.2	115.5	110.0
p-Cl	131.6	160.7	140.2	215.6	117.2	115.5	110.2
p-Br	131.6	160.7	140.1	214.7	117.1	115.4	110.1
p-CN	132.0	160.3	139.7	217.0	117.3	115.7	110.5
p-NO_2	132.2	160.2	139.5	217.6	117.4	115.7	110.7
o2-OH(a)	131.6	160.7	140.0	221.1	118.4	116.1	110.8
o2-OMe(a)	131.5	160.8	140.0	220.5	118.5	115.9	110.7
o2-Me	131.5	160.9	140.6	213.8	118.0	116.1	110.9
o2-F	131.9	160.4	139.8	220.1	118.2	116.0	110.8
o2-Cl	131.9	160.3	139.8	220.8	118.0	116.1	110.9

(continues on next page)

Table B.5 (Continued)

	N-N	N=S	C1-N	O---H	NNH	NNS	NSO
o2-Br	131.9	160.3	139.8	219.2	117.9	115.8	110.8
o2-CN	132.4	159.9	139.5	223.4	118.0	116.6	111.4
o2-NO_2	132.8	159.4	138.9	233.9	120.6	117.4	112.8
o6-OH(a)	131.5	161.1	140.3	210.3	116.2	114.5	110.0
o6-OH(b)	131.4	162.3	140.4	210.5	116.3	115.4	108.5
o6-OMe(a)	131.5	161.1	140.6	211.0	116.1	114.6	110.1
o6-OMe(b)	131.6	161.0	140.5	213.3	116.6	115.0	110.2
o6-Me	131.3	161.5	140.8	210.7	116.5	115.0	110.4
o6-F	131.8	160.8	139.9	211.5	116.5	114.7	110.1
o6-Cl	131.8	160.5	140.5	213.3	116.5	115.0	110.4
o6-Br	131.6	160.9	140.2	210.5	116.0	114.6	110.1
o6-CN	131.9	160.3	139.5	214.8	117.0	115.4	110.3
o6-NO_2	132.1	160.0	139.7	216.8	117.4	115.6	110.6

Table B.6: Electron densities (e/Å^3) at the bond critical point of the N-H bond with all the substituents calculated from B3LYP with three different basis sets.

		6-31+G(d)	6-311+G(2d,p)	cc-pVTZ
H		2.166	2.242	2.323
OH	**m3(a)**	2.167	2.243	2.325
	m3(b)	2.166	2.242	2.324
	m5(a)	2.167	2.243	2.325
	m5(b)	2.166	2.242	2.325
	p(a)	2.161	2.239	2.320
	p(b)	2.161	2.238	2.320
	o2(a)	2.163	2.242	2.325
	o6(a)	2.158	2.236	2.315
	o6(b)	2.152	2.232	2.312
OMe	**m3(a)**	2.166	2.242	2.324
	m3(b)	2.167	2.242	2.325
	m5(a)	2.167	2.244	2.325
	m5(b)	2.167	2.242	2.324
	p(a)	2.162	2.239	2.319
	p(b)	2.161	2.238	2.319
	o2(a)	2.165	2.243	2.326
	o6(a)	2.159	2.238	2.315

(continues on next page)

Table B.6 (Continued)

		6-31+G(d)	6-311+G(2d,p)	cc-pVTZ
	o6(b)	2.162	2.239	2.319
Me	**m3**	2.166	2.242	2.324
	m5	2.166	2.241	2.323
	p	2.165	2.241	2.322
	o2	2.178	2.252	2.333
	o6	2.162	2.239	2.319
F	**m3**	2.166	2.242	2.323
	m5	2.166	2.242	2.323
	p	2.163	2.240	2.321
	o2	2.163	2.242	2.324
	o6	2.158	2.236	2.316
Cl	**m3**	2.165	2.241	2.323
	m5	2.166	2.242	2.324
	p	2.164	2.241	2.323
	o2	2.162	2.240	2.321
	o6	2.162	2.240	2.320
Br	**m3**	2.165	2.242	2.323
	m5	2.165	2.241	2.323
	p	2.164	2.241	2.323

(continues on next page)

Table B.6 (Continued)

		6-31+G(d)	6-311+G(2d,p)	cc-pVTZ
	o2	2.159	2.236	2.317
	o6	2.161	2.241	2.321
CN	**m3**	2.164	2.240	2.321
	m5	2.165	2.241	2.322
	p	2.166	2.241	2.323
	o2	2.155	2.231	2.313
	o6	2.162	2.239	2.320
NO_2	**m3**	2.164	2.212	2.321
	m5	2.165	2.241	2.322
	p	2.166	2.242	2.323
	o2	2.140	2.219	2.299
	o6	2.162	2.240	2.321

Table B.7: Electron densities (e/Å^3) at the bond critical point of the ortho C-H bond with all the substituents calculated from B3LYP with three different basis sets.

		m3		**m5**		**p**		**o6**	
		a	**b**	**a**	**b**	**a**	**b**	**a**	**b**
H	6-31+G(d)	1.860							
	6-311+G(2d,p)	1.900							
	cc-pVTZ	1.967							
OH	6-31+G(d)	1.857	1.836	1.858	1.858	1.864	1.863	1.860	1.863
	6-311+G(2d,p)	1.896	1.876	1.899	1.899	1.904	1.903	1.903	1.900
	cc-pVTZ	1.967	1.944	1.969	1.969	1.975	1.973	1.972	1.969
Ome	6-31+G(d)	1.857	1.862	1.858	1.858	1.862	1.862	1.863	1.863
	6-311+G(2d,p)	1.897	1.902	1.898	1.898	1.903	1.902	1.903	1.903
	cc-pVTZ	1.967	1.972	1.968	1.968	1.973	1.972	1.971	1.972
Me	6-31+G(d)	1.851		1.858		1.859		1.860	
	6-311+G(2d,p)	1.890		1.899		1.900		1.900	
	cc-pVTZ	1.960		1.969		1.970		1.970	

(continues on next page)

Table B.7 (Continued)

		m3	m5	p	o6
F	6-31+G(d)	1.858	1.862	1.865	1.863
	6-311+G(2d,p)	1.898	1.902	1.906	1.903
	cc-pVTZ	1.968	1.972	1.976	1.973
Cl	6-31+G(d)	1.868	1.863	1.863	1.866
	6-311+G(2d,p)	1.909	1.903	1.904	1.906
	cc-pVTZ	1.981	1.974	1.975	1.975
Br	6-31+G(d)	1.870	1.863	1.863	1.863
	6-311+G(2d,p)	1.911	1.904	1.904	1.907
	cc-pVTZ	1.983	1.974	1.974	1.975
CN	6-31+G(d)	1.874	1.867	1.865	1.865
	6-311+G(2d,p)	1.915	1.907	1.907	1.906
	cc-pVTZ	1.986	1.978	1.977	1.976
NO_2	6-31+G(d)	1.884	1.869	1.867	1.869
	6-311+G(2d,p)	1.914	1.898	1.908	1.909
	cc-pVTZ	1.999	1.980	1.978	1.979

Table B.8: Electron densities (e/Å^3) at the bond critical point of the S=O bond with all the substituents calculated from B3LYP with three different basis sets.

		6-31+G(d)	6-311+G(2d,p)	cc-pVTZ
H		1.704	1.843	1.850
OH	**m3(a)**	1.707	1.852	1.845
	m3(b)	1.703	1.849	1.842
	m5(a)	1.705	1.852	1.844
	m5(b)	1.706	1.853	1.844
	p(a)	1.698	1.842	1.839
	p(b)	1.696	1.842	1.835
	o2(a)	1.710	1.856	1.847
	o6(a)	1.692	1.835	1.839
	o6(b)	1.701	1.847	1.830
OMe	**m3(a)**	1.705	1.849	1.843
	m3(b)	1.702	1.848	1.841
	m5(a)	1.704	1.849	1.843
	m5(b)	1.704	1.849	1.842
	p(a)	1.696	1.840	1.835
	p(b)	1.695	1.839	1.834
	o2(a)	1.707	1.852	1.845

(continues on next page)

Table B.8 (Continued)

		6-31+G(d)	6-311+G(2d,p)	cc-pVTZ
	o6(a)	1.691	1.836	1.828
	o6(b)	1.699	1.843	1.837
Me	**m3**	1.703	1.848	1.842
	m5	1.703	1.847	1.841
	p	1.701	1.846	1.840
	o2	1.701	1.847	1.840
	o6	1.696	1.839	1.835
F	**m3**	1.710	1.857	1.849
	m5	1.709	1.857	1.848
	p	1.705	1.849	1.843
	o2	1.716	1.863	1.853
	o6	1.700	1.846	1.840
Cl	**m3**	1.711	1.855	1.849
	m5	1.709	1.856	1.848
	p	1.707	1.855	1.846
	o2	1.718	1.865	1.857
	o6	1.703	1.850	1.842

(continues on next page)

Table B.8 (Continued)

		6-31+G(d)	6-311+G(2d,p)	cc-pVTZ
Br	**m3**	1.711	1.857	1.850
	m5	1.709	1.857	1.849
	p	1.707	1.854	1.847
	o2	1.718	1.866	1.858
	o6	1.700	1.851	1.842
CN	**m3**	1.716	1.863	1.854
	m5	1.715	1.863	1.854
	p	1.717	1.866	1.857
	o2	1.732	1.881	1.870
	o6	1.712	1.860	1.852
NO_2	**m3**	1.719	1.801	1.856
	m5	1.715	1.862	1.854
	p	1.721	1.870	1.859
	o2	1.744	1.894	1.881
	o6	1.716	1.863	1.854

Appendix C: Supplemental information related to Chapter 5

Table C.1: Selected geometrical parameters (distances in pm, angles in degrees) of chloro and methyl substituted dimers.

	Chloro						
	m3	**m5**	**p**	**o2**	**o6**	**m3-5**	**o2-6**
N-N	130.7	130.7	130.6	131.2	130.9	130.7	131.1
N=S	159.5	159.5	159.6	159.5	159.4	159.5	159.5
C3-N7	141.0	141.0	141.0	140.8	141.4	141.0	140.9
NNH	120.6	120.7	120.6	119.7	120.2	120.7	119.6
NNS	121.5	121.7	121.8	120.9	121.2	121.8	120.9
NSO	113.3	113.6	113.4	113.4	113.5	113.5	113.6
NNSO	-0.3	-0.6	-0.3	-0.2	0.0	-0.3	0.1
	Methyl						
	m3	**m5**	**p**	**o2**	**o6**	**m3-5**	**o2-6**
N-N	130.5	130.5	130.4	130.8	130.6	130.5	130.7
N=S	159.7	159.8	159.9	159.5	160.1	159.7	160.1
C3-N7	141.2	141.2	141.2	142.0	141.7	141.2	141.7
NNH	120.6	120.6	120.6	119.7	119.7	120.6	119.3
NNS	121.9	121.8	121.8	122.5	121.2	121.9	120.8
NSO	113.6	113.6	113.5	114.1	113.3	113.6	112.9
NNSO	-0.4	-0.1	-0.4	0.0	0.5	0.3	0.7

Table C.2: Individual topological properties $\rho(r)$ (e/Å^3) and $\nabla^2\rho(r)$ (e/Å^5) at the BCP of the two of NH---O interactions in chloro and methyl substituted dimers and their average.

	$\rho(r)$			$\nabla^2\rho(r)$		
			Average			Average
PhNHNSO	0.172	0.172	0.172	2.21	2.21	2.21
mCl3	0.171	0.171	0.171	2.22	2.22	2.22
mCl5	0.172	0.172	0.172	2.22	2.22	2.22
pCl	0.170	0.170	0.170	2.22	2.22	2.22
oCl2	0.169	0.169	0.169	2.07	2.07	2.07
oCl6	0.181	0.183	0.182	2.30	2.32	2.31
mCl3-5	0.169	0.176	0.173	2.19	2.28	2.23
oCl2-6	0.163	0.171	0.167	2.07	2.13	2.10
mMe3	0.170	0.170	0.170	2.19	2.19	2.19
mMe5	0.172	0.172	0.172	2.20	2.20	2.20
pMe	0.173	0.173	0.173	2.23	2.23	2.23
oMe2	0.168	0.168	0.168	2.10	2.11	2.10
oMe6	0.171	0.171	0.171	2.16	2.16	2.16
mMe3-5	0.172	0.174	0.173	2.20	2.23	2.22
oMe2-6	0.129	0.183	0.156	1.73	2.21	1.97

Table C.3: Individual topological properties $\rho(r)$ (e/Å^3) and $\nabla^2\rho(r)$ (e/Å^5) at the BCP of the two of CH---O interactions in chloro and methyl substituted dimers and their average.

	$\rho(r)$			$\nabla^2\rho(r)$		
			Average			Average
PhNHNSO	0.079	0.079	0.079	0.98	0.98	0.98
mCl3	0.081	0.081	0.081	1.02	1.02	1.02
mCl5	0.078	0.078	0.078	0.97	0.97	0.97
pCl	0.081	0.081	0.081	1.01	1.01	1.01
oCl6	0.073	0.072	0.073	0.94	0.93	0.94
mCl3-5	0.078	0.081	0.080	0.98	1.02	1.00
oCl2-6	0.066		0.066	0.86		0.86
mMe-3	0.078	0.078	0.078	0.97	0.97	0.97
mMe-5	0.077	0.077	0.077	0.96	0.96	0.96
pMe	0.078	0.078	0.078	0.98	0.98	0.98
oMe-6	0.081	0.080	0.081	1.01	1.01	1.01
mMe3-5	0.079	0.077	0.078	0.97	0.96	0.97
oMe2-6	0.078		0.078	0.99		0.99

Appendix D: Internal coordinates and total energies

D.1. Internal Coordinates and Total Energy (au) of unsubstituted and substituted monomers and dimers

Column 1	Atom number
Column 2	Atom
Column 3	Bond distance (Å)
Column 4	Bond angle (degrees)
Column 5	Dihedral angle (degrees)
Column 6-8	Connectivity of atoms

***Syn*-monomer**

1	C	0	0	0	0	0	0
2	C	1.398	0	0	1	0	0
3	C	1.399	119.5	0	1	2	0
4	H	1.086	120.2	180.0	1	2	3
5	C	1.394	120.4	0	2	1	3
6	C	1.394	120.9	0	3	1	2
7	H	1.087	120.2	180.0	2	1	5
8	H	1.087	120.0	-180.0	3	1	6
9	C	1.403	119.6	0.0	5	2	1
10	H	1.088	120.3	180.0	5	2	9
11	H	1.084	121.1	-180.0	6	3	1
12	N	1.404	118.0	180.0	9	5	2
13	N	1.314	122.9	-180.0	12	9	5
14	H	1.026	120.0	180.0	12	9	13
15	S	1.608	115.6	180.0	13	12	9
16	O	1.517	110.2	0.0	15	13	12

Total energy = --815.004303

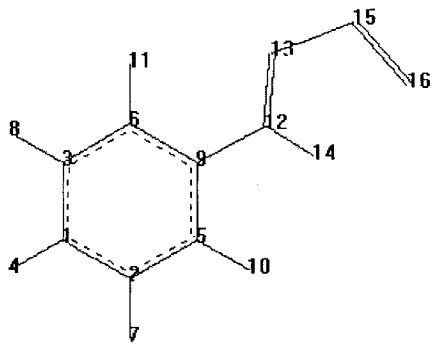

***Sickle*-monomer**

1	C	0	0	0	0	0	0
2	C	1.392	0	0	1	0	0
3	C	1.407	120.2	0	1	2	0
4	H	1.089	119.8	180.0	1	2	3
5	C	1.398	120.2	0	2	1	3
6	C	1.400	120.0	180.0	3	1	4
7	N	1.417	115.1	360.0	3	1	4
8	H	1.087	119.4	0	2	1	4
9	C	1.397	119.0	0	6	3	1
10	N	1.319	135.2	359.8	7	3	6
11	H	1.014	114.4	179.7	7	3	6
12	H	1.084	120.8	180.0	6	3	1
13	H	1.086	120.3	0	5	2	8
14	S	1.578	139.1	179.9	10	7	11
15	H	1.087	118.6	360.0	9	6	12
16	O	1.504	122.4	0	14	10	7

Total Energy = -815.1033238

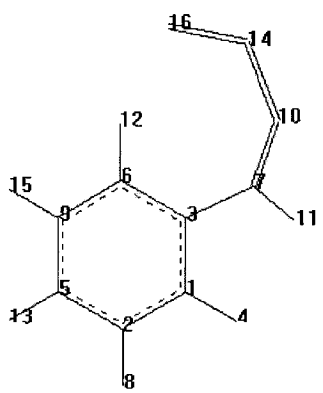

***Anti1*-monomer**

1	C	0	0	0	0	0	0
2	C	1.394	0	0	1	0	0
3	C	1.403	119.7	0	1	2	0
4	H	1.089	120.1	180.0	1	2	3
5	C	1.398	120.4	0.0	2	1	3
6	C	1.402	120.4	0.0	3	1	2
7	N	1.405	118.1	180.0	3	1	6
8	H	1.087	119.3	180.0	2	1	5
9	C	1.400	119.4	0	5	2	1
10	H	1.086	120.3	180.0	5	2	9
11	N	1.325	121.9	180.0	7	3	1
12	H	1.084	119.6	180.0	6	3	1
13	H	1.020	117.3	180.0	7	3	11
14	S	1.604	119.6	180.0	11	7	3
15	H	1.087	120.0	-180.0	9	5	2
16	O	1.496	111.0	180.0	14	11	7

Total Energy = 815.0981818

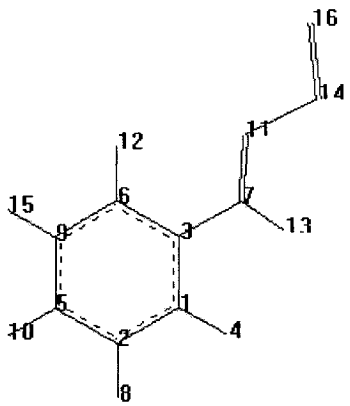

***Anti2*-monomer**

1	C	0	0	0	0	0	0
2	C	1.402	0	0	1	0	0
3	C	1.394	119.2	0	1	2	0
4	H	1.086	120.3	180	1	2	3
5	C	1.389	120.4	0	2	1	3
6	C	1.399	121.2	0	3	1	2
7	H	1.087	120.3	180	2	1	5
8	H	1.087	120.1	-180	3	1	6
9	C	1.411	120.4	0	5	2	1
10	H	1.088	120.0	-180	5	2	9
11	H	1.081	118.9	-180	6	3	1
12	N	1.403	116.1	-180	9	5	2
13	N	1.326	133.5	180.0	12	9	5
14	H	1.013	115.7	180.0	12	9	13
15	S	1.600	127.6	0.0	13	12	9
16	O	1.496	109.4	180.0	15	13	12

Total Energy = -815.0946218

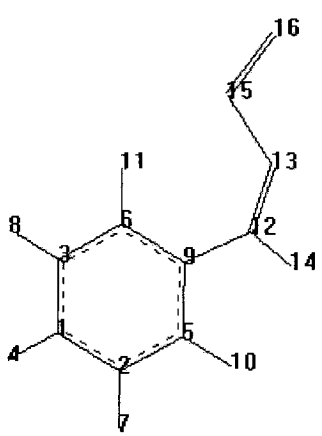

m3-Cl-monomer

1	C	0	0	0	0	0	0
2	C	1.393	0	0	1	0	0
3	C	1.402	118.9	0	1	2	0
4	H	1.084	121.2	180.0	1	2	3
5	C	1.398	121.4	0	2	1	3
6	C	1.403	120.7	0	3	1	2
7	N	1.402	121.6	180.0	3	1	6
8	H	1.086	119.3	180.0	2	1	5
9	C	1.396	118.5	0	5	2	1
10	N	1.317	122.5	0.0	7	3	1
11	H	1.086	120.9	180.0	6	3	1
12	H	1.025	120.2	180.0	7	3	10
13	H	1.084	121.2	180.0	5	2	9
14	S	1.606	115.6	-180.0	10	7	3
15	Cl	1.756	119.5	180.0	9	5	2
16	O	1.515	110.3	0.0	14	10	7

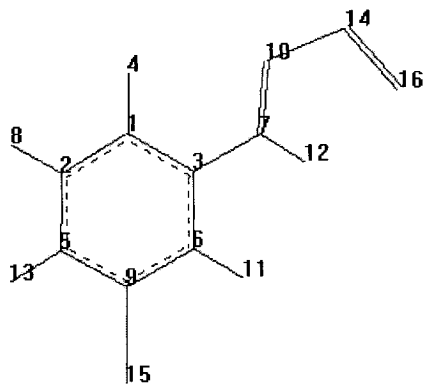

Total Energy = -1274.608312

m5-Cl-monomer

1	C	0	0	0	0	0	0
2	C	1.392	0	0	1	0	0
3	C	1.402	118.4	0	1	2	0
4	H	1.083	121.2	180.0	1	2	3
5	C	1.397	122.1	0	2	1	3
6	C	1.403	120.7	0	3	1	2
7	N	1.402	121	-180.0	3	1	6
8	Cl	1.757	118.7	180.0	2	1	5
9	C	1.397	118.5	0	5	2	1
10	N	1.317	122.7	0	7	3	1
11	H	1.087	120.2	180.0	6	3	1
12	H	1.025	120.1	-180.0	7	3	10
13	H	1.084	120.4	180.0	5	2	9
14	S	1.606	115.6	180.0	10	7	3
15	H	1.086	119.6	180.0	9	5	2
16	O	1.515	110.3	0	14	10	7

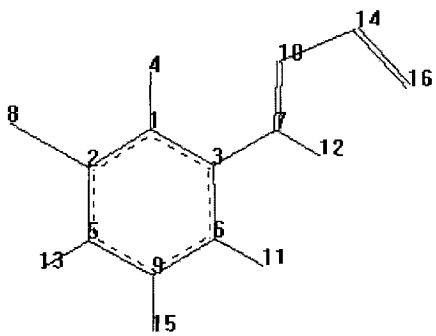

Total Energy = -1274.608533

p-Cl-monomer

1	C	0	0	0	0	0	0
2	C	1.393	0	0	1	0	0
3	C	1.402	119.6	0	1	2	0
4	H	1.084	120.5	180.0	1	2	3
5	C	1.397	119.9	0	2	1	3
6	C	1.403	120.1	0	3	1	2
7	N	1.402	121.6	180.0	3	1	6
8	H	1.085	120.1	180.0	2	1	5
9	C	1.396	120.7	0	5	2	1
10	Cl	1.756	119.7	-180.0	5	2	9
11	N	1.316	122.7	0	7	3	1
12	H	1.087	120.2	180.0	6	3	1
13	H	1.026	120.1	180.0	7	3	11
14	S	1.608	115.5	-180.0	11	7	3
15	H	1.085	120.3	180.0	9	5	2
16	O	1.516	110.2	0	14	11	7

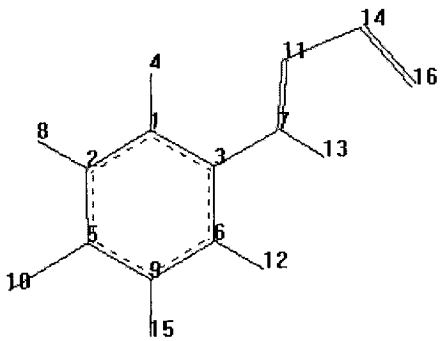

Total Energy = -1274.608544

o2-Cl-monomer

1	C	0	0	0	0	0	0
2	C	1.396	0	0	1	0	0
3	C	1.399	119.7	0	1	2	0
4	H	1.086	119.7	180.0	1	2	3
5	C	1.393	119.9	0	2	1	3
6	C	1.392	120.6	0	3	1	2
7	H	1.085	121.0	180.0	2	1	5
8	H	1.086	120.2	180.0	3	1	6
9	C	1.407	120.8	0	5	2	1
10	Cl	1.759	119.2	180.0	5	2	9
11	H	1.084	121.1	180.0	6	3	1
12	N	1.398	120.0	180.0	9	5	2
13	N	1.319	121.8	180.0	12	9	5
14	H	1.025	120.2	180.0	12	9	13
15	S	1.603	116.1	180.0	13	12	9
16	O	1.512	110.9	0	15	13	12

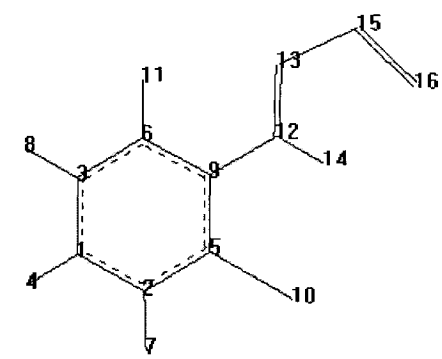

Total Energy = -1274.606920

o6-Cl-monomer

1	C	0	0	0	0	0	0
2	C	1.409	0	0	1	0	0
3	C	1.398	119.8	0	1	2	0
4	Cl	1.750	122.6	-177.6	1	2	3
5	N	1.405	125.2	179.7	2	1	3
6	C	1.407	118.6	-177.9	2	1	5
7	C	1.394	120.9	-1.3	3	1	2
8	H	1.085	118.5	-178.9	3	1	7
9	N	1.318	124.7	30.6	5	2	1
10	C	1.390	121.3	-0.9	6	2	1
11	H	1.026	118.3	171.9	5	2	9
12	H	1.088	118.6	-179.0	6	2	10
13	H	1.086	119.7	-179.7	7	3	1
14	S	1.606	115.0	175.9	9	5	2
15	H	1.086	119.6	-179.8	10	6	2
16	O	1.517	110.4	-0.5	14	9	5

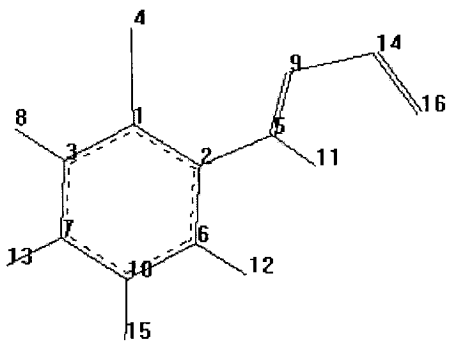

Total Energy = -1274.598042

m3-Me monomer

1	C	0	0	0	0	0	0
2	C	1.392	0	0	1	0	0
3	C	1.402	118.5	0	1	2	0
4	H	1.084	121.5	180.0	1	2	3
5	C	1.399	121.0	0	2	1	3
6	C	1.401	120.7	0	3	1	2
7	N	1.405	121.5	180.0	3	1	6
8	H	1.087	119.3	-180.0	2	1	5
9	C	1.401	120.6	0	5	2	1
10	N	1.314	122.9	0	7	3	1
11	H	1.089	119.6	180.0	6	3	1
12	H	1.026	120.0	180.0	7	3	10
13	H	1.087	119.8	-180.0	5	2	9
14	S	1.609	115.5	180.0	10	7	3
15	C	1.512	121.4	179.9	9	5	2
16	O	1.518	110.1	0	14	10	7
17	H	1.094	111.3	0.9	15	9	5
18	H	1.097	111.3	120.2	15	9	17
19	H	1.097	111.3	-120.2	15	9	17

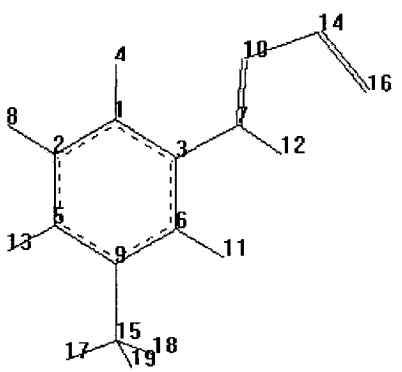

Total Energy = -854.295707

m5-Me-monomer

1	C	0	0	0	0	0	0
2	C	1.397	0	0	1	0	0
3	C	1.402	120.2	0	1	2	0
4	H	1.085	120.6	-180.0	1	2	3
5	C	1.406	119.0	0.1	2	1	3
6	C	1.401	120.6	0	3	1	2
7	N	1.405	121.3	-179.9	3	1	6
8	C	1.512	120.6	-179.7	2	1	5
9	C	1.395	120.6	-0.1	5	2	1
10	N	1.314	123.0	-0.1	7	3	1
11	H	1.088	120.4	-179.9	6	3	1
12	H	1.026	119.9	-180.0	7	3	10
13	H	1.088	119.6	180.0	5	2	9
14	H	1.097	111.2	-125.9	8	2	1
15	H	1.094	111.5	120.5	8	2	14
16	H	1.098	111.1	-119.3	8	2	14
17	S	1.609	115.6	-180.0	10	7	3
18	H	1.087	120.0	180.0	9	5	2
19	O	1.517	110.2	0	17	10	7

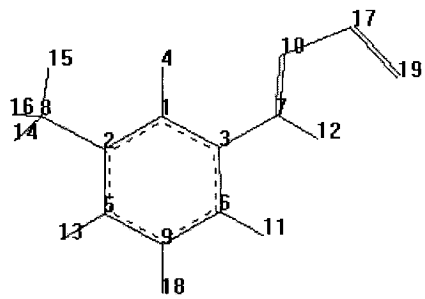

Total Energy =-854.295758

p-Me-monomer

1	C	0	0	0	0	0	0
2	C	1.392	0	0	1	0	0
3	C	1.402	119.3	0	1	2	0
4	H	1.084	121.0	180.0	1	2	3
5	C	1.405	121.9	0	2	1	3
6	C	1.400	119.9	0	3	1	2
7	N	1.404	121.7	180.0	3	1	6
8	H	1.088	118.7	-180.0	2	1	5
9	C	1.401	117.7	0	5	2	1
10	N	1.313	122.9	0	7	3	1
11	H	1.088	120.2	180.0	6	3	1
12	H	1.026	120.0	180.0	7	3	10
13	C	1.511	120.8	180.0	5	2	9
14	S	1.610	115.5	180.0	10	7	3
15	H	1.087	119.6	-180.0	9	5	2
16	H	1.098	111.4	-60.2	13	5	2
17	H	1.097	111.4	119.5	13	5	16
18	H	1.095	111.4	-120.2	13	5	16
19	O	1.518	110.1	0	14	10	7

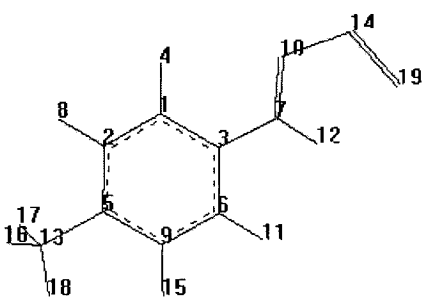

Total Energy = -854.295478

o2-Me-monomer

1	C	0	0	0	0	0	0
2	C	1.397	0	0	1	0	0
3	C	1.398	119.5	0	1	2	0
4	H	1.086	120.0	-180.0	1	2	3
5	C	1.399	121.9	0	2	1	3
6	C	1.393	120.2	0	3	1	2
7	H	1.088	119.6	-180.0	2	1	5
8	H	1.087	120.4	180.0	3	1	6
9	C	1.413	117.4	0	5	2	1
10	C	1.511	120.9	180.0	5	2	9
11	H	1.084	121.0	-180.0	6	3	1
12	N	1.406	118.3	180.0	9	5	2
13	H	1.094	110.4	0	10	5	2
14	H	1.099	112.2	-119.5	10	5	13
15	H	1.099	112.2	119.5	10	5	13
16	N	1.315	122.8	180.0	12	9	5
17	H	1.024	120.5	180.0	12	9	16
18	S	1.609	115.4	180.0	16	12	9
19	O	1.518	110.0	0	18	16	12

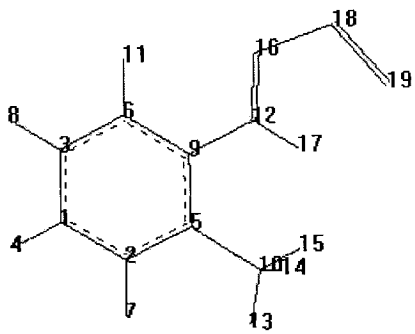

Total Energy = -854.294344

o6-Me-monomer

1	C	0	0	0	0	0	0
2	C	1.396	0	0	1	0	0
3	C	1.397	119.4	0	1	2	0
4	H	1.086	120.1	180.0	1	2	3
5	C	1.403	122.9	0	2	1	3
6	C	1.390	119.4	0	3	1	2
7	H	1.087	119.2	-180.0	2	1	5
8	H	1.086	120.8	-180.0	3	1	6
9	C	1.415	116.7	0	5	2	1
10	C	1.511	119.1	-180.0	5	2	9
11	H	1.088	119.9	-180.0	6	3	1
12	N	1.408	124.6	-180.0	9	5	2
13	H	1.095	109.7	0.1	10	5	2
14	H	1.095	112.0	-120.3	10	5	13
15	H	1.095	112.0	120.3	10	5	13
16	N	1.313	126.1	-0.2	12	9	5
17	H	1.028	117.9	-180.0	12	9	16
18	S	1.615	114.8	-180.0	16	12	9
19	O	1.520	109.8	0	18	16	12

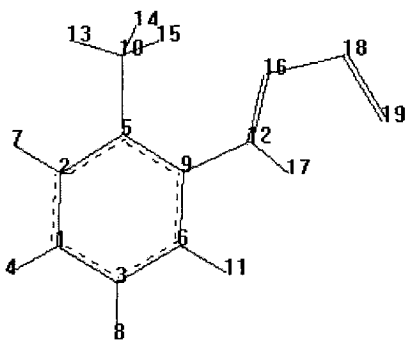

Total Energy = -854.290146

m3-Br-monomer

1	C	0	0	0	0	0	0
2	C	1.393	0	0	1	0	0
3	C	1.398	121.3	0	2	1	0
4	C	1.395	118.6	0	3	2	1
5	C	1.401	118.9	0	1	2	3
6	C	1.391	121.7	0	4	3	2
7	N	1.402	121.5	180.0	5	1	2
8	N	1.316	122.6	0	7	5	1
9	S	1.606	115.6	180.0	8	7	5
10	O	1.515	110.3	0	9	8	7
11	H	1.084	121.3	180.0	1	2	3
12	H	1.086	119.3	180.0	2	1	5
13	H	1.086	120.5	180.0	6	4	3
14	H	1.025	120.2	180.0	7	5	1
15	Br	1.903	119.5	180.0	4	3	2
16	H	1.084	120.9	0	3	2	12

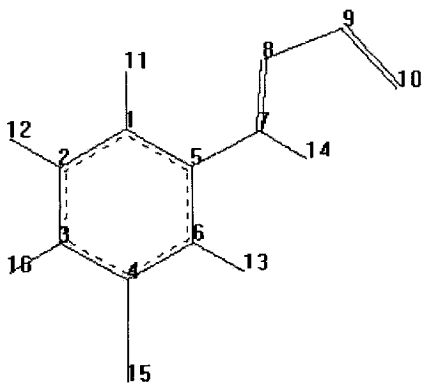

Total Energy = -3386.140502

m5-Br-monomer

1	C	0	0	0	0	0	0
2	C	1.391	0	0	1	0	0
3	C	1.397	122.0	0	2	1	0
4	C	1.397	118.6	0	3	2	1
5	C	1.401	118.3	0	1	2	3
6	C	1.393	120.9	0	4	3	2
7	N	1.401	121.0	180.0	5	1	2
8	N	1.317	122.6	0	7	5	1
9	S	1.606	115.6	180.0	8	7	5
10	O	1.515	110.2	0	9	8	7
11	H	1.083	121.4	180.0	1	2	3
12	H	1.086	119.6	180.0	4	3	2
13	H	1.087	120.5	180.0	6	4	3
14	H	1.025	120.1	180.0	7	5	1
15	H	1.084	120.5	180.0	3	2	1
16	Br	1.904	118.8	0	2	1	11

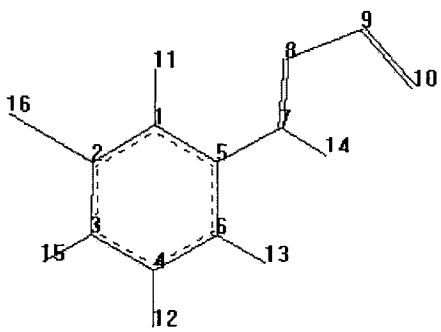

Total Energy = -3386.140598

p-Br-monomer

1	C	0	0	0	0	0	0
2	C	1.393	0	0	1	0	0
3	C	1.396	120.0	0	2	1	0
4	C	1.395	120.7	0	3	2	1
5	C	1.401	119.5	0	1	2	3
6	C	1.393	119.6	0	4	3	2
7	Br	1.901	119.6	180.0	3	2	1
8	N	1.401	121.5	180.0	5	1	2
9	N	1.316	122.7	0	8	5	1
10	S	1.607	115.4	180.0	9	8	5
11	O	1.516	110.1	0	10	9	8
12	H	1.084	120.6	180.0	1	2	3
13	H	1.085	119.9	180.0	2	1	5
14	H	1.085	120.4	180.0	4	3	2
15	H	1.087	119.8	180.0	6	4	3
16	H	1.026	120.2	180.0	8	5	1

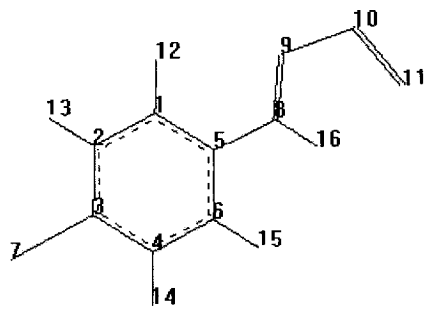

Total Energy = -3386.140407

o2-Br-monomer

1	C	0	0	0	0	0	0
2	C	1.396	0	0	1	0	0
3	C	1.393	120.1	0	2	1	0
4	C	1.406	120.4	0	3	2	1
5	C	1.404	119.1	0	4	3	2
6	N	1.398	119.8	180.0	4	3	2
7	C	1.391	120.1	0	5	4	3
8	N	1.319	122.1	0	6	4	5
9	S	1.603	115.8	180.0	8	6	4
10	H	1.086	119.7	180.0	1	2	3
11	H	1.085	120.5	180.0	2	1	7
12	Br	1.906	119.5	180.0	3	2	1
13	H	1.084	118.7	0	5	4	6
14	H	1.025	120.0	180.0	6	4	5
15	H	1.086	119.3	0	7	5	13
16	O	1.512	110.8	0	9	8	6

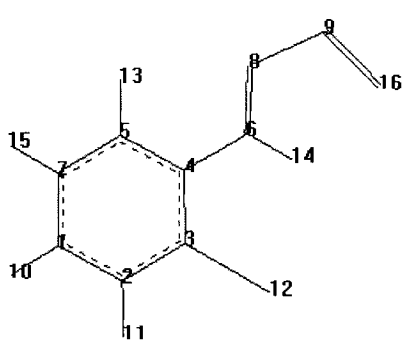

Total Energy = -3386.139987

o6-Br-monomer

1	C	0	0	0	0	0	0
2	C	1.408	0	0	1	0	0
3	N	1.402	126.9	0	2	1	0
4	N	1.316	126.7	0	3	2	1
5	S	1.609	114.6	180.0	4	3	2
6	C	1.399	119.4	180.0	1	2	3
7	C	1.410	118.6	180.0	2	1	3
8	C	1.388	121.6	180.0	7	2	3
9	C	1.393	121.5	0	6	1	2
10	Br	1.899	124.1	0	1	2	3
11	H	1.027	117.3	180.0	3	2	1
12	O	1.518	110.1	0	5	4	3
13	H	1.088	118.6	0	7	2	3
14	H	1.085	118.4	180.0	6	1	2
15	H	1.086	119.8	180.0	9	6	1
16	H	1.086	119.6	0	8	7	13

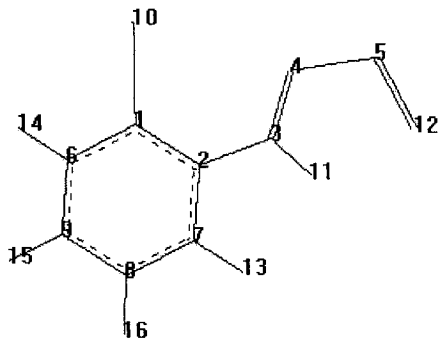

Total Energy = -3386.130953

m3-NO_2-monomer

1	C	0	0	0	0	0	0
2	C	1.394	0	0	1	0	0
3	C	1.397	121.1	0	2	1	0
4	C	1.394	117.9	0	3	2	1
5	C	1.405	119.6	0	1	2	3
6	C	1.391	122.7	0	4	3	2
7	N	1.400	121.5	180.0	5	1	2
8	N	1.320	122.2	180.0	7	5	6
9	S	1.603	115.7	180.0	8	7	5
10	O	1.512	110.6	0	9	8	7
11	H	1.084	120.9	180.0	1	2	3
12	H	1.086	119.3	180.0	2	1	5
13	H	1.084	119.8	180.0	6	4	3
14	H	1.025	120.3	0	7	5	6
15	N	1.477	119.1	180.0	4	3	2
16	H	1.083	122.0	0	3	2	12
17	O	1.230	117.6	180.0	15	4	6
18	O	1.232	117.7	0	15	4	6

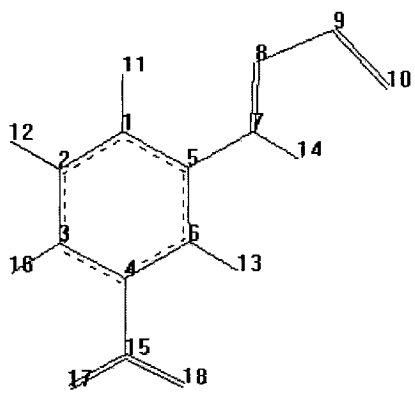

Total Energy = -1019.509821

m5-NO_2-monomer

1	C	0	0	0	0	0	0
2	C	1.391	0	0	1	0	0
3	C	1.395	123.1	0	2	1	0
4	C	1.396	117.9	0	3	2	1
5	C	1.400	117.9	0	1	2	3
6	C	1.394	120.7	0	4	3	2
7	N	1.400	121.2	180.0	5	1	2
8	N	1.319	122.4	0	7	5	1
9	S	1.603	115.6	180.0	8	7	5
10	O	1.513	110.4	0	9	8	7
11	H	1.082	120.8	180.0	1	2	3
12	H	1.086	119.8	180.0	4	3	2
13	H	1.087	120.1	180.0	6	4	3
14	H	1.025	120.3	180.0	7	5	1
15	H	1.083	120.1	180.0	3	2	1
16	N	1.479	118.1	0	2	1	11
17	O	1.231	117.6	180.0	16	2	1
18	O	1.231	117.8	0	16	2	1

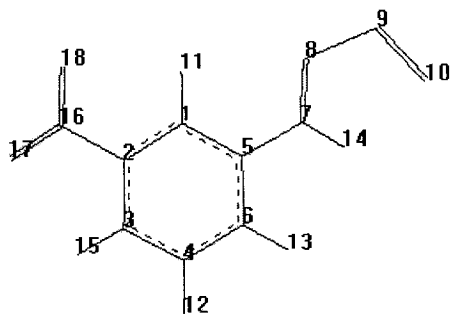

Total Energy = -1019.509572

p-NO_2-monomer

1	C	0	0	0	0	0	0
2	C	1.389	0	0	1	0	0
3	C	1.398	119.5	0	2	1	0
4	C	1.397	121.5	0	3	2	1
5	C	1.405	119.5	0	1	2	3
6	C	1.388	119.1	0	4	3	2
7	N	1.466	119.3	180.0	3	2	1
8	N	1.395	121.4	180.0	5	1	2
9	N	1.322	122.4	0	8	5	1
10	S	1.602	115.7	180.0	9	8	5
11	O	1.511	110.7	0	10	9	8
12	H	1.084	120.7	180.0	1	2	3
13	H	1.083	120.9	180.0	2	1	5
14	H	1.083	119.8	180.0	4	3	2
15	H	1.087	119.9	180.0	6	4	3
16	H	1.025	120.2	180.0	8	5	1
17	O	1.234	117.8	0	7	3	4
18	O	1.233	117.8	180.0	7	3	4

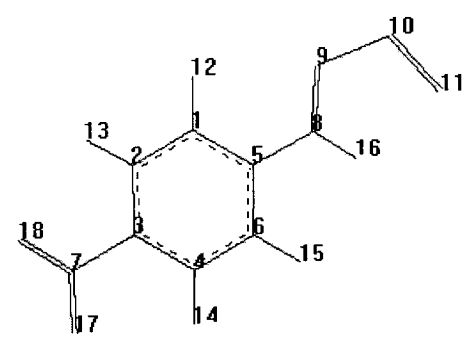

Total Energy = -1019.512267

o2-NO_2-monomer

1	C	0	0	0	0	0	0
2	C	1.386	0	0	1	0	0
3	C	1.402	120.6	0	2	1	0
4	C	1.421	120.7	0	3	2	1
5	C	1.410	117.6	0	4	3	2
6	N	1.389	122.7	180.0	4	3	2
7	C	1.387	121.0	0	5	4	3
8	N	1.328	120.7	0	6	4	5
9	S	1.594	117.4	180.0	8	6	4
10	H	1.085	120.1	180.0	1	2	3
11	H	1.083	121.4	180.0	2	1	7
12	N	1.459	116.7	180.0	3	2	1
13	H	1.083	118.2	0	5	4	6
14	H	1.025	118.7	180.0	6	4	5
15	H	1.087	119.0	0	7	5	13
16	O	1.503	112.8	0	9	8	6
17	O	1.244	118.5	180.0	12	3	2
18	O	1.230	118.4	0	12	3	2

Total Energy = -1019.508711

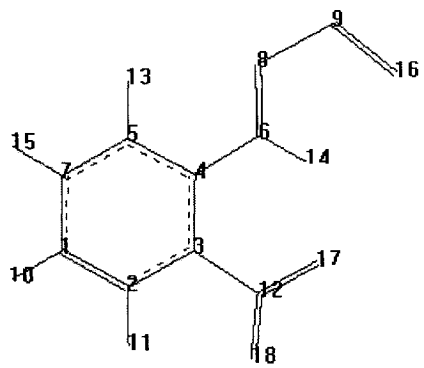

o6-NO_2-monomer

1	C	0	0	0	0	0	0
2	C	1.407	0	0	1	0	0
3	N	1.397	124.3	0	2	1	0
4	N	1.321	122.7	25.8	3	2	1
5	S	1.600	115.6	178.4	4	3	2
6	C	1.395	121.0	185.4	1	2	3
7	C	1.405	118.0	177.9	2	1	3
8	C	1.392	120.9	177.1	7	2	3
9	C	1.393	120.1	356.8	6	1	2
10	N	1.473	122.5	10.6	1	2	3
11	H	1.025	119.7	22.4	3	2	7
12	O	1.513	110.6	359.6	5	4	3
13	H	1.087	118.8	358.9	7	2	3
14	H	1.085	118.5	178.5	6	1	2
15	H	1.085	119.9	181.2	9	6	1
16	H	1.086	119.3	358.1	8	7	13
17	O	1.229	117.4	229.8	10	1	6
18	O	1.231	117.2	46.3	10	1	6

Total Energy = -1019.496304

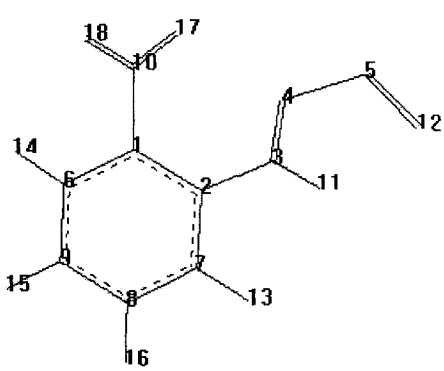

m3-F-monomer

1	C	0	0	0	0	0	0
2	C	1.394	0	0	1	0	0
3	C	1.399	121.4	0	2	1	0
4	C	1.390	117.7	0	3	2	1
5	C	1.403	119.1	0	1	2	3
6	C	1.387	123.0	0	4	3	2
7	N	1.402	121.6	180.0	5	1	2
8	N	1.317	122.6	0	7	5	1
9	S	1.606	115.6	180.0	8	7	5
10	O	1.515	110.3	360.0	9	8	7
11	H	1.084	121.1	180.0	1	2	3
12	H	1.086	119.2	180.0	2	1	5
13	H	1.086	120.0	180.0	6	4	3
14	H	1.025	120.2	180.0	7	5	1
15	F	1.357	118.9	180.0	4	3	2
16	H	1.085	122.2	0	3	2	12

Total Energy = -914.25340

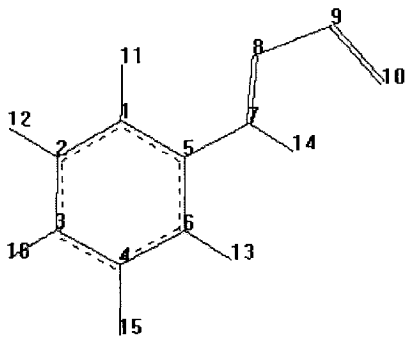

m5-F-monomer

1	C	0	0	0	0	0	0
2	C	1.387	0	0	1	0	0
3	C	1.391	123.4	0	2	1	0
4	C	1.398	117.7	0	3	2	1
5	C	1.402	117.6	0	1	2	3
6	C	1.394	121.0	0	4	3	2
7	N	1.401	121.0	180.0	5	1	2
8	N	1.317	122.7	0	7	5	1
9	S	1.606	115.6	180.0	8	7	5
10	O	1.515	110.3	360.0	9	8	7
11	H	1.083	120.9	180.0	1	2	3
12	H	1.086	119.6	180.0	4	3	2
13	H	1.087	120.4	180.0	6	4	3
14	H	1.025	120.0	180.0	7	5	1
15	H	1.085	120.1	180.0	3	2	1
16	F	1.357	118.0	0	2	1	11

Total Energy = -914.25385

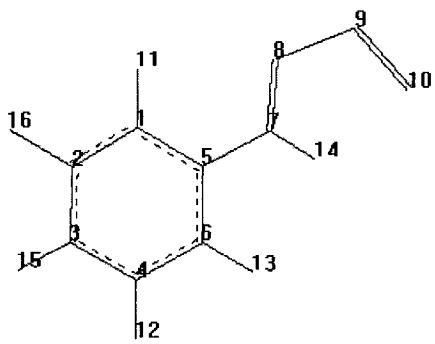

p-F-monomer

1	C	0	0	0	0	0	0
2	C	1.394	0	0	1	0	0
3	C	1.391	119.1	0	2	1	0
4	C	1.390	122.2	0	3	2	1
5	C	1.403	119.6	0	1	2	3
6	C	1.394	118.7	0	4	3	2
7	F	1.359	118.9	180.0	3	2	1
8	N	1.404	121.5	180.0	5	1	2
9	N	1.315	122.7	0	8	5	1
10	S	1.609	115.5	180.0	9	8	5
11	O	1.517	110.0	0	10	9	8
12	H	1.084	120.6	180.0	1	2	3
13	H	1.085	121.1	180.0	2	1	5
14	H	1.085	120.0	0	4	3	7
15	H	1.087	119.7	180.0	6	4	3
16	H	1.026	120.1	180.0	8	5	1

Total Energy = -914.25283

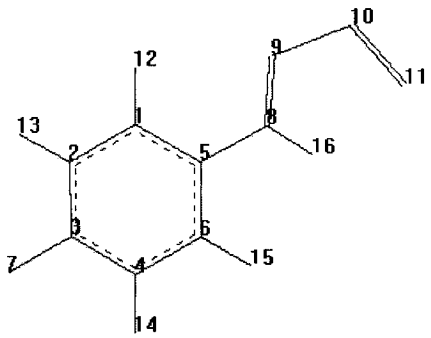

o2-F-monomer

1	C	0	0	0	0	0	0
2	C	1.399	0	0	1	0	0
3	C	1.384	118.7	0	2	1	0
4	C	1.401	122.5	0	3	2	1
5	C	1.402	118.3	0	4	3	2
6	N	1.398	118.5	180.0	4	3	2
7	C	1.395	119.8	0	5	4	3
8	N	1.319	121.8	180.0	6	4	3
9	S	1.604	116.0	180.0	8	6	4
10	H	1.086	119.7	180.0	1	2	3
11	H	1.085	122.1	180.0	2	1	7
12	F	1.362	119.8	180.0	3	2	1
13	H	1.084	118.9	0	5	4	6
14	H	1.024	120.0	0	6	4	3
15	H	1.086	119.2	0	7	5	13
16	O	1.513	110.8	0	9	8	6

Total Energy = -914.25117

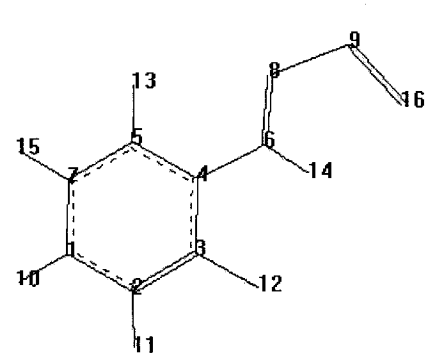

o6-F-monomer

1	C	0	0	0	0	0	0
2	C	1.404	0	0	1	0	0
3	N	1.399	124.8	0	2	1	0
4	N	1.318	125.2	0.9	3	2	1
5	S	1.608	114.7	179.9	4	3	2
6	C	1.389	121.5	180.0	1	2	3
7	C	1.407	117.7	180.1	2	1	3
8	C	1.392	121.1	180.0	7	2	3
9	C	1.396	120.0	360.0	6	1	2
10	F	1.351	120.4	0.1	1	2	3
11	H	1.027	118.3	180.7	3	2	1
12	O	1.518	110.1	0	5	4	3
13	H	1.088	118.8	0.1	7	2	3
14	H	1.086	118.2	359.9	6	1	10
15	H	1.086	119.9	180.0	9	6	1
16	H	1.086	119.5	0	8	7	13

Total Energy = -914.24465

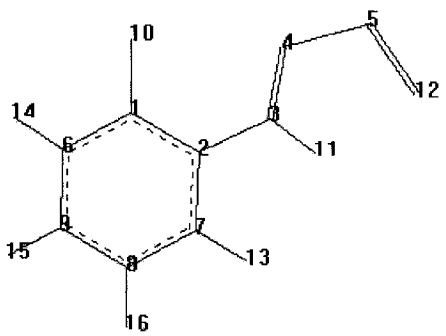

m3-CN-monomer

1	C	0	0	0	0	0	0
2	C	1.393	0	0	1	0	0
3	C	1.395	121.1	0	2	1	0
4	C	1.405	119.1	0	3	2	1
5	C	1.403	119.4	0	1	2	3
6	C	1.400	120.4	0	5	1	2
7	N	1.400	121.5	180.0	5	1	2
8	N	1.319	122.3	180.0	7	5	6
9	S	1.604	115.6	180.0	8	7	5
10	O	1.513	110.4	0	9	8	7
11	H	1.084	121.0	180.0	1	2	3
12	H	1.086	119.3	180.0	2	1	5
13	H	1.086	120.7	0	6	5	7
14	H	1.025	120.3	0	7	5	6
15	C	1.436	120.0	180.0	4	3	2
16	H	1.085	121.0	0	3	2	12
17	N	1.163	179.9	180.2	15	4	6

Total Energy = -907.249326

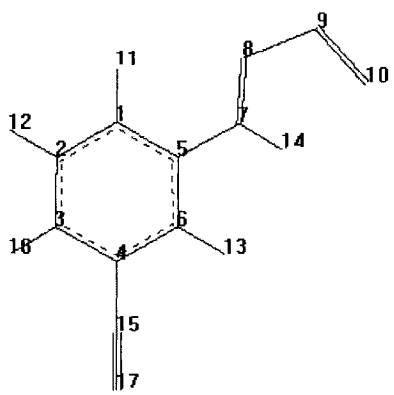

m5-CN-monomer

1	C	0	0	0	0	0	0
2	C	1.402	0	0	1	0	0
3	C	1.406	121.0	0	2	1	0
4	C	1.395	119.1	0	3	2	1
5	C	1.399	119.0	0	1	2	3
6	C	1.394	120.7	0	4	3	2
7	N	1.400	121.2	180.0	5	1	2
8	N	1.319	122.4	0	7	5	1
9	S	1.604	115.6	180.0	8	7	5
10	O	1.513	110.4	0	9	8	7
11	H	1.083	120.8	180.0	1	2	3
12	H	1.086	119.9	180.0	4	3	2
13	H	1.087	120.2	180.0	6	4	3
14	H	1.025	120.2	180.0	7	5	1
15	H	1.085	119.9	180.0	3	2	1
16	C	1.437	119.3	0	2	1	11
17	N	1.163	179.6	180.0	16	2	1

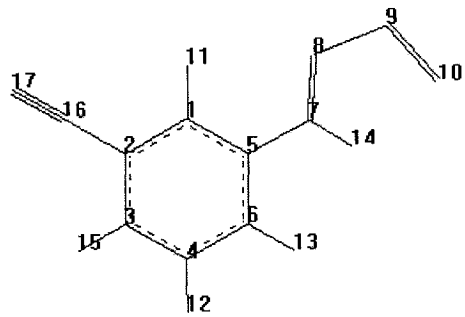

Total Energy = -907.249299

p-CN-monomer

1	C	0	0	0	0	0	0
2	C	1.389	0	0	1	0	0
3	C	1.408	120.6	0	2	1	0
4	C	1.407	119.4	0	3	2	1
5	C	1.404	119.5	0	1	2	3
6	C	1.389	120.2	0	4	3	2
7	C	1.432	120.3	180.0	3	2	1
8	N	1.397	121.5	180.0	5	1	2
9	N	1.320	122.5	0	8	5	1
10	S	1.603	115.7	180.0	9	8	5
11	O	1.512	110.5	0	10	9	8
12	H	1.084	120.8	180.0	1	2	3
13	H	1.085	119.8	180.0	2	1	5
14	H	1.085	119.8	180.0	4	3	2
15	H	1.087	119.9	180.0	6	4	3
16	H	1.025	120.2	180.0	8	5	1
17	N	1.164	179.9	359.2	7	3	4

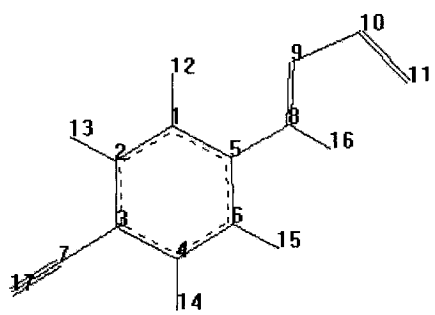

Total Energy = -907.251208

o2-CN-monomer

1	C	0	0	0	0	0	0
2	C	1.391	0	0	1	0	0
3	C	1.406	120.4	0	2	1	0
4	C	1.416	119.8	0	3	2	1
5	C	1.402	119.4	0	4	3	2
6	N	1.395	119.3	180.0	4	3	2
7	C	1.392	119.9	0	5	4	3
8	N	1.324	121.4	0	6	4	5
9	S	1.599	116.6	180.0	8	6	4
10	H	1.085	120.1	180.0	1	2	3
11	H	1.085	120.8	180.0	2	1	7
12	C	1.431	120.0	180.0	3	2	1
13	H	1.084	119.1	0	5	4	6
14	H	1.026	120.6	180.0	6	4	5
15	H	1.086	119.0	0	7	5	13
16	O	1.508	111.4	0	9	8	6
17	N	1.165	178.9	180.0	12	3	2

Total Energy = -907.248830

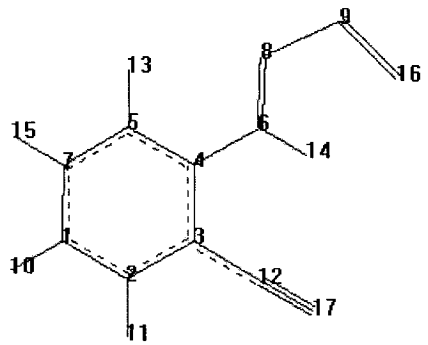

o6-CN-monomer

1	C	0	0	0	0	0	0
2	C	1.416	0	0	1	0	0
3	N	1.395	124.3	0	2	1	0
4	N	1.319	124.1	0.5	3	2	1
5	S	1.603	115.4	180.0	4	3	2
6	C	1.410	118.7	180.0	1	2	3
7	C	1.406	119.3	180.0	2	1	3
8	C	1.389	120.9	180.0	7	2	3
9	C	1.390	121.5	360.0	6	1	2
10	C	1.434	124.6	0.1	1	2	3
11	H	1.026	118.9	0.3	3	2	7
12	O	1.514	110.3	0	5	4	3
13	H	1.087	119.0	0	7	2	3
14	H	1.085	118.0	180.0	6	1	2
15	H	1.085	120.1	180.0	9	6	1
16	H	1.086	119.4	0	8	7	13
17	N	1.164	173.4	358.9	10	1	6

Total Energy = -907.243615

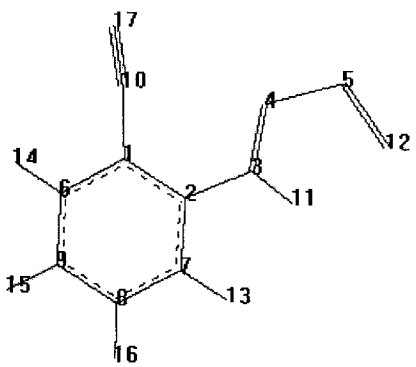

m3-OH(a)-monomer

1	C	0	0	0	0	0	0
2	C	1.393	0	0	1	0	0
3	C	1.398	121.5	0	2	1	0
4	C	1.400	119.1	0	3	2	1
5	C	1.403	118.5	0	1	2	3
6	C	1.396	120.5	0	4	3	2
7	N	1.404	121.4	180.0	5	1	2
8	N	1.315	122.7	180.0	7	5	6
9	S	1.607	115.7	180.0	8	7	5
10	O	1.516	110.3	0	9	8	7
11	H	1.083	121.4	180.0	1	2	3
12	H	1.087	119.3	180.0	2	1	5
13	H	1.086	119.2	180.0	6	4	3
14	H	1.025	120.0	0	7	5	6
15	O	1.369	122.8	180.0	4	3	2
16	H	1.088	120.5	0	3	2	12
17	H	0.970	110.0	180	15	4	6

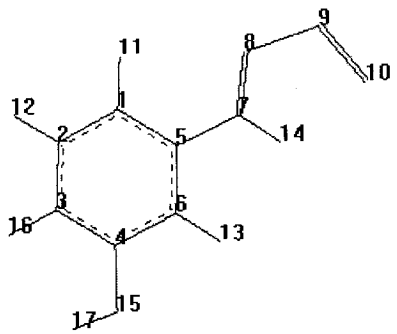

Total Energy = -890.221814

m3-OH(b)-monomer

1	C	0	0	0	0	0	0
2	C	1.396	0	0	1	0	0
3	C	1.395	121.7	0	2	1	0
4	C	1.400	119.1	0	3	2	1
5	C	1.400	118.5	0	1	2	3
6	C	1.396	120.5	0	4	3	2
7	N	1.404	121.6	180.0	5	1	2
8	N	1.315	122.8	0	7	5	1
9	S	1.608	115.4	180.0	8	7	5
10	O	1.517	110.1	0	9	8	7
11	H	1.083	121.5	180	1	2	3
12	H	1.087	119.1	180	2	1	5
13	H	1.089	120.4	180.0	6	4	3
14	H	1.026	120.1	180.0	7	5	1
15	O	1.369	117.2	180.0	4	3	2
16	H	1.085	121.7	0	3	2	12
17	H	0.970	110.4	0	15	4	6

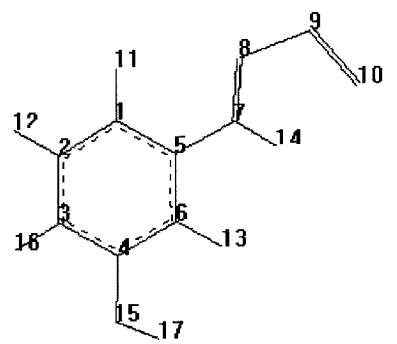

Total Energy = -890.221255

m5-OH(a)-monomer

1	C	0	0	0	0	0	0
2	C	1.396	0	0	1	0	0
3	C	1.401	120.9	0	2	1	0
4	C	1.397	119.2	0	3	2	1
5	C	1.397	118.8	0	1	2	3
6	C	1.392	121.0	0	4	3	2
7	N	1.403	121.0	180.0	5	1	2
8	N	1.315	122.9	0	7	5	1
9	S	1.607	115.6	180.0	8	7	5
10	O	1.517	110.3	0	9	8	7
11	H	1.083	120.1	180.0	1	2	3
12	H	1.086	119.5	180.0	4	3	2
13	H	1.087	120.7	180.0	6	4	3
14	H	1.025	119.9	180.0	7	5	1
15	H	1.088	120.4	180.0	3	2	1
16	O	1.369	116.6	0	2	1	11
17	H	0.970	110.0	180.0	16	2	1

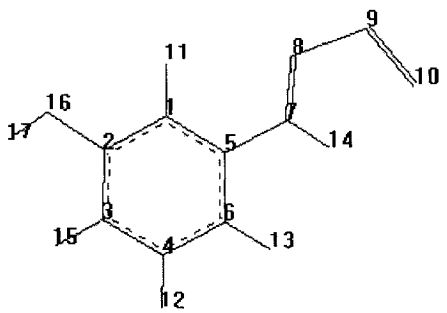

Total Energy = -890.221987

m5-OH(b)-monomer

1	C	0	0	0	0	0	0
2	C	1.396	0	0	1	0	0
3	C	1.402	121.0	0	2	1	0
4	C	1.394	119.1	0	3	2	1
5	C	1.401	118.9	0	1	2	3
6	C	1.396	121.2	0	4	3	2
7	N	1.403	120.8	180.0	5	1	2
8	N	1.315	122.8	0	7	5	1
9	S	1.609	115.7	180.0	8	7	5
10	O	1.516	110.2	0	9	8	7
11	H	1.086	121.3	180.0	1	2	3
12	H	1.086	119.5	180.0	4	3	2
13	H	1.087	120.7	180.0	6	4	3
14	H	1.025	119.9	180.0	7	5	1
15	H	1.085	119.3	180.0	3	2	1
16	O	1.368	122.0	0	2	1	11
17	H	0.970	110.2	0	16	2	1

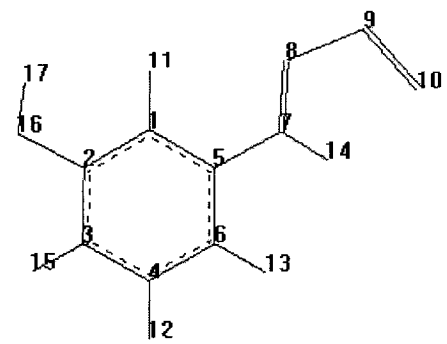

Total Energy = -890.222349

p-OH(a)-monomer

1	C	0	0	0	0	0	0
2	C	1.394	0	0	1	0	0
3	C	1.400	120.5	0	2	1	0
4	C	1.400	119.8	0	3	2	1
5	C	1.400	119.7	0	1	2	3
6	C	1.391	119.9	0	4	3	2
7	O	1.370	122.9	180.0	3	2	1
8	N	1.405	121.7	180.0	5	1	2
9	N	1.312	122.9	0	8	5	1
10	S	1.613	115.3	180.0	9	8	5
11	O	1.519	109.8	0	10	9	8
12	H	1.084	120.5	180.0	1	2	3
13	H	1.088	119.4	180.0	2	1	5
14	H	1.085	119.2	0	4	3	7
15	H	1.087	119.6	180.0	6	4	3
16	H	1.026	120.0	180.0	8	5	1
17	H	0.970	110.1	180.0	7	3	4

Total Energy = -890.220781

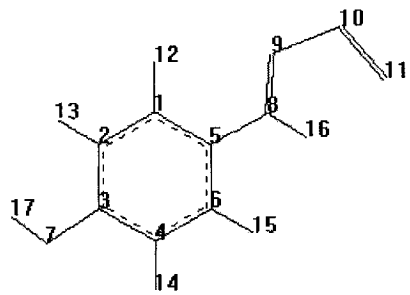

p-OH(b)-monomer

1	C	0	0	0	0	0	0
2	C	1.390	0	0	1	0	0
3	C	1.401	120.4	0	2	1	0
4	C	1.399	119.8	0	3	2	1
5	C	1.403	119.8	0	1	2	3
6	C	1.394	120.0	0	4	3	2
7	O	1.370	117.2	180.0	3	2	1
8	N	1.405	121.7	180.0	5	1	2
9	N	1.312	122.9	180.0	8	5	6
10	S	1.613	115.3	180.0	9	8	5
11	O	1.520	109.7	360.0	10	9	8
12	H	1.084	120.5	180.0	1	2	3
13	H	1.086	120.6	180.0	2	1	5
14	H	1.088	120.4	0	4	3	7
15	H	1.087	119.7	180.0	6	4	3
16	H	1.026	120.1	0	8	5	6
17	H	0.970	110.2	0	7	3	4

Total Energy = -890.220661

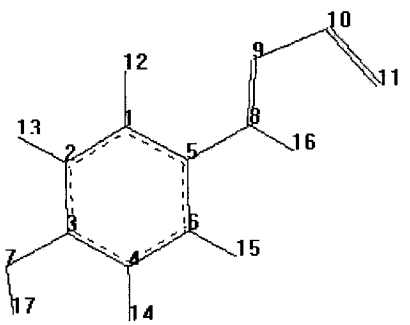

o2-OH(a)-monomer

1	C	0	0	0	0	0	0
2	C	1.408	0	0	1	0	0
3	N	1.400	117.5	0	2	1	0
4	N	1.316	122.1	180.0	3	2	1
5	S	1.607	116.1	180.0	4	3	2
6	C	1.393	120.1	180.0	1	2	3
7	C	1.399	119.7	180.0	2	1	3
8	C	1.395	120.0	180.0	7	2	3
9	C	1.398	120.3	0	8	7	2
10	O	1.373	116.0	180.0	1	2	7
11	H	1.025	119.5	180.0	3	2	7
12	O	1.515	110.8	0	5	4	3
13	H	1.084	118.9	0	7	2	3
14	H	1.088	119.5	0	6	1	10
15	H	1.086	120.5	180.0	9	8	7
16	H	1.086	119.5	0	8	7	13
17	H	0.969	110.6	0.1	10	1	6

Total Energy = -890.221374

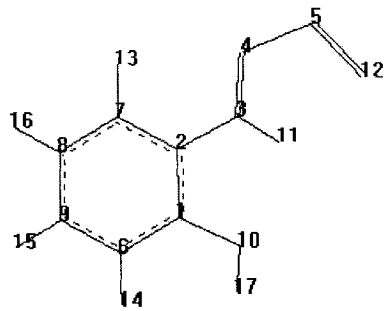

o6-OH(a)-monomer

1	C	0	0	0	0	0	0
2	C	1.412	0	0	1	0	0
3	N	1.403	124.2	0	2	1	0
4	N	1.315	125.7	344.6	3	2	1
5	S	1.611	114.5	181.1	4	3	2
6	C	1.399	119.0	180.7	1	2	3
7	C	1.404	119.0	178.5	2	1	3
8	C	1.392	121.4	178.9	7	2	3
9	C	1.395	121.4	0.7	6	1	2
10	O	1.364	119.0	359.9	1	2	3
11	H	1.028	118.0	349.1	3	2	7
12	O	1.521	110.0	0.3	5	4	3
13	H	1.088	118.6	358.6	7	2	3
14	H	1.089	118.6	1.0	6	1	10
15	H	1.086	119.7	179.8	9	6	1
16	H	1.086	119.8	0.2	8	7	13
17	H	0.970	109.3	2.0	10	1	6

Total Energy = -890.212299

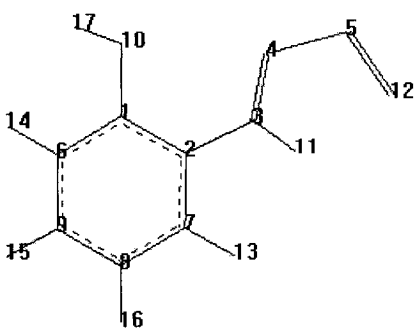

o6-OH(b)-monomer

1	C	0	0	0	0	0	0
2	C	1.415	0	0	1	0	0
3	N	1.404	122.6	0	2	1	0
4	N	1.314	124.0	359.9	3	2	1
5	S	1.623	115.4	180.0	4	3	2
6	C	1.400	118.6	180.0	1	2	3
7	C	1.405	119.9	180.0	2	1	3
8	C	1.390	120.7	180.0	7	2	3
9	C	1.392	121.0	0	6	1	2
10	O	1.358	123.7	0	1	2	3
11	H	1.028	119.7	360.0	3	2	7
12	O	1.518	108.5	0	5	4	3
13	H	1.088	119.0	0	7	2	3
14	H	1.086	117.6	0	6	1	10
15	H	1.086	119.6	180.0	9	6	1
16	H	1.086	119.8	0	8	7	13
17	H	0.980	109.7	180.1	10	1	6

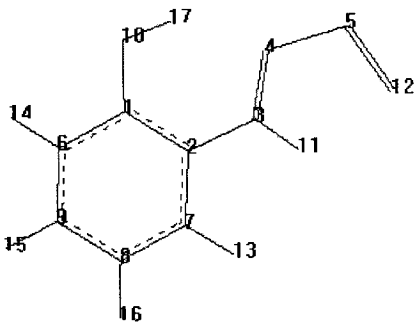

Total Energy = -890.223247

m3-OMe(a)-monomer

1	C	0	0	0	0	0	0
2	C	1.391	0	0	1	0	0
3	C	1.401	121.9	0	2	1	0
4	C	1.401	119.0	0	3	2	1
5	C	1.404	118.3	0	1	2	3
6	C	1.397	121.0	0	5	1	2
7	N	1.404	121.4	180.0	5	1	2
8	N	1.314	122.8	180.0	7	5	6
9	S	1.608	115.7	180.0	8	7	5
10	O	1.517	110.3	0	9	8	7
11	H	1.083	121.5	180.0	1	2	3
12	H	1.087	119.2	180.0	2	1	5
13	H	1.087	121.4	180.0	6	5	1
14	H	1.025	120.0	0	7	5	6
15	O	1.365	124.6	180.0	4	3	2
16	H	1.084	119.7	0	3	2	12
17	C	1.423	118.6	180.0	15	4	6
18	H	1.098	111.2	61.3	17	15	4
19	H	1.098	111.2	298.7	17	15	4
20	H	1.091	105.6	180.0	17	15	4

Total Energy = -929.498452

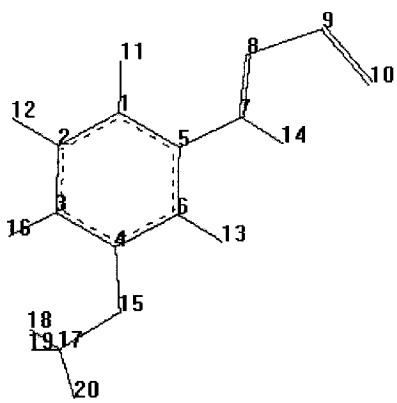

m3-OMe(b)-monomer

1	C	0	0	0	0	0	0
2	C	1.398	0	0	1	0	0
3	C	1.392	121.5	0	2	1	0
4	C	1.405	119.5	0	3	2	1
5	C	1.397	118.3	0	1	2	3
6	C	1.398	120.1	0	4	3	2
7	N	1.405	121.6	180.0	5	1	2
8	N	1.314	122.9	0	7	5	1
9	S	1.609	115.5	180.0	8	7	5
10	O	1.518	110.2	0	9	8	7
11	H	1.083	121.5	180.0	1	2	3
12	H	1.087	119.2	180.0	2	1	5
13	H	1.085	121.3	180.0	6	4	3
14	H	1.026	120.0	180.0	7	5	1
15	O	1.364	115.8	180.0	4	3	2
16	H	1.085	121.7	0	3	2	12
17	C	1.423	118.9	0	15	4	6
18	H	1.098	111.3	61.3	17	15	4
19	H	1.098	111.3	298.6	17	15	4
20	H	1.091	105.7	179.9	17	15	4

Total Energy = -929.498452

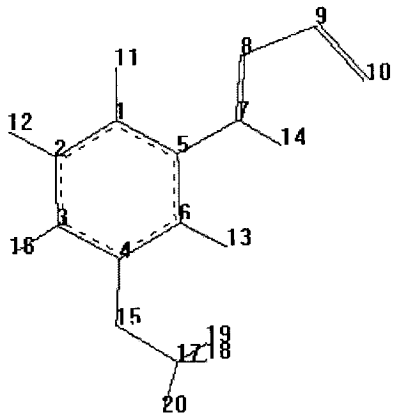

m5-OMe(a)-monomer

1	C	0	0	0	0	0	0
2	C	1.401	0	0	1	0	0
3	C	1.403	120.6	0	2	1	0
4	C	1.400	119.0	0	3	2	1
5	C	1.394	119.3	0	1	2	3
6	C	1.390	121.4	0	4	3	2
7	N	1.404	121.2	180.0	5	1	2
8	N	1.314	122.9	0	7	5	1
9	S	1.608	115.6	180.0	8	7	5
10	O	1.517	110.3	0	9	8	7
11	H	1.083	119.7	180.0	1	2	3
12	H	1.087	119.2	180.0	4	3	2
13	H	1.087	120.8	180.0	6	4	3
14	H	1.025	119.9	180.0	7	5	1
15	H	1.083	121.3	180.0	3	2	1
16	O	1.364	115.1	0	2	1	11
17	C	1.423	118.8	180.0	16	2	1
18	H	1.098	111.3	61.3	17	16	2
19	H	1.098	111.3	298.7	17	16	2
20	H	1.091	105.6	180.0	17	16	2

Total Energy = -929.498534

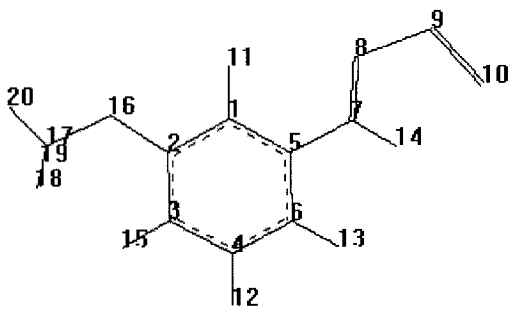

m5-OMe(b)-monomer

1	C	0	0	0	0	0	0
2	C	1.397	0	0	1	0	0
3	C	1.407	120.5	0	2	1	0
4	C	1.391	119.5	0	3	2	1
5	C	1.403	118.8	0	1	2	3
6	C	1.398	121.1	0	4	3	2
7	N	1.404	120.6	180.0	5	1	2
8	N	1.314	123.0	180.0	7	5	6
9	S	1.609	115.6	180.0	8	7	5
10	O	1.517	110.2	0	9	8	7
11	H	1.082	122.2	180.0	1	2	3
12	H	1.086	119.6	180.0	4	3	2
13	H	1.087	120.8	180.0	6	4	3
14	H	1.025	119.8	0	7	5	6
15	H	1.085	118.9	180.0	3	2	1
16	O	1.363	123.8	0	2	1	11
17	C	1.424	118.8	0	16	2	1
18	H	1.097	111.2	61.2	17	16	2
19	H	1.097	111.2	298.8	17	16	2
20	H	1.091	105.6	180.0	17	16	2

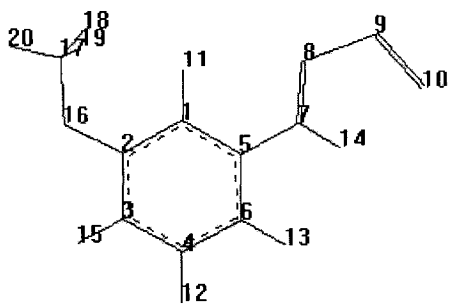

Total Energy = -929.499186

p-OMe(a)-monomer

1	C	0	0	0	0	0	0
2	C	1.397	0	0	1	0	0
3	C	1.402	120.2	0	2	1	0
4	C	1.404	119.4	0	3	2	1
5	C	1.397	120.1	0	1	2	3
6	C	1.388	120.3	0	4	3	2
7	O	1.365	124.7	180.0	3	2	1
8	N	1.405	121.9	180.0	5	1	2
9	N	1.312	123.0	0	8	5	1
10	S	1.613	115.3	180.0	9	8	5
11	O	1.520	109.8	0	10	9	8
12	H	1.084	120.2	180.0	1	2	3
13	H	1.084	118.7	180.0	2	1	5
14	H	1.086	118.8	0	4	3	7
15	H	1.088	119.7	180.0	6	4	3
16	H	1.026	120.0	180.0	8	5	1
17	C	1.423	118.6	0	7	3	2
18	H	1.098	111.3	61.3	17	7	3
19	H	1.098	111.3	298.7	17	7	3
20	H	1.091	105.7	180.0	17	7	3

Total Energy = -929.497600

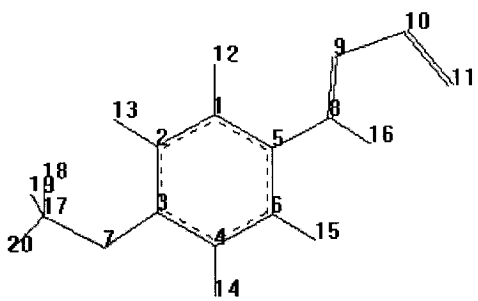

p-OMe(b)-monomer

1	C	0	0	0	0	0	0
2	C	1.387	0	0	1	0	0
3	C	1.406	120.8	0	2	1	0
4	C	1.401	119.5	0	3	2	1
5	C	1.405	119.7	0	1	2	3
6	C	1.397	119.8	0	4	3	2
7	O	1.365	115.8	180.0	3	2	1
8	N	1.405	121.7	180.0	5	1	2
9	N	1.312	123.0	180.0	8	5	6
10	S	1.613	115.3	180.0	9	8	5
11	O	1.520	109.7	0	10	9	8
12	H	1.084	120.6	180.0	1	2	3
13	H	1.086	120.6	180.0	2	1	5
14	H	1.084	121.3	0	4	3	7
15	H	1.088	119.4	180.0	6	4	3
16	H	1.026	120.0	0	8	5	6
17	C	1.422	118.6	0	7	3	4
18	H	1.098	111.3	61.3	17	7	3
19	H	1.098	111.3	298.7	17	7	3
20	H	1.091	105.7	180.0	17	7	3

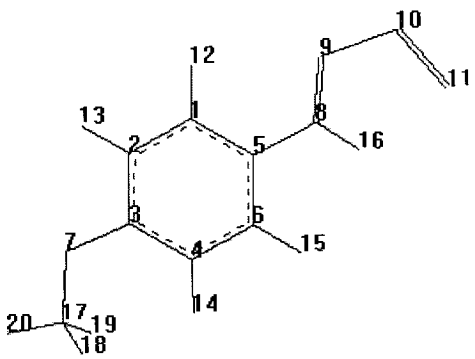

Total Energy = -929.497635

o2-OMe(a)-monomer

1	C	0	0	0	0	0	0
2	C	1.414	0	0	1	0	0
3	N	1.400	117.2	0	2	1	0
4	N	1.315	122.4	180.0	3	2	1
5	S	1.608	115.9	180.0	4	3	2
6	C	1.395	119.7	180.0	1	2	3
7	C	1.397	120.1	180.0	2	1	3
8	C	1.397	119.9	180.0	7	2	3
9	C	1.395	120.1	0	8	7	2
10	O	1.367	114.9	180.0	1	2	7
11	H	1.025	119.1	180.0	3	2	7
12	O	1.516	110.7	0	5	4	3
13	H	1.084	118.9	0	7	2	3
14	H	1.084	120.3	0	6	1	10
15	H	1.086	120.4	180.0	9	8	7
16	H	1.086	119.5	0	8	7	13
17	C	1.425	118.9	0.2	10	1	6
18	H	1.097	111.0	61.0	17	10	1
19	H	1.097	111.0	298.6	17	10	1
20	H	1.091	105.6	179.8	17	10	1

Total Energy = -929.498505

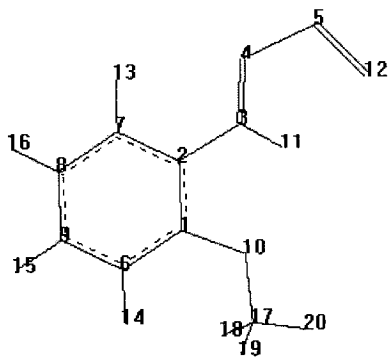

o6-OMe(a)-monomer

1	C	0	0	0	0	0	0
2	C	1.418	0	0	1	0	0
3	N	1.406	123.7	0	2	1	0
4	N	1.315	125.7	24.2	3	2	1
5	S	1.611	114.6	177.8	4	3	2
6	C	1.401	118.7	178.9	1	2	3
7	C	1.401	119.5	182.3	2	1	3
8	C	1.394	121.3	181.6	7	2	3
9	C	1.395	119.3	359.6	8	7	2
10	O	1.357	117.2	182.4	1	2	7
11	H	1.027	118.0	16.7	3	2	7
12	O	1.521	110.1	359.5	5	4	3
13	H	1.088	118.6	2.1	7	2	3
14	H	1.084	119.7	358.5	6	1	10
15	H	1.086	120.5	180.5	9	8	7
16	H	1.086	119.9	359.6	8	7	13
17	C	1.423	119.0	359.2	10	1	6
18	H	1.097	111.2	62.3	17	10	1
19	H	1.098	111.3	299.6	17	10	1
20	H	1.091	105.4	180.9	17	10	1

Total Energy = -929.488875

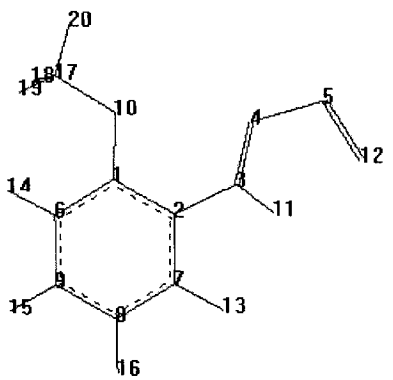

o6-OMe(b)-monomer

1	C	0	0	0	0	0	0
2	C	1.412	0	0	1	0	0
3	N	1.405	123.3	0	2	1	0
4	N	1.316	124.3	331.9	3	2	1
5	S	1.610	115.0	180.6	4	3	2
6	C	1.398	119.0	181.2	1	2	3
7	C	1.405	119.5	177.5	2	1	3
8	C	1.392	120.8	178.7	7	2	3
9	C	1.395	121.2	0.6	6	1	2
10	O	1.371	120.8	173.4	1	2	7
11	H	1.026	119.0	338.2	3	2	7
12	O	1.519	110.2	0.3	5	4	3
13	H	1.088	119.0	358.0	7	2	3
14	H	1.087	118.0	3.8	6	1	10
15	H	1.086	119.9	179.5	9	6	1
16	H	1.086	119.6	0.5	8	7	13
17	C	1.433	116.1	278.2	10	1	6
18	H	1.098	110.9	58.1	17	10	1
19	H	1.096	110.6	295.7	17	10	1
20	H	1.092	106.0	177.0	17	10	1

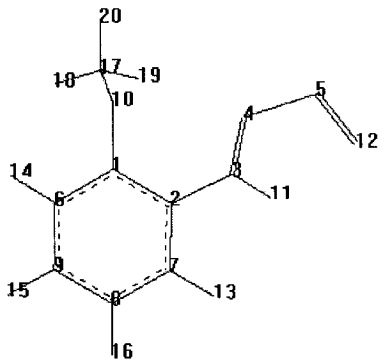

Total energy = -929.487022

PhNHNSO-dimer

1	C	0	0	0	0	0	0
2	C	1.403	0	0	1	0	0
3	C	1.395	119.3	0	1	2	0
4	H	1.085	119.5	180.2	1	2	3
5	N	1.412	118.0	180.0	2	1	3
6	C	1.402	120.6	180.2	2	1	4
7	C	1.398	120.6	179.8	3	1	4
8	H	1.087	119.2	359.9	3	1	4
9	N	1.305	120.7	1.1	5	2	6
10	C	1.394	119.2	0	6	2	1
11	H	1.086	120.3	360.0	7	3	8
12	H	1.084	119.8	179.9	6	2	1
13	H	1.032	118.7	181.3	5	2	6
14	S	1.597	121.9	179.8	9	5	2
15	H	1.087	119.2	0.0	10	6	12
16	O	1.525	113.6	359.7	14	9	5
17	H	1.908	156.8	43.3	16	14	9
18	N	1.032	160.4	124.1	17	16	14
19	C	1.412	118.7	2.6	18	17	16
20	N	1.305	120.6	182.8	18	17	16
21	C	1.403	118.0	1.3	19	18	17
22	C	1.402	121.3	181.3	19	18	17
23	S	1.597	121.9	359.6	20	18	17
24	C	1.395	119.3	0	21	19	22
25	C	1.394	119.2	0	22	19	21
26	O	1.525	113.6	359.7	23	20	18
27	H	1.086	119.5	180.2	21	19	22
28	H	1.084	119.8	179.9	22	19	21
29	C	1.398	120.6	179.8	24	21	27
30	H	1.087	119.2	0.0	25	22	28
31	H	1.087	119.2	359.9	24	21	27
32	H	1.086	120.3	180.0	29	24	21

Total energy = -1630.026781

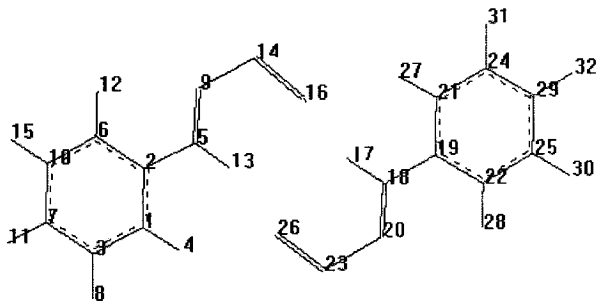

mCl3-dimer

1	C	0	0	0	0	0	0
2	C	1.395	0	0	1	0	0
3	C	1.398	118.4	0	1	2	0
4	H	1.085	120.4	-180.0	1	2	3
5	C	1.392	121.9	0	2	1	3
6	C	1.393	121.3	0	3	1	2
7	H	1.087	119.4	180.0	3	1	6
8	Cl	1.758	119.3	-180.0	2	1	5
9	C	1.403	118.5	0	5	2	1
10	H	1.085	121.3	179.9	5	2	9
11	H	1.084	121.1	-180.0	6	3	1
12	N	1.410	117.6	180.0	9	5	2
13	N	1.307	120.6	-179.2	12	9	5
14	H	1.032	118.8	-179.9	12	9	13
15	S	1.595	121.5	179.7	13	12	9
16	O	1.524	113.3	-0.3	15	13	12
17	C	6.898	141.5	20.5	15	13	16
18	C	1.395	21.7	177.9	17	15	13
19	C	1.398	97.1	170.0	17	15	18
20	H	1.085	141.5	-15.7	17	15	18
21	C	1.392	121.9	11.3	18	17	15
22	C	1.393	121.3	-4.1	19	17	15
23	H	1.087	119.4	180.0	19	17	22
24	Cl	1.758	119.3	-180.0	18	17	21
25	C	1.403	118.5	0	21	18	17
26	H	1.085	121.3	179.9	21	18	25
27	H	1.084	121.1	-180.0	22	19	17
28	N	1.410	117.6	180.0	25	21	18
29	N	1.307	120.6	-179.2	28	25	21
30	H	1.032	118.8	-179.9	28	25	29
31	S	1.595	121.5	179.7	29	28	25
32	O	1.524	113.3	-0.3	31	29	28

Total energy = -2549.236064

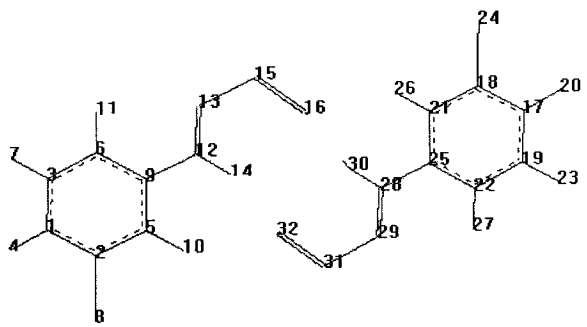

mCl5-dimer

1	C	0	0	0	0	0	0
2	C	1.397	0	0	1	0	0
3	C	1.397	118.5	0	1	2	0
4	H	1.085	121.2	180.0	1	2	3
5	C	1.394	121.1	360.0	2	1	3
6	C	1.391	122.0	180.0	3	1	4
7	H	1.086	119.5	0	2	1	4
8	Cl	1.758	119.2	360.0	3	1	4
9	C	1.402	118.4	0	6	3	1
10	H	1.085	121.3	359.9	5	2	7
11	H	1.083	121.0	180.1	6	3	1
12	N	1.410	120.8	180.1	9	6	3
13	N	1.307	120.7	1.2	12	9	6
14	H	1.032	118.6	181.4	12	9	6
15	S	1.595	121.8	179.6	13	12	9
16	O	1.524	113.5	359.7	15	13	12
17	C	5.690	138.8	152.6	16	15	13
18	C	1.397	29.5	31.6	17	16	15
19	C	1.397	89.0	209.4	17	16	15
20	H	1.085	150.7	27.4	17	16	15
21	C	1.394	121.1	360.0	18	17	19
22	C	1.391	122.0	180.0	19	17	20
23	H	1.086	119.5	0	18	17	20
24	Cl	1.758	119.3	360.0	19	17	20
25	C	1.402	118.4	0.0	22	19	17
26	H	1.085	121.3	359.9	21	18	23
27	H	1.083	121.0	180.1	22	19	17
28	N	1.410	120.8	180.1	25	22	19
29	N	1.307	120.7	1.2	28	25	22
30	H	1.032	118.6	181.5	28	25	22
31	S	1.595	121.8	179.6	29	28	25
32	O	1.524	113.5	359.7	31	29	28

Total energy = -2549.236088

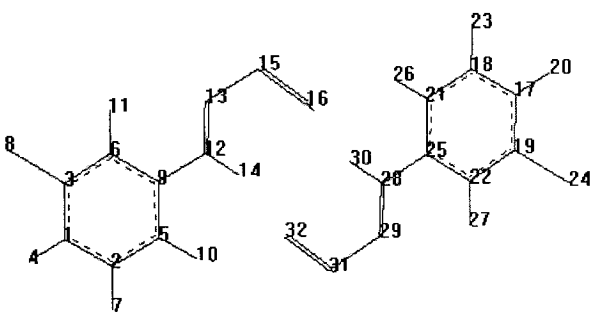

pCl-dimer

1	C	0	0	0	0	0	0
2	C	1.393	0	0	1	0	0
3	C	1.402	119.7	0	1	2	0
4	H	1.084	120.4	180.1	1	2	3
5	C	1.397	119.8	360.0	2	1	3
6	C	1.402	120.4	180.0	3	1	4
7	N	1.410	121.4	0	3	1	4
8	H	1.085	120.1	0	2	1	4
9	C	1.394	119.8	360.0	6	3	1
10	Cl	1.757	119.6	0	5	2	8
11	N	1.306	120.6	0.7	7	3	1
12	H	1.085	119.6	180.1	6	3	1
13	H	1.032	118.7	180.8	7	3	1
14	S	1.596	121.8	179.6	11	7	3
15	H	1.085	120.2	360.0	9	6	12
16	O	1.525	113.4	359.7	14	11	7
17	C	4.937	162.5	129.8	16	14	11
18	C	1.393	124.4	47.9	17	16	14
19	C	1.402	4.8	58.2	17	16	14
20	H	1.084	115.3	228.8	17	16	14
21	C	1.397	119.8	360.0	18	17	19
22	C	1.402	120.4	180.0	19	17	20
23	N	1.410	121.4	0.1	19	17	20
24	H	1.085	120.1	0	18	17	20
25	C	1.394	119.8	360.0	22	19	17
26	Cl	1.757	119.6	0	21	18	24
27	N	1.306	120.6	0.6	23	19	17
28	H	1.085	119.6	180.1	22	19	17
29	H	1.032	118.7	180.8	23	19	17
30	S	1.596	121.8	179.6	27	23	19
31	H	1.085	120.2	360.0	25	22	28
32	O	1.525	113.4	359.7	30	27	23

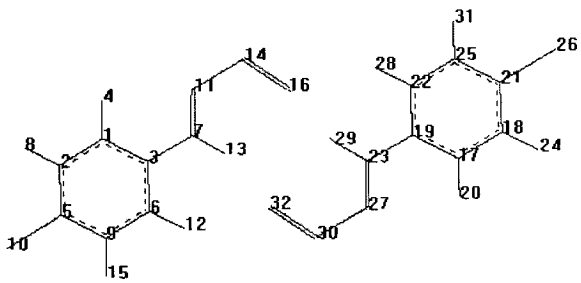

Total energy = -2549.236490

oCl2-dimer

1	C	0	0	0	0	0	0
2	C	1.395	0	0	1	0	0
3	C	1.398	119.8	0.0	1	2	0
4	H	1.086	119.7	179.7	1	2	3
5	C	1.395	120.0	0.1	2	1	3
6	C	1.392	120.3	179.5	3	1	4
7	H	1.085	120.9	0.8	2	1	4
8	H	1.086	120.3	0.2	3	1	4
9	C	1.404	120.5	0.4	6	3	1
10	Cl	1.755	118.7	2.1	5	2	7
11	H	1.084	121.0	0.1	6	3	8
12	N	1.408	120.8	180.1	9	6	3
13	N	1.312	119.5	339.9	12	9	6
14	H	1.032	119.3	146.2	12	9	6
15	S	1.596	120.9	176.7	13	12	9
16	O	1.518	113.3	0.2	15	13	12
17	H	1.941	137.7	273.8	16	15	13
18	N	1.032	146.2	191.0	17	16	15
19	C	1.408	119.3	69.4	18	17	16
20	N	1.312	119.7	263.1	18	17	16
21	C	1.406	120.4	34.3	19	18	17
22	C	1.404	120.8	213.7	19	18	17
23	S	1.595	121.0	349.4	20	18	17
24	C	1.395	120.6	1.4	21	19	22
25	C	1.392	120.5	359.3	22	19	21
26	O	1.518	113.4	359.8	23	20	18
27	Cl	1.755	120.6	183.5	21	19	22
28	H	1.084	118.5	179.8	22	19	21
29	C	1.395	120.0	359.0	24	21	19
30	H	1.086	119.4	359.9	25	22	28
31	H	1.085	119.1	179.9	24	21	19
32	H	1.086	119.7	180.2	29	24	21

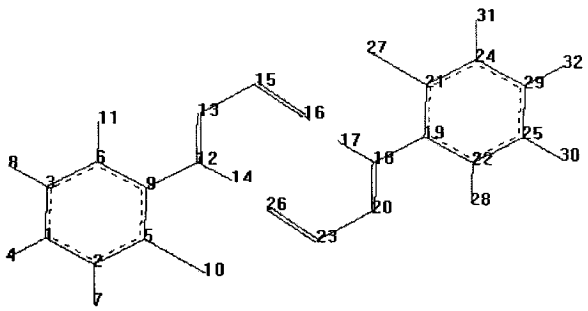

Total energy = -2549.220689

oCl6-dimer

1	C	0	0	0	0	0	0
2	C	1.397	0	0	1	0	0
3	C	1.395	119.8	0	1	2	0
4	H	1.086	120.6	179.3	1	2	3
5	C	1.392	120.0	1.3	2	1	3
6	C	1.397	120.6	180.3	3	1	4
7	H	1.086	120.5	359.9	2	1	4
8	H	1.085	120.7	359.1	3	1	4
9	C	1.405	120.8	180.3	5	2	7
10	H	1.086	121.0	0.3	5	2	7
11	Cl	1.752	117.7	356.9	6	3	8
12	N	1.414	117.1	0.4	9	5	10
13	N	1.309	121.1	218.9	12	9	5
14	H	1.033	117.7	27.4	12	9	5
15	S	1.594	121.2	178.7	13	12	9
16	O	1.526	113.5	0.8	15	13	12
17	H	1.892	152.6	299.6	16	15	13
18	N	1.033	156.7	201.2	17	16	15
19	C	1.414	117.7	34.6	18	17	16
20	N	1.309	120.1	226.1	18	17	16
21	C	1.405	117.1	332.9	19	18	17
22	C	1.408	124.0	151.1	19	18	17
23	S	1.594	121.2	349.6	20	18	17
24	C	1.392	120.8	1.4	21	19	22
25	C	1.397	119.9	357.7	22	19	21
26	H	1.086	118.2	181.4	21	19	22
27	Cl	1.752	122.4	174.7	22	19	21
28	O	1.526	113.4	359.2	23	20	18
29	C	1.395	120.6	1.4	25	22	19
30	H	1.086	119.6	359.8	24	21	26
31	H	1.085	118.7	180.2	25	22	19
32	H	1.086	119.6	179.7	29	25	22

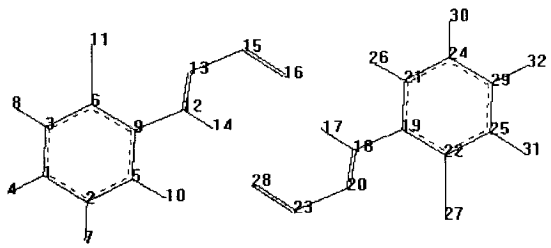

Total energy = -2549.215527

mCl3-5-dimer

1	C	0	0	0	0	0	0
2	C	1.393	0	0	1	0	0
3	C	1.402	119.0	0	1	2	0
4	H	1.084	121.1	180.0	1	2	3
5	C	1.398	121.3	360.0	2	1	3
6	C	1.403	120.9	180.0	3	1	4
7	N	1.410	121.4	0	3	1	4
8	H	1.087	119.4	0	2	1	4
9	C	1.392	118.5	0	6	3	1
10	N	1.307	120.5	1.0	7	3	1
11	H	1.084	120.2	180.2	6	3	1
12	H	1.032	118.8	181.3	7	3	1
13	H	1.085	121.2	0.0	5	2	8
14	S	1.595	121.8	359.5	10	7	12
15	Cl	1.758	118.8	359.8	9	6	11
16	O	1.524	113.6	359.8	14	10	7
17	C	4.946	160.1	121.1	16	14	10
18	C	1.391	123.6	55.1	17	16	14
19	C	1.402	5.4	70.3	17	16	14
20	H	1.083	115.4	236.6	17	16	14
21	C	1.397	122.0	0	18	17	19
22	C	1.402	120.9	180.0	19	17	20
23	N	1.410	120.8	0.0	19	17	20
24	Cl	1.758	118.8	0.1	18	17	20
25	C	1.394	119.1	0	22	19	17
26	N	1.307	120.7	1.1	23	19	17
27	H	1.085	119.6	180.1	22	19	17
28	H	1.032	118.7	181.4	23	19	17
29	H	1.085	120.3	180.0	21	18	17
30	S	1.595	121.8	359.4	26	23	28
31	H	1.086	119.4	360.0	25	22	27
32	O	1.524	113.4	359.7	30	26	23

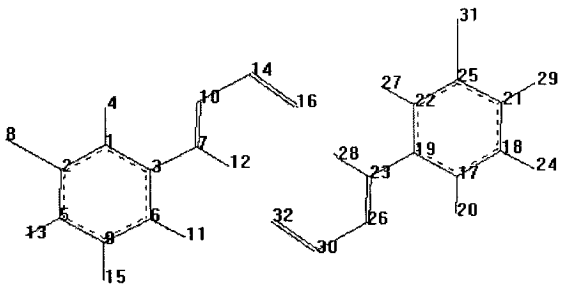

Total energy = -2549.236055

oCl2-6-dimer

1	C	0	0	0	0	0	0
2	C	1.395	0	0	1	0	0
3	C	1.399	119.7	0	1	2	0
4	H	1.086	119.7	179.8	1	2	3
5	C	1.394	120.0	0.1	2	1	3
6	C	1.392	120.3	179.6	3	1	4
7	H	1.085	120.9	0.6	2	1	4
8	H	1.086	120.3	0.2	3	1	4
9	C	1.403	120.4	0.3	6	3	1
10	Cl	1.755	118.8	1.7	5	2	7
11	H	1.084	121.0	0.1	6	3	8
12	N	1.408	121.0	179.8	9	6	3
13	N	1.311	119.7	346.7	12	9	6
14	H	1.030	118.8	150.5	12	9	6
15	S	1.592	122.4	178.0	13	12	9
16	O	1.519	114.8	1.0	15	13	12
17	C	4.883	173.9	229.2	16	15	13
18	C	1.409	14.7	10.1	17	16	15
19	C	1.398	122.4	285.3	17	16	15
20	Cl	1.753	117.6	125.1	17	16	15
21	N	1.410	125.1	180.8	18	17	19
22	C	1.407	118.6	2.5	18	17	19
23	C	1.394	120.8	358.5	19	17	18
24	H	1.085	118.5	179.7	19	17	18
25	N	1.311	122.5	209.1	21	18	22
26	C	1.391	121.1	358.3	22	18	17
27	H	1.034	117.5	22.0	21	18	22
28	H	1.085	118.2	178.0	22	18	17
29	H	1.086	119.7	359.1	23	19	24
30	S	1.598	119.4	5.1	25	21	27
31	H	1.086	119.5	0.6	26	22	28
32	O	1.523	112.3	359.2	30	25	21

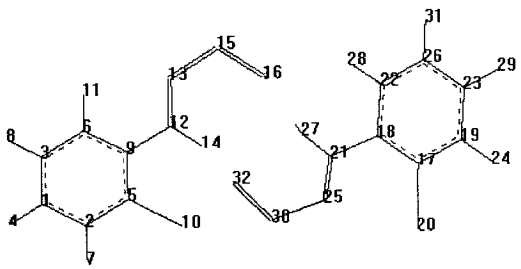

Total energy = -2549.217564

mMe3-dimer

1	C	0	0	0	0	0	0
2	C	1.395	0	0	1	0	0
3	C	1.400	118.6	0	1	2	0
4	H	1.084	121.2	180.2	1	2	3
5	C	1.397	120.9	360.0	2	1	3
6	C	1.403	120.8	179.9	3	1	4
7	N	1.412	121.4	0.1	3	1	4
8	H	1.087	119.3	0.1	2	1	4
9	C	1.398	120.4	360.0	6	3	1
10	N	1.305	120.7	1.0	7	3	1
11	H	1.086	119.0	180.1	6	3	1
12	H	1.032	118.7	181.2	7	3	1
13	H	1.088	119.8	360.0	5	2	8
14	S	1.597	121.9	359.1	10	7	12
15	C	1.512	120.6	359.6	9	6	11
16	O	1.525	113.6	359.6	14	10	7
17	H	1.098	111.2	243.8	15	9	6
18	H	1.095	111.4	4.1	15	9	6
19	H	1.097	111.3	124.5	15	9	6
20	C	4.960	157.1	118.9	16	14	10
21	C	1.395	123.8	57.5	20	16	14
22	C	1.400	5.3	70.9	20	16	14
23	H	1.084	115.0	238.6	20	16	14
24	C	1.397	120.9	360.0	21	20	22
25	C	1.403	120.8	179.9	22	20	23
26	N	1.412	121.4	0.1	22	20	23
27	H	1.087	119.3	0.1	21	20	23
28	C	1.398	120.4	360.0	25	22	20
29	N	1.305	120.7	0.9	26	22	20
30	H	1.086	119.0	180.1	25	22	20
31	H	1.032	118.7	181.2	26	22	20
32	H	1.088	119.8	360.0	24	21	27
33	S	1.597	121.9	359.1	29	26	31
34	C	1.512	120.6	359.6	28	25	30
35	O	1.525	113.6	359.6	33	29	26
36	H	1.097	111.3	125.1	34	28	25
37	H	1.098	111.2	244.4	34	28	25
38	H	1.095	111.4	4.6	34	28	25

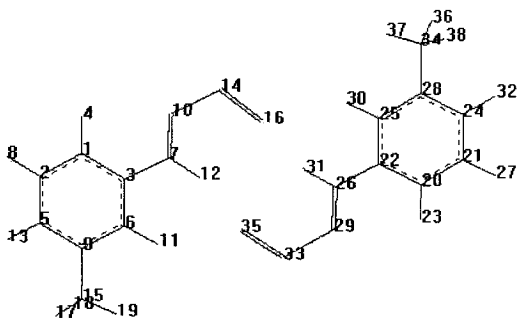

Total energy = -1708.609310

mMe5-dimer

1	C	0	0	0	0	0	0
2	C	1.397	0	0	1	0	0
3	C	1.403	120.3	0	1	2	0
4	H	1.085	120.4	180.0	1	2	3
5	C	1.406	118.9	0	2	1	3
6	C	1.400	120.8	180.0	3	1	4
7	N	1.412	121.1	0	3	1	4
8	C	1.512	120.6	0.2	2	1	4
9	C	1.395	120.5	359.9	5	2	1
10	N	1.305	120.8	178.7	7	3	6
11	H	1.085	119.8	179.9	6	3	1
12	H	1.033	118.6	358.3	7	3	6
13	H	1.088	119.6	179.9	5	2	1
14	H	1.097	111.2	236.3	8	2	1
15	H	1.095	111.5	356.8	8	2	1
16	H	1.097	111.2	117.0	8	2	1
17	S	1.598	121.8	0.6	10	7	12
18	H	1.087	119.9	0	9	5	13
19	O	1.525	113.5	0.3	17	10	7
20	C	4.955	154.7	245.0	19	17	10
21	C	1.397	125.5	300.6	20	19	17
22	C	1.403	5.5	282.6	20	19	17
23	H	1.085	114.1	118.8	20	19	17
24	C	1.406	118.9	0.1	21	20	22
25	C	1.400	120.8	180.0	22	20	23
26	N	1.412	121.1	0.1	22	20	23
27	C	1.512	120.6	0.2	21	20	23
28	C	1.395	120.5	359.9	24	21	20
29	N	1.305	120.9	178.4	26	22	25
30	H	1.085	119.8	179.9	25	22	20
31	H	1.033	118.6	358.0	26	22	25
32	H	1.088	119.6	179.9	24	21	20
33	H	1.097	111.2	236.1	27	21	20
34	H	1.095	111.5	356.5	27	21	20
35	H	1.097	111.2	116.7	27	21	20
36	S	1.598	121.8	0.6	29	26	31
37	H	1.087	119.9	0.1	28	24	32
38	O	1.525	113.5	0.3	36	29	26

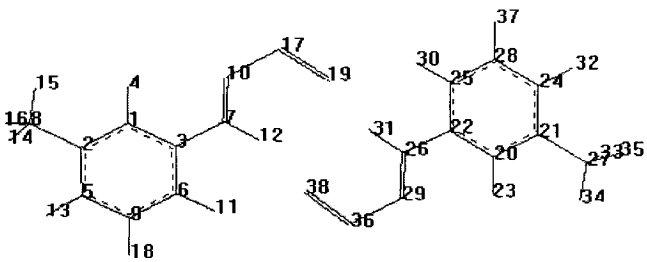

Total energy = -1708.609288

pMe-dimer

1	C	0	0	0	0	0	0
2	C	1.392	0	0	1	0	0
3	C	1.403	119.3	0	1	2	0
4	H	1.084	120.8	180.1	1	2	3
5	C	1.406	121.8	360.0	2	1	3
6	C	1.400	120.1	179.9	3	1	4
7	N	1.412	121.5	0	3	1	4
8	H	1.088	118.8	0.1	2	1	4
9	C	1.395	119.4	360.0	6	3	1
10	N	1.304	120.8	181.2	7	3	6
11	H	1.086	119.6	180.2	6	3	1
12	H	1.033	118.6	1.4	7	3	6
13	C	1.511	120.8	0.2	5	2	8
14	S	1.599	121.8	359.3	10	7	12
15	H	1.088	118.8	359.9	9	6	11
16	H	1.097	111.4	123.0	13	5	9
17	H	1.098	111.4	242.5	13	5	9
18	H	1.095	111.4	2.7	13	5	9
19	O	1.526	113.5	359.6	14	10	7
20	C	4.945	156.7	118.0	19	14	10
21	C	1.392	124.2	57.9	20	19	14
22	C	1.403	5.0	72.6	20	19	14
23	H	1.084	115.0	239.1	20	19	14
24	C	1.406	121.8	359.9	21	20	22
25	C	1.400	120.1	179.9	22	20	23
26	N	1.412	121.5	0	22	20	23
27	H	1.088	118.8	0.1	21	20	23
28	C	1.395	119.4	360.0	25	22	20
29	N	1.304	120.8	181.2	26	22	25
30	H	1.086	119.6	180.2	25	22	20
31	H	1.033	118.6	1.5	26	22	25
32	C	1.511	120.8	0.2	24	21	27
33	S	1.599	121.8	359.3	29	26	31
34	H	1.088	118.8	359.9	28	25	30
35	H	1.097	111.4	122.9	32	24	28
36	H	1.098	111.4	242.4	32	24	28
37	H	1.095	111.4	2.6	32	24	28
38	O	1.526	113.5	359.6	33	29	26

Total energy = -1708.608979

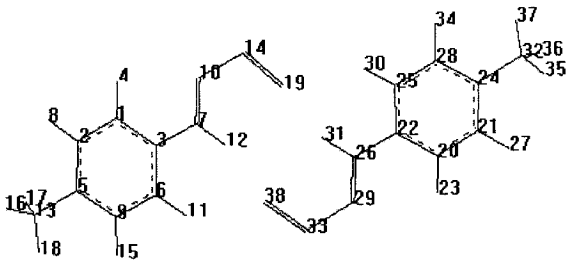

oMe2-dimer

1	C	0	0	0	0	0	0
2	C	1.397	0	0	1	0	0
3	C	1.396	119.6	0	1	2	0
4	H	1.087	120.4	179.7	1	2	3
5	C	1.393	119.8	0.7	2	1	3
6	C	1.401	122.0	180.2	3	1	4
7	H	1.087	120.5	359.7	2	1	4
8	H	1.088	119.6	359.2	3	1	4
9	C	1.401	120.0	180.4	5	2	7
10	C	1.510	120.7	358.5	6	3	8
11	H	1.085	120.9	360.0	5	2	7
12	N	1.420	119.6	180.1	9	5	2
13	H	1.098	111.4	234.9	10	6	3
14	H	1.094	110.4	354.7	10	6	3
15	H	1.095	111.7	115.1	10	6	3
16	H	1.032	119.7	216.5	12	9	5
17	N	1.308	119.4	24.3	12	9	5
18	S	1.595	122.5	351.7	17	12	16
19	O	1.524	114.1	0.1	18	17	12
20	C	5.869	141.5	166.4	19	18	17
21	C	1.397	78.6	171.3	20	19	18
22	C	1.396	46.3	324.0	20	19	18
23	H	1.087	152.0	35.1	20	19	18
24	C	1.393	119.8	359.3	21	20	22
25	C	1.401	122.0	179.8	22	20	23
26	H	1.087	120.5	0.3	21	20	23
27	H	1.088	119.6	0.8	22	20	23
28	C	1.401	120.0	179.6	24	21	26
29	C	1.510	120.7	1.5	25	22	27
30	H	1.085	120.9	0.0	24	21	26
31	N	1.420	119.6	179.9	28	24	21
32	H	1.095	111.6	245.2	29	25	22
33	H	1.094	110.4	5.6	29	25	22
34	H	1.098	111.4	125.5	29	25	22
35	H	1.032	119.8	143.4	31	28	24
36	N	1.308	119.4	335.6	31	28	24
37	S	1.595	122.5	8.3	36	31	35
38	O	1.524	114.1	359.9	37	36	31

Total energy = -1708.598338

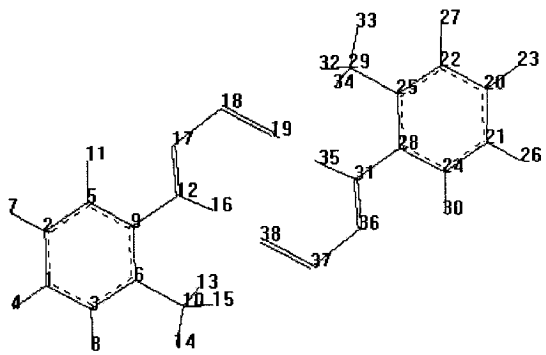

oMe6-dimer

1	C	0	0	0	0	0	0
2	C	1.396	0	0	1	0	0
3	C	1.396	119.4	0	1	2	0
4	H	1.087	120.0	179.4	1	2	3
5	C	1.403	122.7	0.4	2	1	3
6	C	1.391	119.6	179.8	3	1	4
7	H	1.088	119.3	0.6	2	1	4
8	H	1.087	120.7	0.1	3	1	4
9	C	1.406	120.5	360.0	6	3	1
10	C	1.512	118.8	1.2	5	2	7
11	H	1.086	120.7	359.6	6	3	8
12	N	1.417	115.2	180.1	9	6	3
13	H	1.095	109.6	9.2	10	5	2
14	H	1.095	112.2	248.9	10	5	2
15	H	1.095	111.9	129.3	10	5	2
16	N	1.306	122.8	160.0	12	9	6
17	H	1.034	117.4	344.5	12	9	6
18	S	1.601	121.2	181.9	16	12	9
19	O	1.526	113.3	0.5	18	16	12
20	C	5.607	130.8	218.7	19	18	16
21	C	1.396	90.4	130.3	20	19	18
22	C	1.396	29.9	297.2	20	19	18
23	H	1.087	148.7	323.8	20	19	18
24	C	1.403	122.7	0.4	21	20	22
25	C	1.391	119.6	179.8	22	20	23
26	H	1.088	119.3	0.6	21	20	23
27	H	1.087	120.7	0.1	22	20	23
28	C	1.406	120.5	360.0	25	22	20
29	C	1.512	118.8	1.2	24	21	26
30	H	1.086	120.7	359.6	25	22	27
31	N	1.417	115.2	180.1	28	25	22
32	H	1.095	109.6	9.3	29	24	21
33	H	1.095	112.2	248.9	29	24	21
34	H	1.095	111.9	129.3	29	24	21
35	N	1.306	122.8	160.1	31	28	25
36	H	1.034	117.4	344.5	31	28	25
37	S	1.601	121.2	181.9	35	31	28
38	O	1.526	113.3	0.5	37	35	31

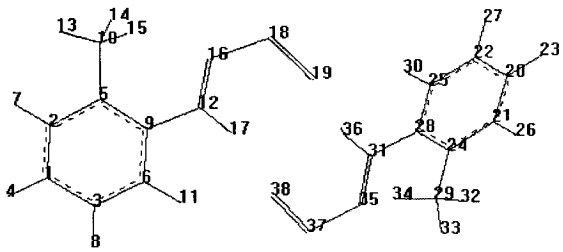

Total energy = -1708.596679

mMe3-5-dimer

1	C	0	0	0	0	0	0
2	C	1.394	0	0	1	0	0
3	C	1.401	118.6	0	1	2	0
4	H	1.084	121.3	179.7	1	2	3
5	C	1.398	120.9	0.1	2	1	3
6	C	1.402	120.8	180.3	3	1	4
7	N	1.412	121.3	0	3	1	4
8	H	1.087	119.3	360.0	2	1	4
9	C	1.399	120.4	359.9	6	3	1
10	N	1.305	120.7	358.6	7	3	1
11	H	1.086	119.0	179.7	6	3	1
12	H	1.033	118.7	178.3	7	3	1
13	H	1.088	119.8	0	5	2	8
14	S	1.597	121.9	0.6	10	7	12
15	C	1.512	120.4	1.5	9	6	11
16	O	1.525	113.6	0.3	14	10	7
17	H	1.096	111.4	215.3	15	9	6
18	H	1.095	111.5	336.0	15	9	6
19	H	1.098	111.0	95.8	15	9	6
20	C	4.951	154.6	245.3	16	14	10
21	C	1.397	125.5	300.1	20	16	14
22	C	1.403	5.5	281.8	20	16	14
23	H	1.085	114.1	118.3	20	16	14
24	C	1.406	118.9	0	21	20	22
25	C	1.400	120.8	180.1	22	20	23
26	N	1.412	121.1	0.0	22	20	23
27	C	1.512	120.7	360.0	21	20	23
28	C	1.395	120.5	360.0	24	21	20
29	N	1.305	120.8	178.4	26	22	25
30	H	1.085	119.8	179.8	25	22	20
31	H	1.033	118.5	358.0	26	22	25
32	H	1.088	119.6	180.0	24	21	20
33	H	1.097	111.2	239.8	27	21	20
34	H	1.095	111.5	0.1	27	21	20
35	H	1.097	111.2	120.4	27	21	20
36	S	1.598	121.9	0.7	29	26	31
37	H	1.087	119.9	0	28	24	32
38	O	1.525	113.6	0.3	36	29	26

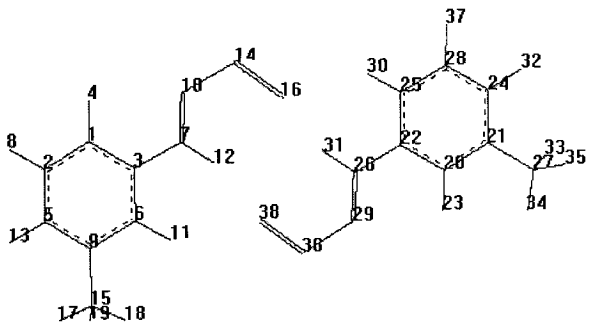

Total energy = -1708.609245

oMe2-6-dimer

1	C	0	0	0	0	0	0
2	C	1.396	0	0	1	0	0
3	C	1.397	119.6	0	1	2	0
4	H	1.087	120.0	179.8	1	2	3
5	C	1.401	122.0	0.1	2	1	3
6	C	1.393	119.9	179.7	3	1	4
7	H	1.087	119.6	0.6	2	1	4
8	H	1.087	120.5	0.3	3	1	4
9	C	1.401	119.8	0.2	6	3	1
10	C	1.510	120.8	1.4	5	2	7
11	H	1.084	120.9	0.1	6	3	8
12	N	1.417	119.9	179.7	9	6	3
13	H	1.094	110.4	2.0	10	5	2
14	H	1.096	111.8	241.5	10	5	2
15	H	1.098	111.4	121.5	10	5	2
16	N	1.306	120.6	342.2	12	9	6
17	H	1.029	119.6	150.6	12	9	6
18	S	1.600	120.5	178.2	16	12	9
19	O	1.527	112.5	1.0	18	16	12
20	C	5.607	129.1	199.7	19	18	16
21	C	1.396	90.1	113.5	20	19	18
22	C	1.396	30.3	280.0	20	19	18
23	H	1.087	148.9	307.7	20	19	18
24	C	1.403	122.7	0.4	21	20	22
25	C	1.392	119.6	179.8	22	20	23
26	H	1.088	119.3	0.6	21	20	23
27	H	1.087	120.7	0.1	22	20	23
28	C	1.406	120.5	0.0	25	22	20
29	C	1.512	118.9	1.3	24	21	26
30	H	1.085	120.7	359.6	25	22	27
31	N	1.417	115.4	179.9	28	25	22
32	H	1.095	109.7	10.3	29	24	21
33	H	1.095	112.1	249.9	29	24	21
34	H	1.095	111.9	130.3	29	24	21
35	N	1.307	122.6	157.4	31	28	25
36	H	1.035	117.4	342.4	31	28	25
37	S	1.601	121.1	181.9	35	31	28
38	O	1.524	113.3	0.3	37	35	31

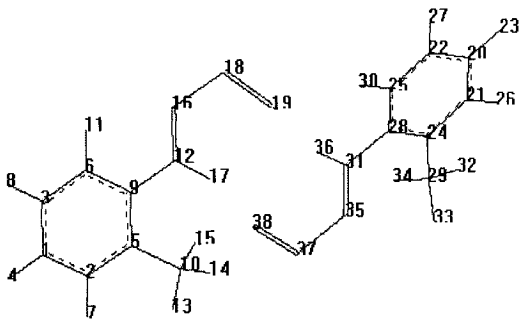

Total energy = -1708.598235

Appendix E: Contour plots and molecular graph

E.1 Contour maps of the election density of PhNHNSO and substituted PhNHNSO monomers from B3LYP/6-31+G(d)

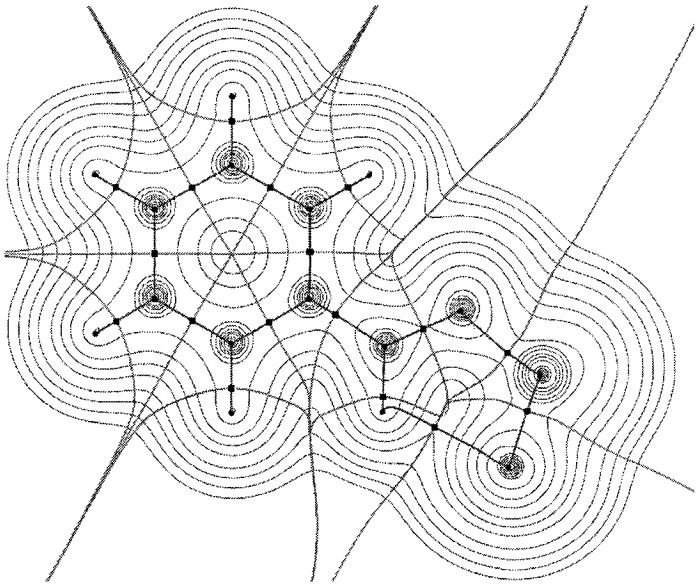

Fig. E.1.1: PhNHNSO

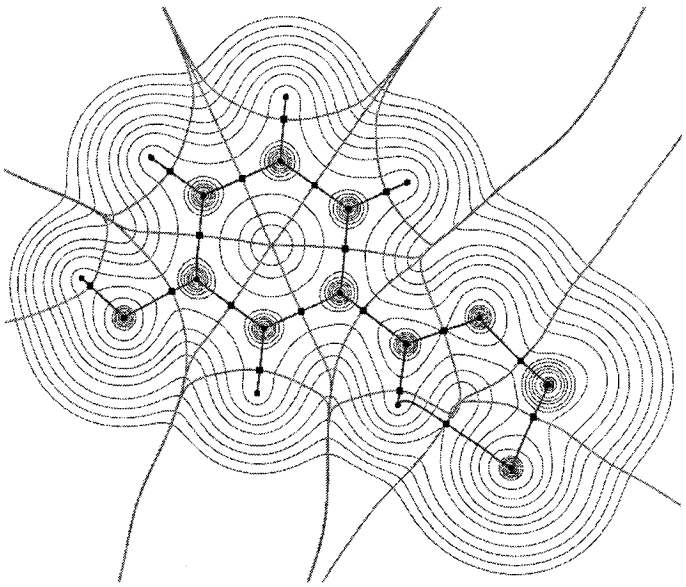

Fig. E.1.2: **m3-OH(a)**

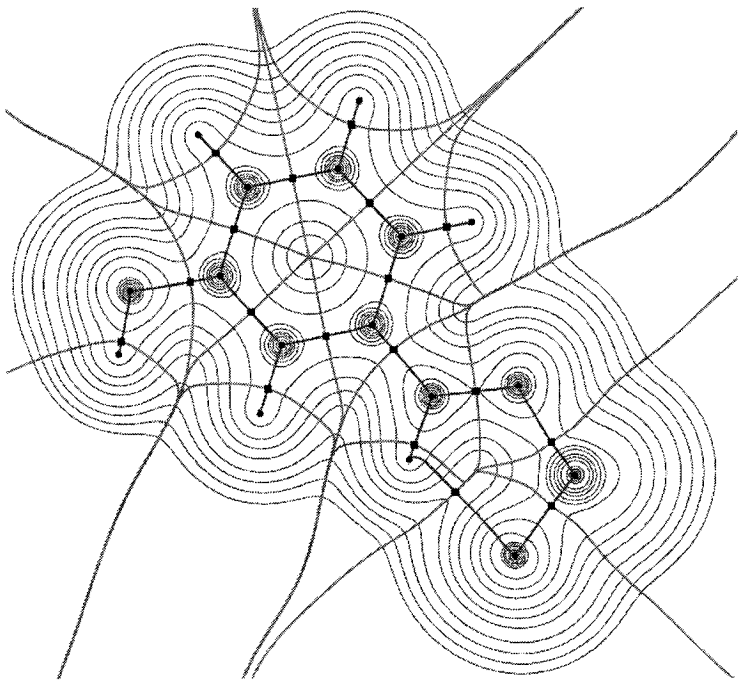

Fig. E.1.3: **m3-OH(b)**

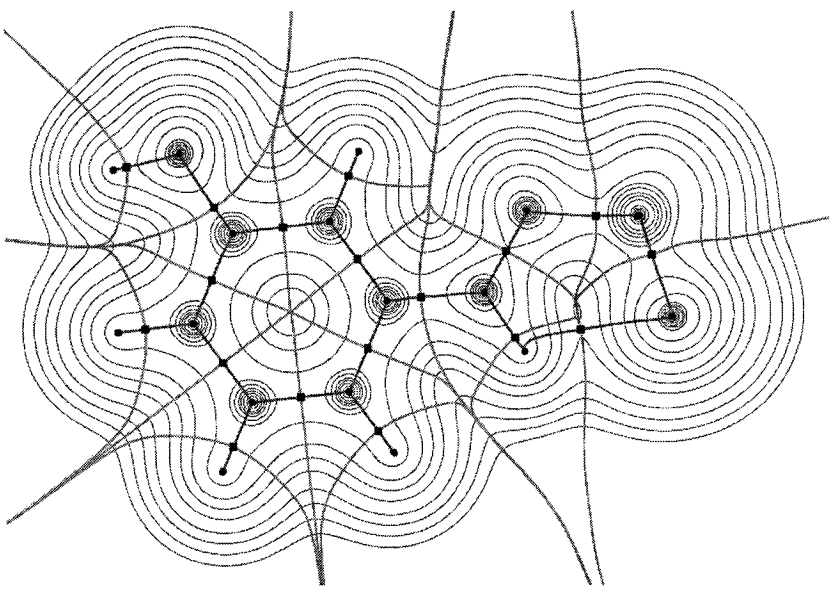

Fig. E.1.4: **m5-OH(a)**

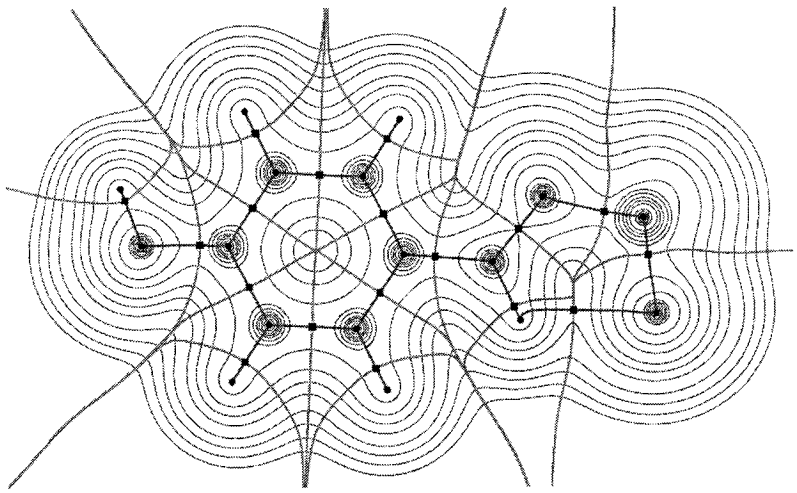

Fig. E.1.5: **p-OH(a)**

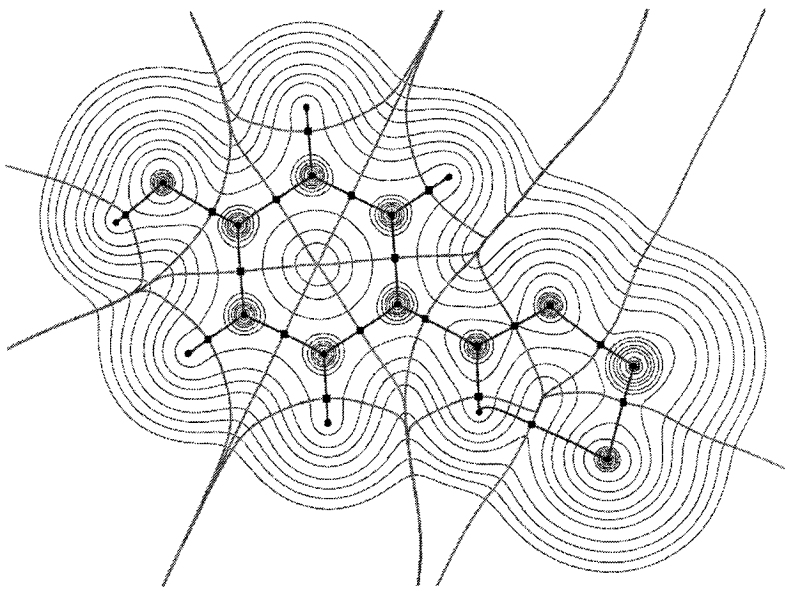

Fig. E.1.6: **p-OH(b)**

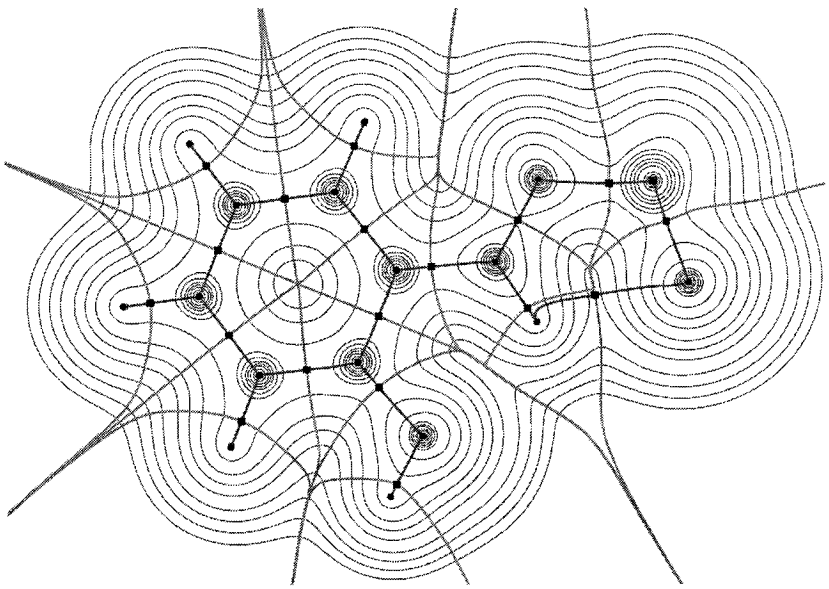

Fig. E.1.7: **o2-OH(a)**

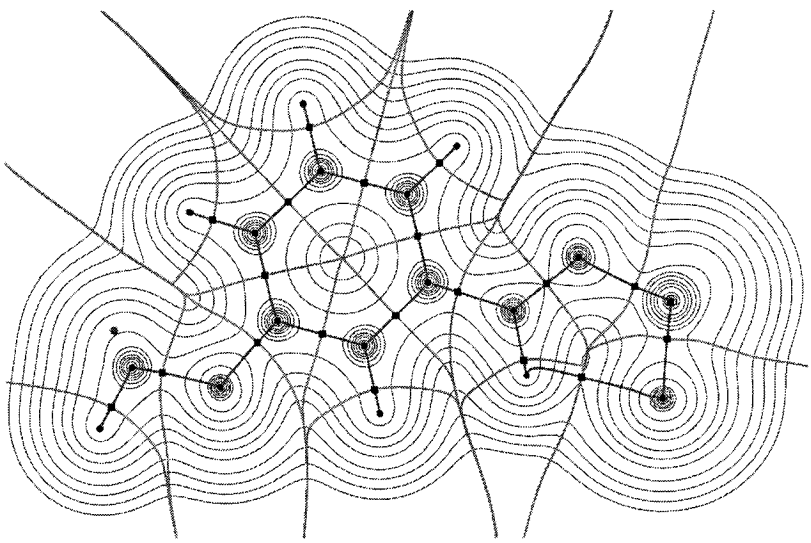

Fig. E.1.8: **m3-OMe(a)**

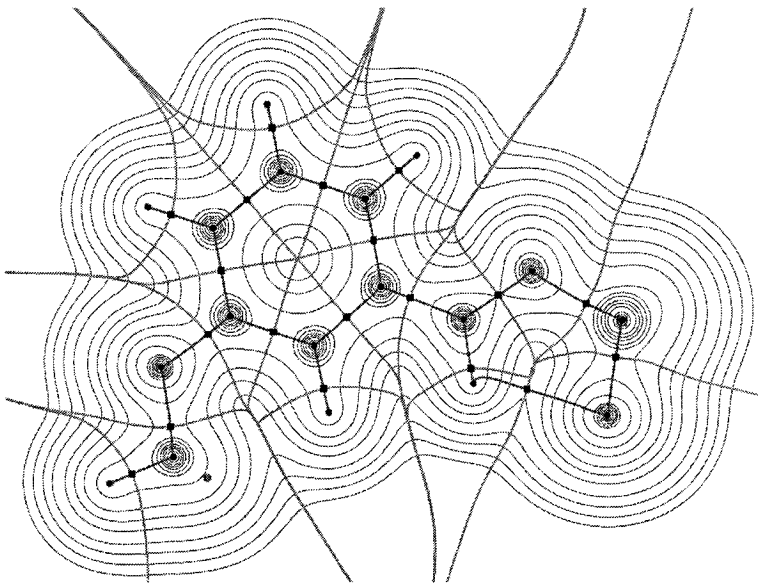

Fig. E.1.9: **m3-OMe(b)**

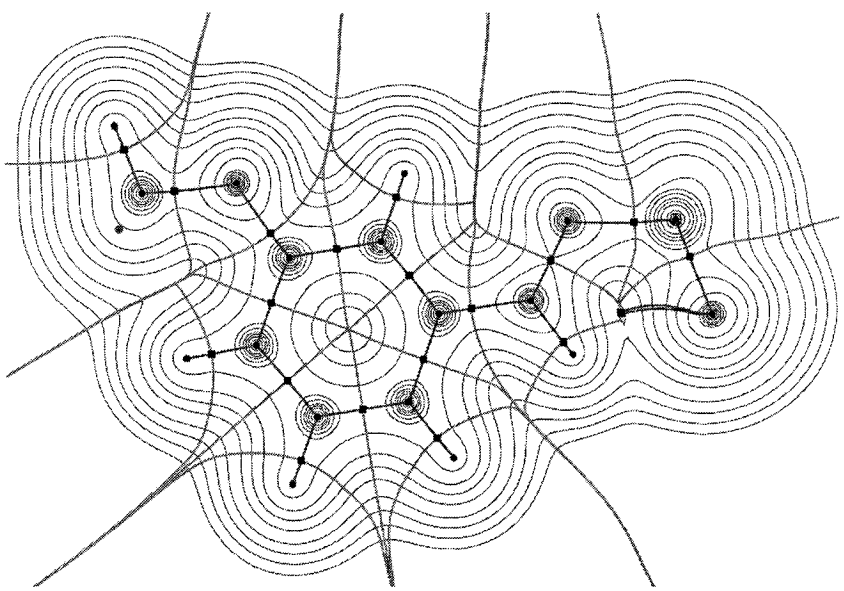

Fig. E.1.10: **m5-OMe(a)**

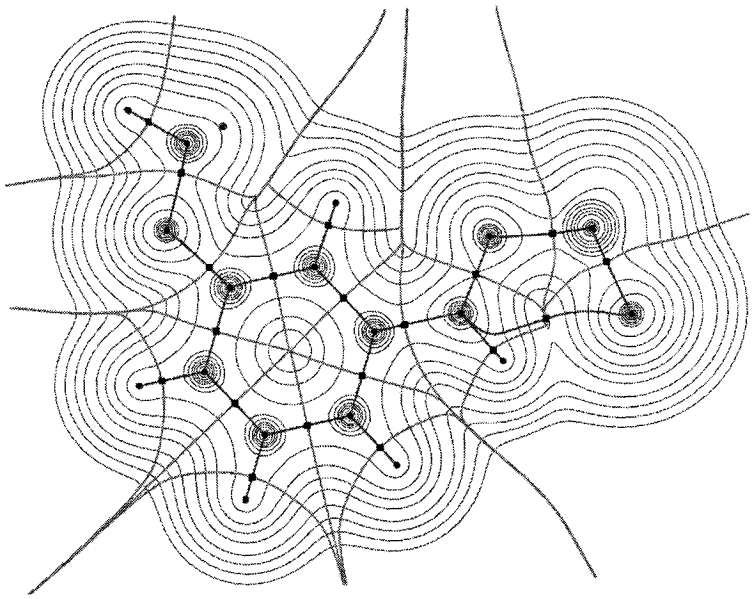

Fig. E.1.11: **m5-OMe(b)**

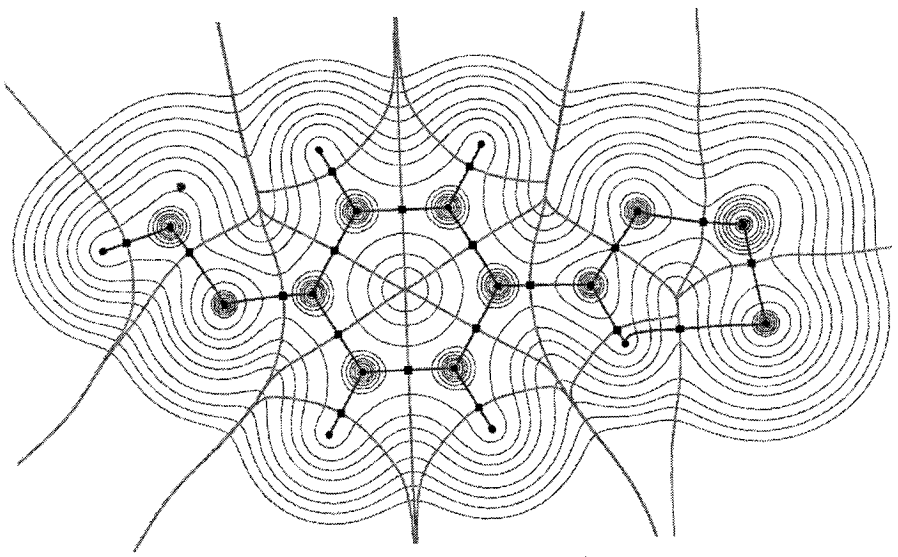

Fig. E.1.12: **p-OMe(a)**

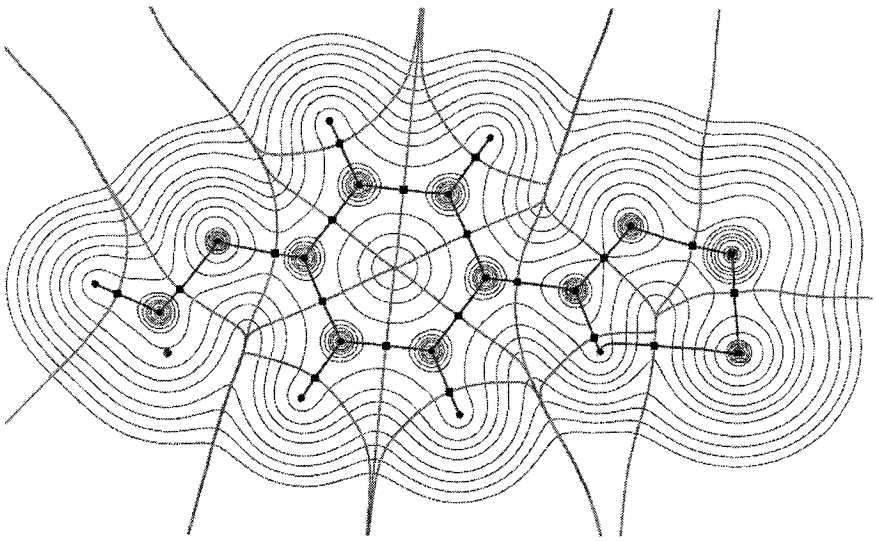

Fig. E.1.13: **p-OMe(b)**

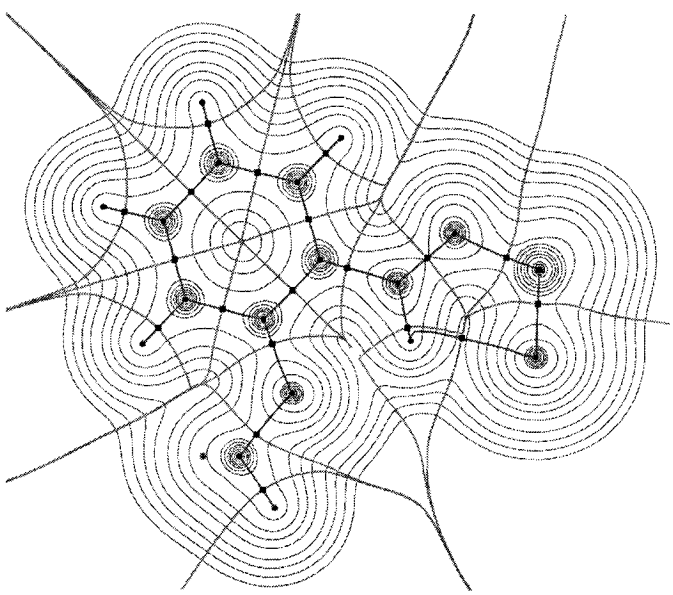

Fig. E.1.14: **o2-OMe(a)**

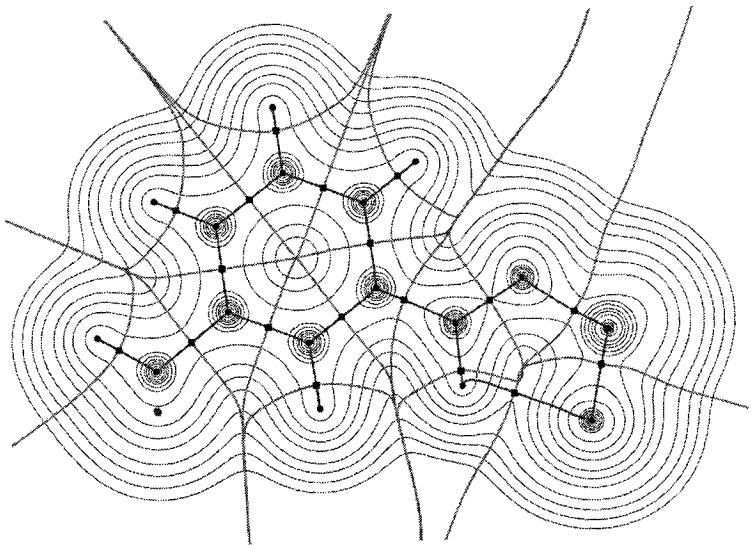

Fig. E.1.15: **m3-Me**

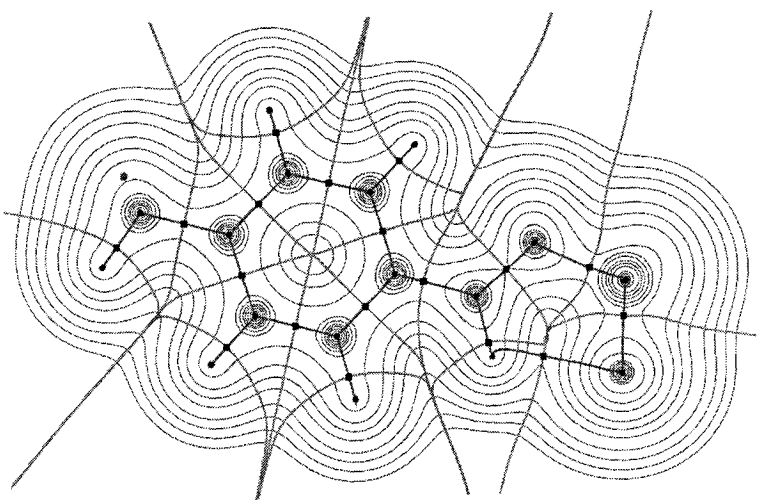

Fig. E.1.16: **p-Me**

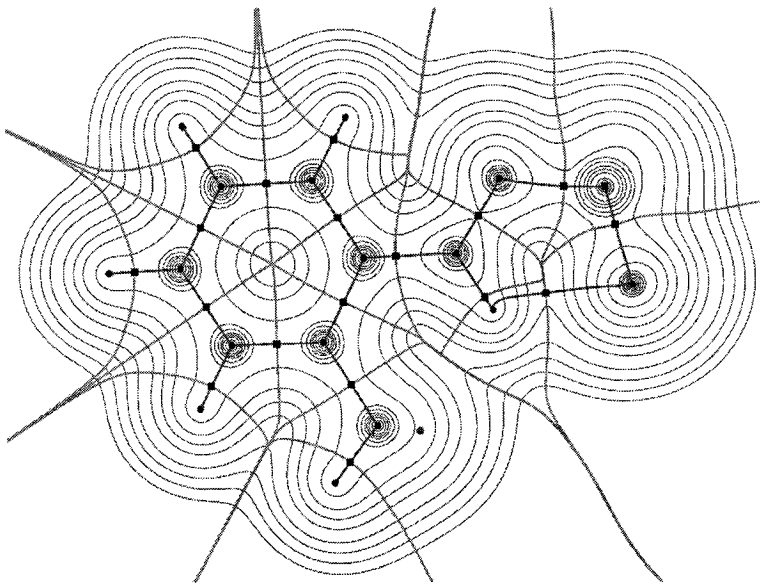

Fig. E.1.17: **o2-Me**

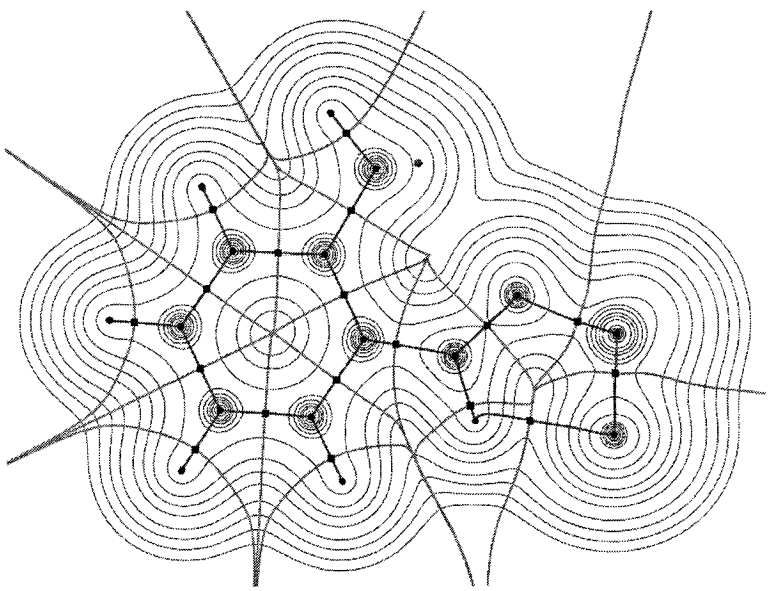

Fig. E.1.18: **o6-Me**

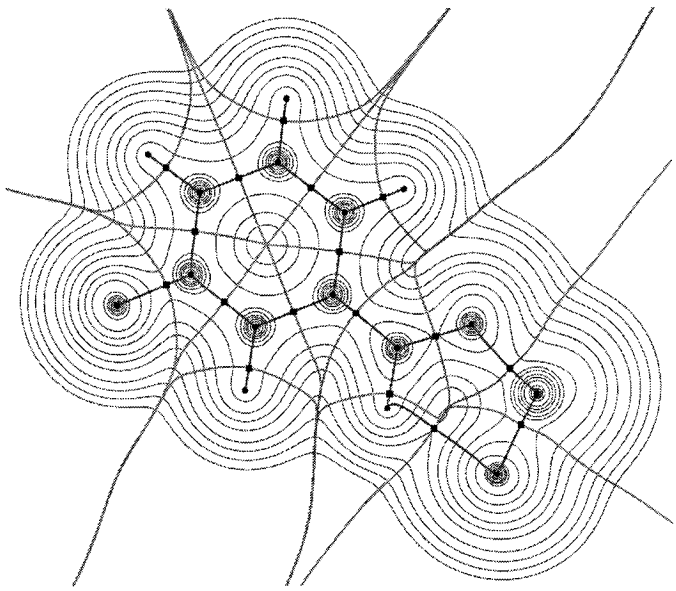

Fig. E.1.19: **m3-F**

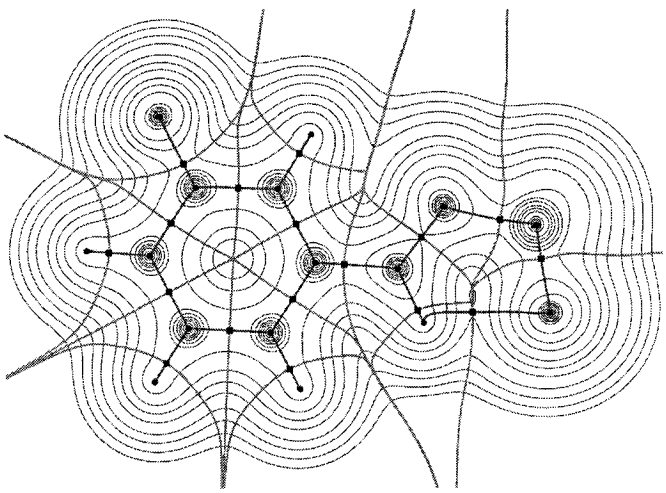

Fig. E.1.20: **m5-F**

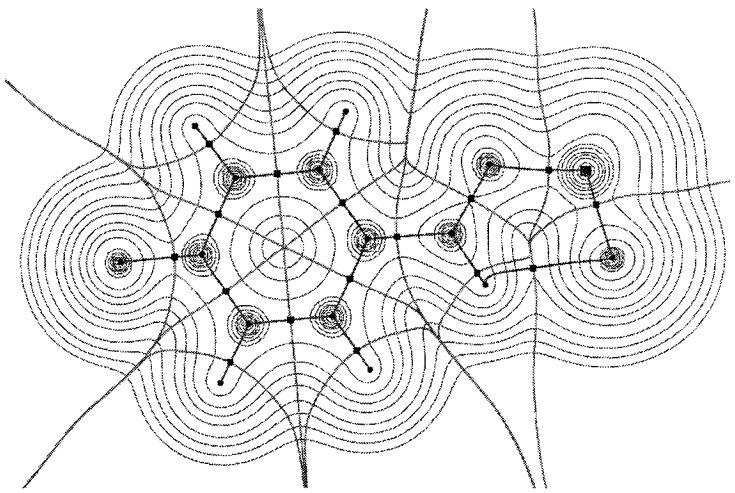

Fig. E.1.21: **p-F**

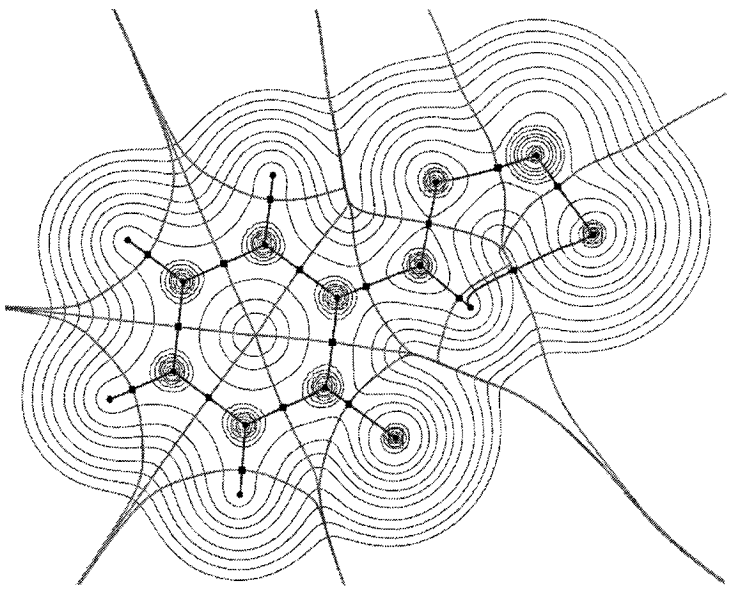

Fig. E.1.22: **o2-F**

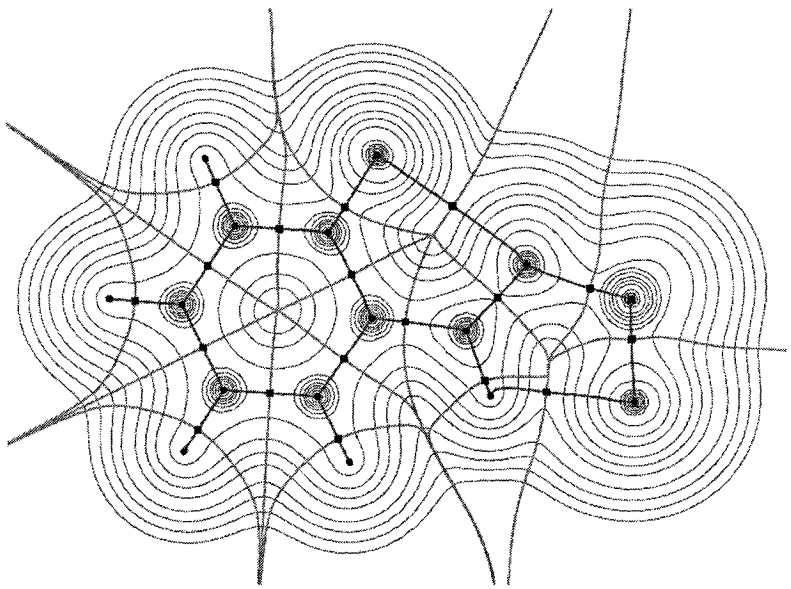

Fig. E.1.23: **o6-F**

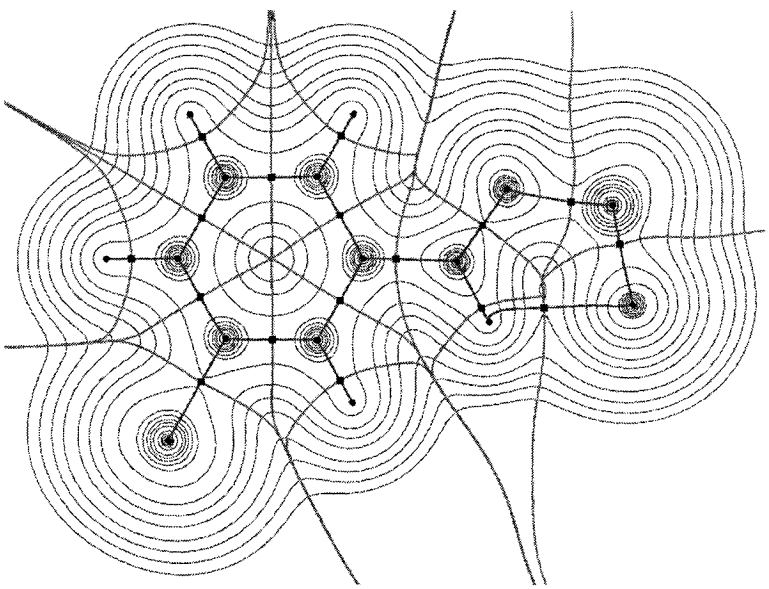

Fig. E.1.24: **m3-Cl**

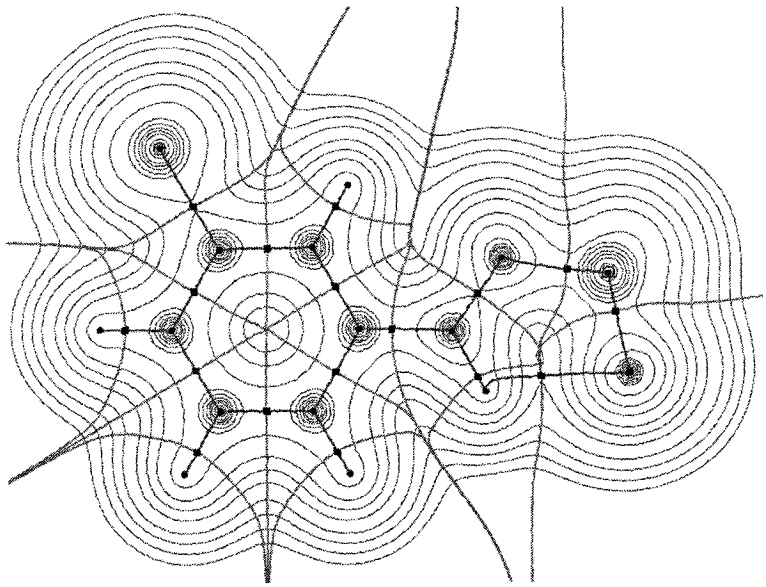

Fig. E.1.25: **m5-Cl**

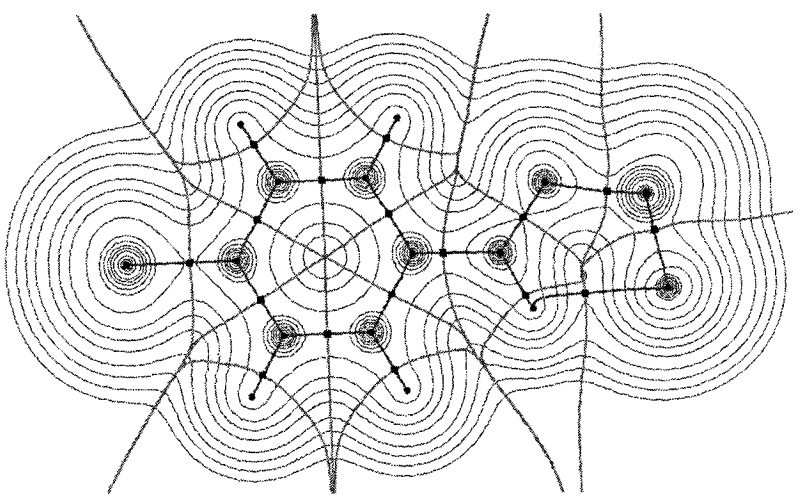

Fig. E.1.26: **p-Cl**

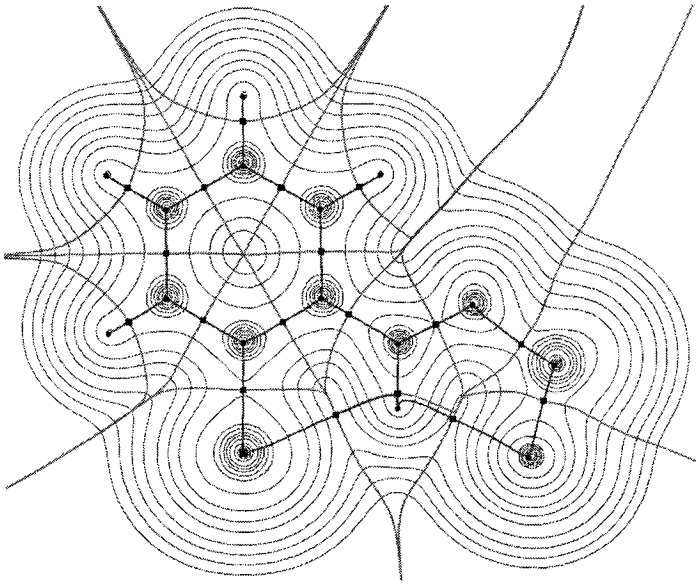

Fig. E.1.27: **o2-Cl**

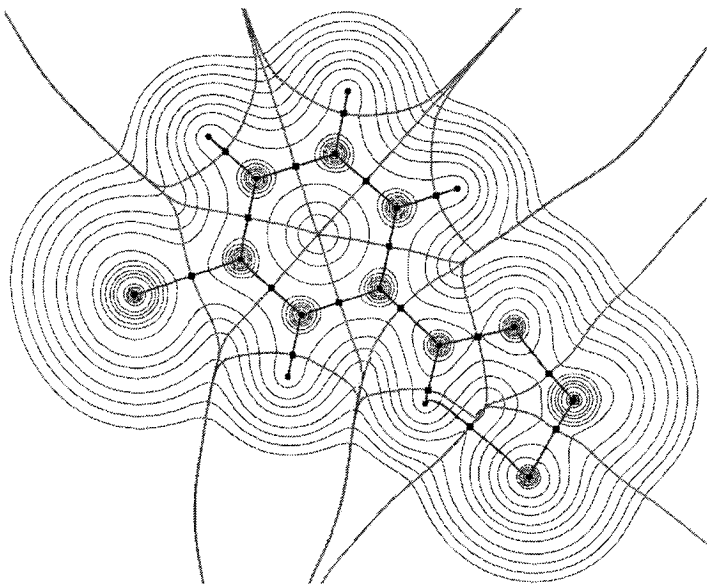

Fig. E.1.28: **m3-Br**

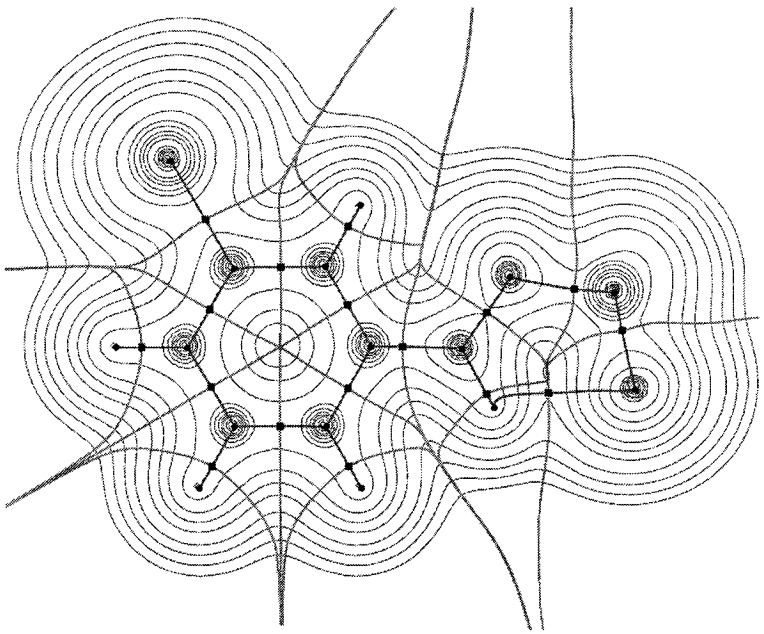

Fig. E.1.29: **m5-Br**

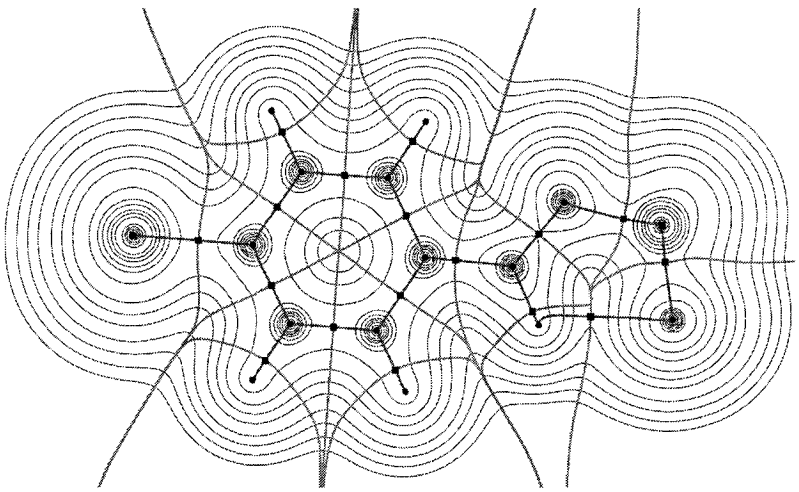

Fig. E.1.30: **p-Br**

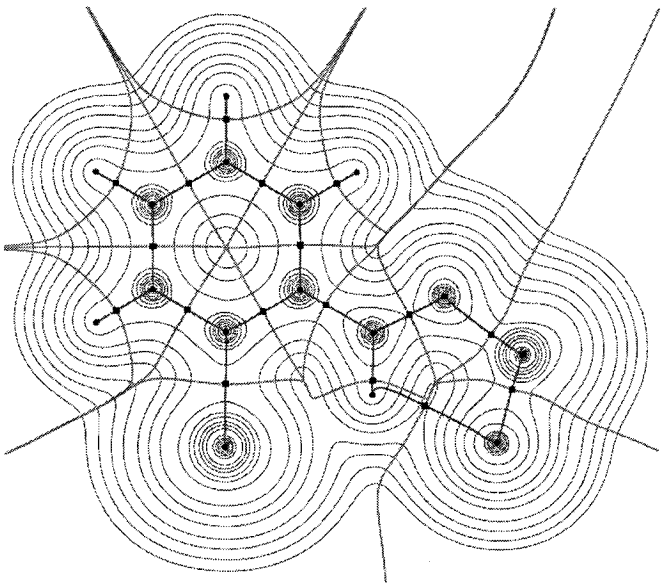

Fig. E.1.31: **o2-Br**

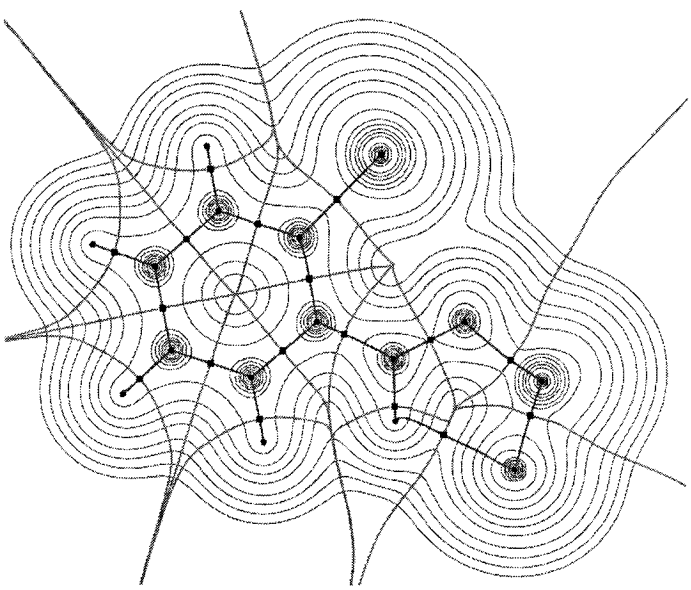

Fig. E.1.32: **o6-Br**

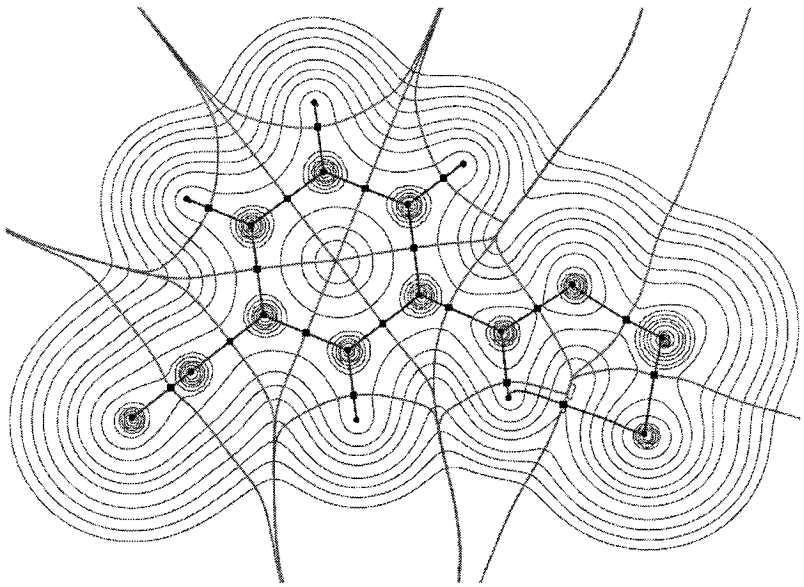

Fig. E.1.33: **m3-CN**

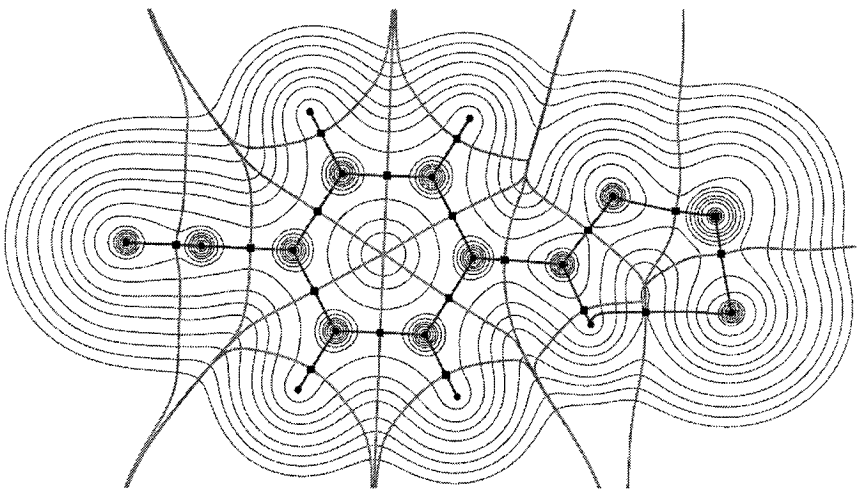

Fig. E.1.34: **p-CN**

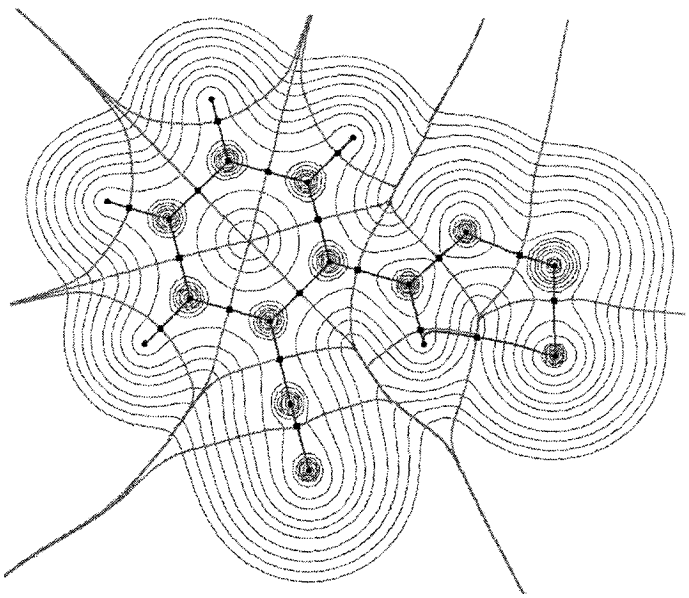

Fig. E.1.35: **o2-CN**

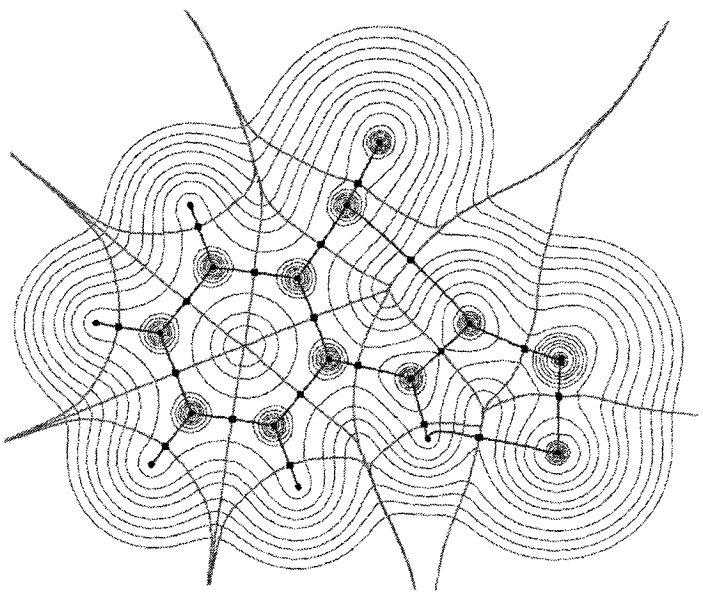

Fig. E.1.36: **o6-CN**

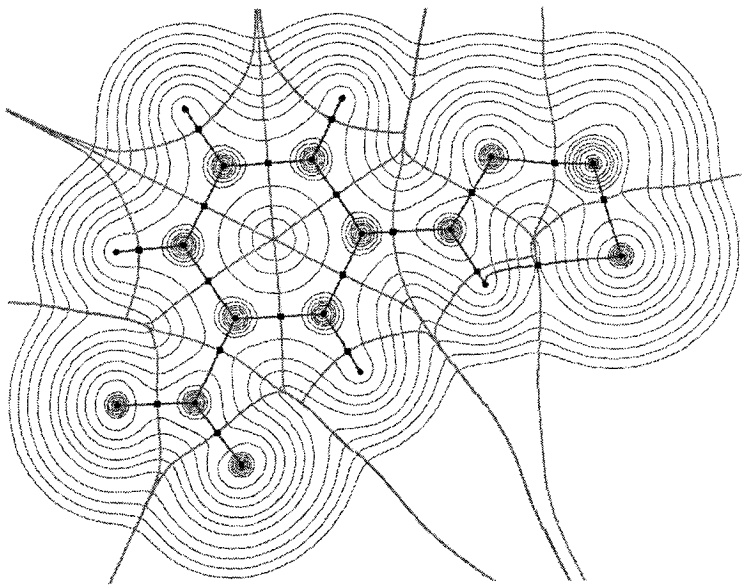

Fig. E.1.37: **m3-NO_2**

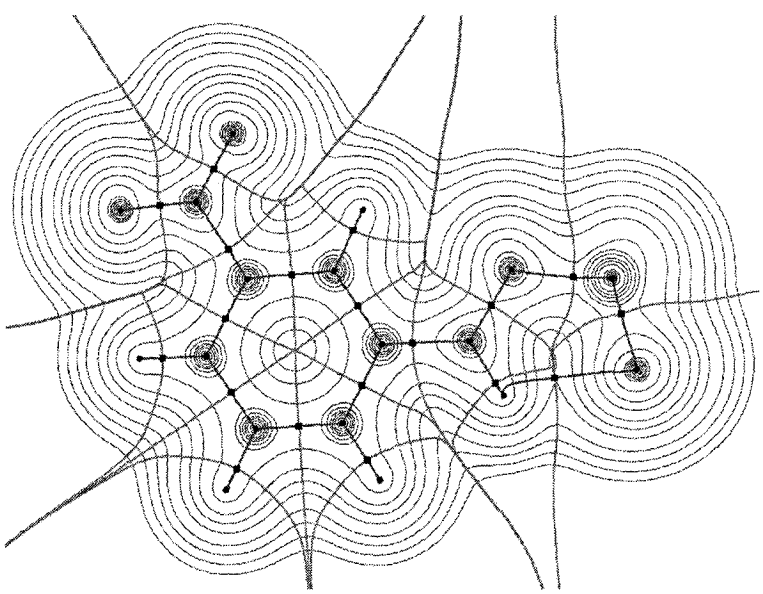

Fig. E.1.38: **m5-NO_2**

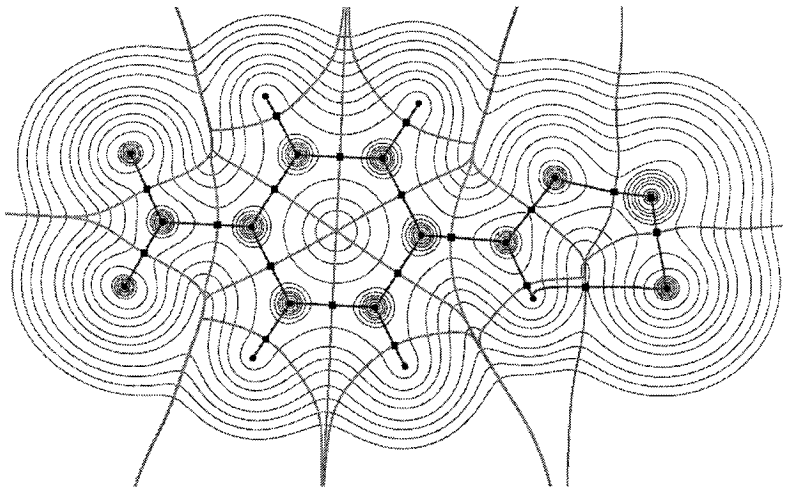

Fig. E.1.39: **p-NO_2**

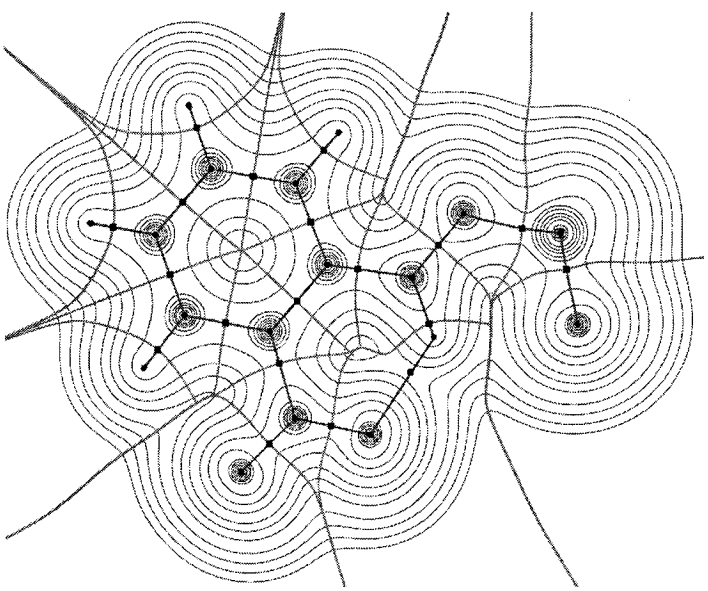

Fig. E.1.40: **o2-NO_2**

E.2 Contour maps of the election density of substituted PhNHNSO dimers

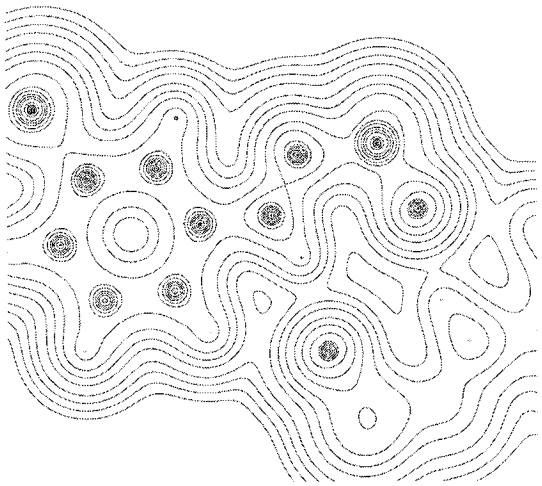

Fig. E.2. 1: **mCl5**

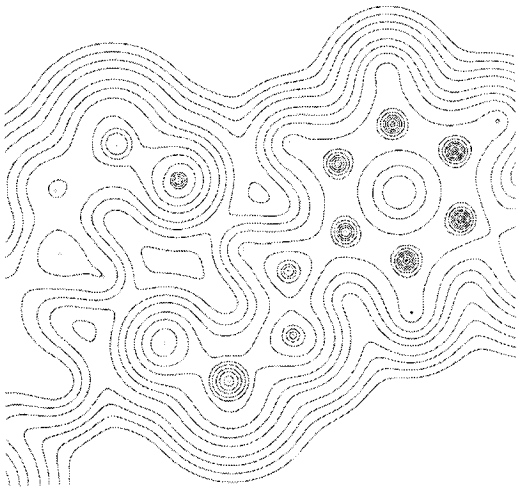

Fig. E.2. 2: **mCl3-5**

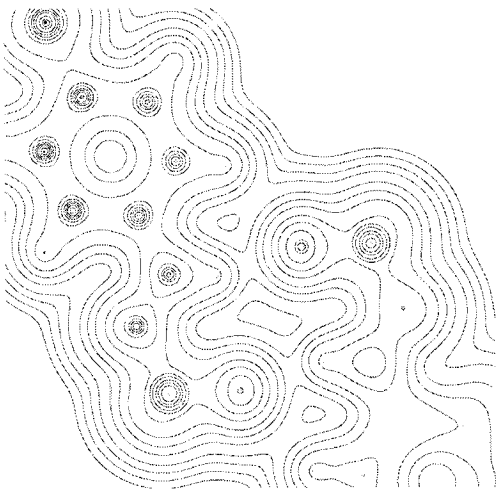

Fig. E.2. 3: **pCl**

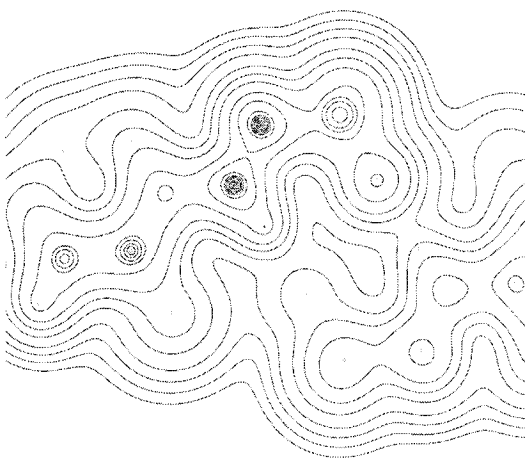

Fig. E.2. 4**: oCl6**

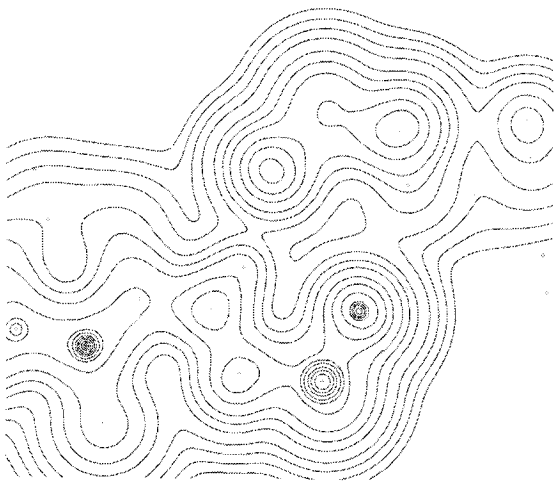

Fig. E.2. 5: **oCl2-6**

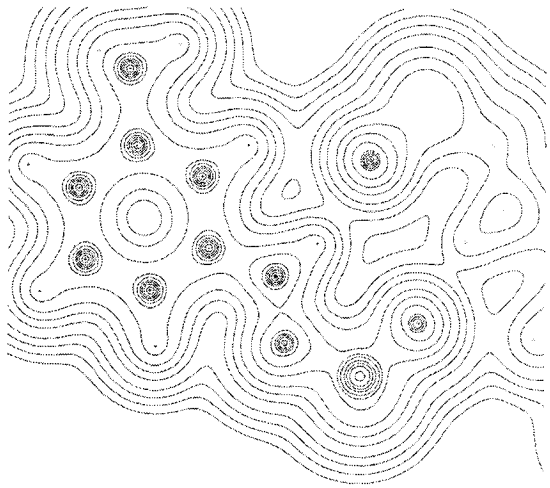

Fig. E.2. 6: **mMe3**

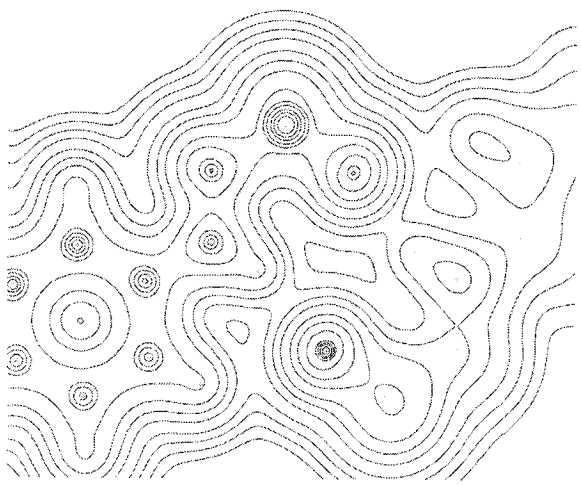

Fig. E.2. 7**: mMe5**

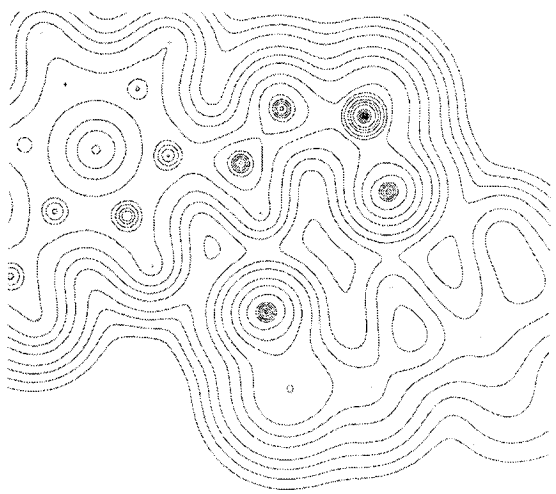

Fig. E.2. 8: **mMe3-5**

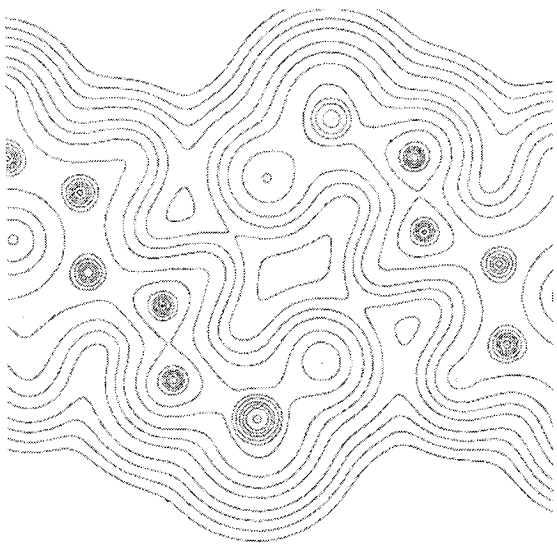

Fig. E.2. 9: **pMe**

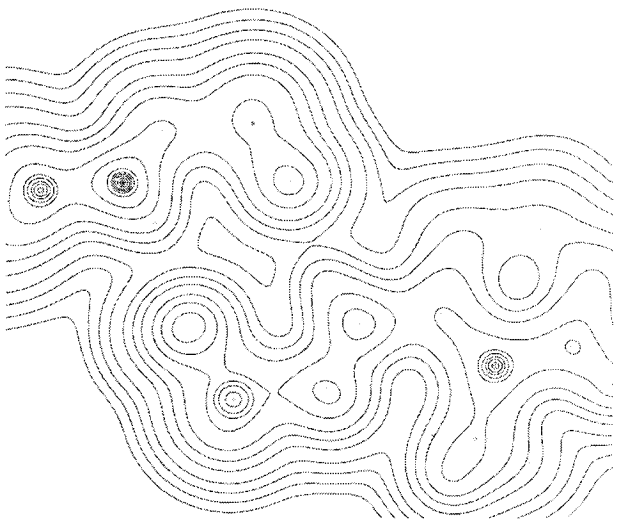

Fig. E.2. 11: **oMe2**

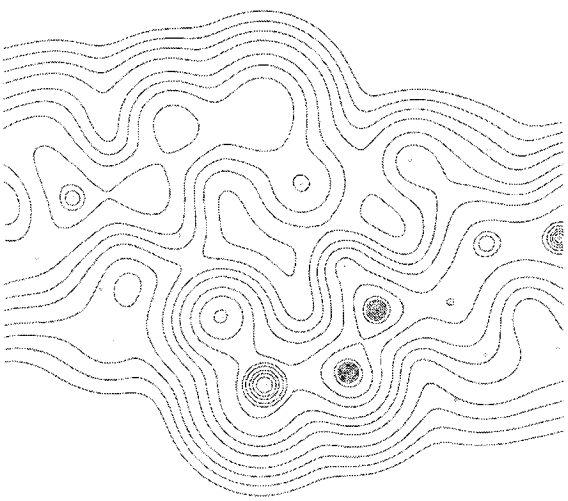

Fig. E.2. 10: **oMe6**

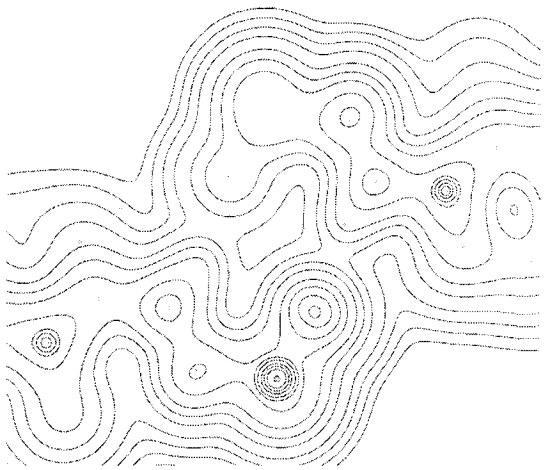

Fig. E.2. 12: **oMe2-6**

E.3 Molecular graph of PhNHNSO monomer from B3LYP/6-311+G(2d,p)

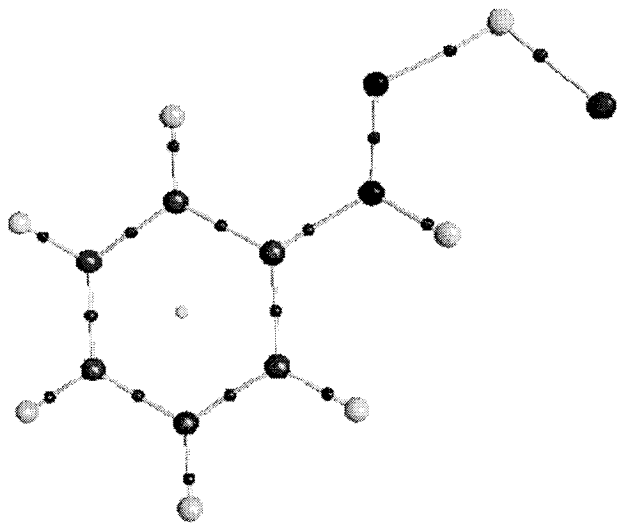

Fig. E.3. 1: PhNHNSO monomer